1998

12 Gene transfer using Starburst™ dendrimers

J.F. Kukowska-Latallo, A.U. Bielinska, C. Chen, M. Rymaszewski, D.A Tomalia and J.R. Baker, Jr.

Chemistry and characterization of dendrimers

The new class of synthetic, highly branched, spherical Starburst™ polyamidoamine (PAMAM) dendrimer polymers is unique in structure. These molecules are uniform in size with a high density of charged primary amino groups restricted to the surface, as well as being highly soluble and stable in aqueous solution. The major structural differences in PAMAM dendrimers relate to the initiator molecule, either ammonia (NH_3) as trivalent or ethylenediamine (EDA) as a tetravalent core, that starts the stepwise polymerization process and determines the overall shape, density, and surface charge of the molecule. With each new layer, or generation, the molecular weight of the polymer more than doubles and the number of surface amino groups exactly doubles. Dendrimers range in size from 10 to 130 Å, with each polymerization step adding approximately 10 Å to the diameter of the molecule. At least 10 generations of both types of PAMAM dendrimers (NH_3 and EDA core) can be synthesized (Tomalia *et al.*, 1990). Each final dendrimer preparation is purified using ultrafiltration and structurally characterized using a number of techniques including electrospray-ionization mass spectroscopy, ^{13}C and ^{1}H nuclear magnetic resonance spectroscopy, size exclusion chromatography, capillary electrophoresis, high performance liquid chromatography (HPLC), and gel electrophoresis (Tomalia *et al.*, 1990). Starburst™ PAMAM dendrimers are identified using a standard nomenclature; for example G10 EDA is the 10th generation of an EDA core dendrimer. PAMAM dendrimers are currently the only class of dendritic macromolecules that are reliably produced in large quantities and that can be precisely synthesized over a broad range of molecular weights. The defined size, structure, and large number of surface amino groups of PAMAM dendrimers have enabled polymers to be employed as a substrate for the attachment of antibodies, contrast agents, and radionuclides for applications in different areas of biology and medicine. Studies using antibody–dendrimer conjugates *in vitro* and *in vivo* in

Self-assembling Complexes for Gene Delivery: From Laboratory to Clinical Trial.
Edited by A.V. Kabanov, P.L. Felgner and L.W. Seymour.

experimental animals have documented these conjugates to be nontoxic and able to target biological agents to specific cells (Wiener *et al.*, 1994; Barth *et al.*, 1994).

It has been demonstrated that PAMAM dendrimers, with defined numbers of amino groups on the surface and positively charged at physiologic pH, interact with biologically relevant polyanions including nucleic acids. Dendrimer–DNA complexes transfect cells in a manner similar to DNA–polylysine complexes (Behr *et al.*, 1994) but with better efficiency given the high solubility and defined architecture of this polymer.

Transfer of genetic material using Starburst™ dendrimers

In vivo and *ex vivo* gene therapies require efficient delivery of genetic material into a cell and preferably high levels of expression of the transferred gene. Existing transfection systems that mediate efficient transfection, such as viral vectors or liposomes, pose problems because of limited cargo space, recombination, mutagenesis, targeting, immunogenicity, and inflammation. Dendrimers are nonimmunogenic and can mediate the delivery of single-stranded and double-stranded, natural or synthetic DNA or RNA of any kind and any size (Kukowska-Latallo *et al.*, 1996; Bielinska *et al.*, 1996). Several models of gene delivery have been evaluated using dendrimers complexed with reporter plasmids, containing genes under the control of different viral promoters, and with respect to specific biology of the cell. The reporter genes included chloramphenicol acetyltransferase (CAT), β-galactosidase (β-gal), luciferase (luc), or green fluorescence protein (GFP). Most of these vectors can also be used to determine the cellular localization of the expressed reporter gene product *in vitro* and *in vivo* (β-gal, CAT, GFP).

In vitro gene transfer

In vitro gene transfer using synthetic dendritic polymers has recently experienced rapid growth. The efforts to understand the structure of the DNA–dendrimer complex and its mechanism of transfection are crucial to expand the application of this technology to *ex vivo* and *in vivo* approaches. Dendrimers, like all nonviral vectors, induce condensation of DNA and may share some other features, ultimately leading to transgene expression from the nucleus. Natural polyamines and polylysine have been known to condense DNA into toroidal and rod-like structures which have been associated with transfection capabilities (Boussif *et al.*, 1995; Remy *et al.*, 1995). Dendritic polymers have an increased overall ionic interaction with DNA compared with natural polyamines, polylysine, and liposomes, and produce very stable and highly soluble DNA complexes.

Formation of a DNA–dendrimer complex

The complex used to transfect cells is composed of two components: a dendritic polymer and DNA. The proportion of each of the components can be optimized for a particular application. Binding and condensation are based on the

electrostatic interactions of the negatively charged DNA and the positively charged dendrimer. The net charge of the complex is neutral when DNA is completely bound to dendrimer in an equal number of positive amino charges on the polymer to the number of negative phosphate groups on DNA. Formation of the complex takes place within seconds to minutes after mixing the components and yields salt-resistant particles stable at a wide range of pH (Kukowska-Latallo *et al.*, 1996). The binding of plasmid DNA to the dendrimer appears to alter the secondary and tertiary, but not the primary structure, of the DNA. The dendrimer condenses the plasmid DNA and the degree of condensation appears to depend on the size of dendrimer, the concentration of the DNA, and the DNA:dendrimer charge ratio used (Bielinska *et al.*, 1996). The appearance of DNA–dendrimer complexes on electronmicrographs is not uniform and ranges from a few to several hundred nanometers. This correlates with the size of dendrimer and to some degree with the transfection activity. In general, higher expression from delivered genetic material *in vitro* is achieved with higher generation dendrimers, i.e. G5 EDA (28.8 kD), G7 EDA (116 kD), and G9 EDA (467 kD). Complexes formed at a fivefold to 20-fold excess of positive (dendrimer) charge, show improved expression, and/or transfer of genetic material. Upon binding to the dendrimer, the DNA is protected against degradation by either specific nucleases or cellular extracts containing nuclease activity (Figure 12.1). The strength of the coulombic interaction between the dendrimer and the DNA resulting in the stability of the complex is probably an important determinant of the transfection activity of the DNA–dendrimer complex. It seems that only the DNA–dendrimer complexes in which DNA is both protected from nucleolitic activity and still transcriptionally active are efficient for gene transfer and expression. At present, preliminary *in vitro* studies indicate that while the initiation of transcription from T7 or CMV promoters (using either T7 polymerase or eucaryotic RNA polymerase II) can be inhibited by complexing DNA to a dendrimer at high excess of positive charge, the elongation of the RNA transcript and translation do not appear to be affected (Bielinska *et al.*, 1998). There were no abortive RNA transcripts generated from the dendrimer-complexed DNA template, regardless of the DNA:dendrimer charge ratio, suggesting that the formation of the transcriptional complex and/or the initiation of transcription rather than the elongation of the nascent RNA was inhibited by complexing the DNA template with the dendrimer. This is reminiscent of the alterations in DNA function when complexed with naturally occurring polycations such as nonacetylated histones.

Characterization of the transfectionally active fraction of DNA–dendrimer complex

Formation of condensed toroid structures by plasmid DNA, as assessed by electron microscopy (EM), is associated with the development of an active transfection complex. Fractionation of the overall complex on density gradients and functional analysis of the fractions revealed that not all of the fractions of the DNA–dendrimer

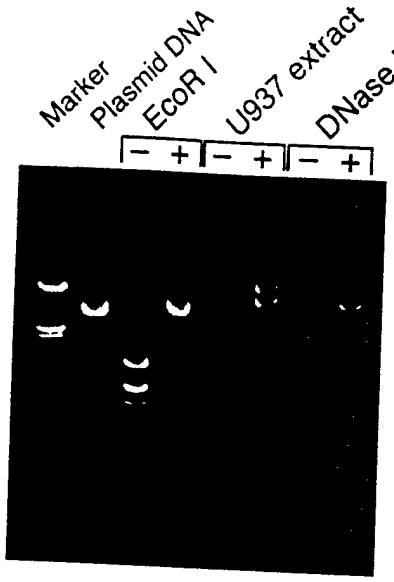

Figure 12.1 *In vitro* nuclease protection of plasmid DNA complexed with a dendrimer. Plasmid pRSVLuc DNA before and after complexing with G5 EDA dendrimer at 1:5 charge ratio was incubated with EcoRI restriction endonuclease, DNaseI nuclease or cellular extract containing nucleases from U937 lymphoma cells. After complexing with G5 EDA, plasmid DNA could be dissociated from the dendrimer using 1% SDS. Whenever plasmid DNA was complexed with the dendrimer (+ lanes), it was fully protected against degradation by specific restriction endonucleases and its integrity was almost fully preserved even when nonspecific cellular nucleases were employed as shown by ethidium bromide stained agarose gel. Formation of DNA–dendrimer complexes at charge ratios greater than 1:1 (i.e. 3:1) provided incomplete protection from nuclease activity (data not shown).

complex are equally active in transfection and expression. The transfectionally active particles appear to constitute less then 10% of the entire complexed DNA, although the nonactive complexes may undergo further alterations either in the culture medium or when associated with cells, and yield a higher transfection efficiency. The optimized proportions of each component indicate that an excess of positive charge in the complex may facilitate its binding to the negatively charged phospholipids in the plasma membrane of the cell. Our unpublished results suggest that by decreasing the DNA to dendrimer charge ratio (e.g. from 1:0.1 to 1:5.0) the formation of biologically functional complexes increases, probably through the generation of more soluble and lower density DNA–dendrimer structures. Dynamic light scattering of DNA–dendrimer complexes revealed polydispersed populations with diameters ranging from 20 nm to 200 μm (Figure 12.2). The sizes and distribution of the complexes depend on DNA concentration, the charge ratio of DNA to dendrimer in the complex, and the type and generation of dendrimer.

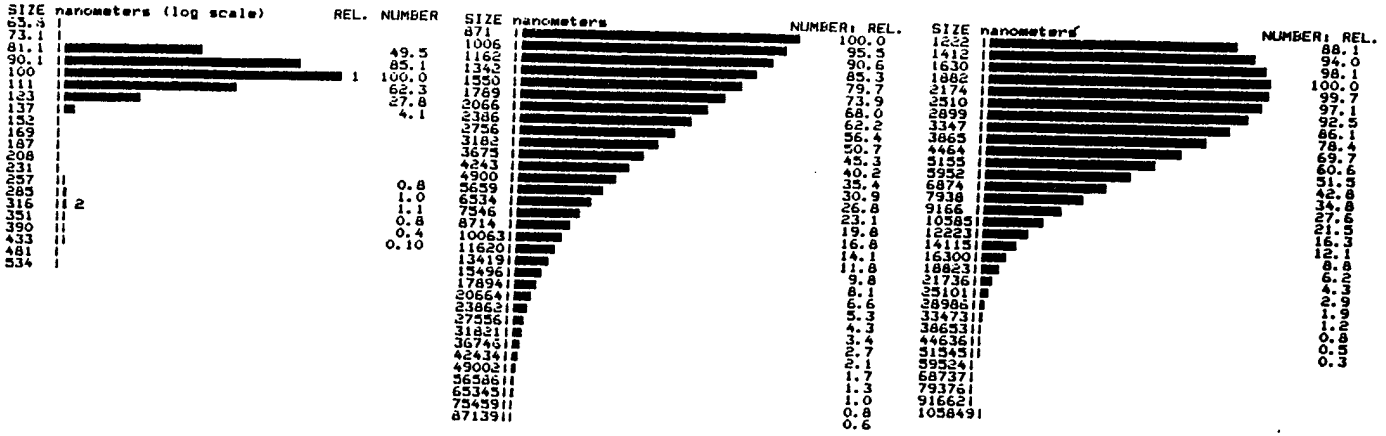

Figure 12.2 Dynamic laser light scattering (DLLS) particle size analysis using NICOMP Model 370 analyzer. All complexes were generated in a water solution at 50 μg/ml DNA concentration and an increasing amount of G7 EDA dendrimer. Non-Gaussian distribution of particles complexed at 1:0.1 DNA to dendrimer charge ratio reveals two major populations of particles with mean diameters of 98.6 and 310.7 nm (left panel). Complexes formed at 1:1 (middle panel) and 1:5 (right panel) DNA to G7 EDA charge ratio generate heterologous populations of particles with near-Gaussian size distribution and mean diameter of particles of 1558.6 nm and 2983 nm, respectively.

Mechanism of intracellular delivery

While most transfection experiments measure the endpoint of gene transfer they are very limited in monitoring all the other intracellular processes leading to gene expression. This is particularly true of the early stages of the transfer: uptake and entry of genetic material into the cell, transit from the cytoplasm to the nucleus, and the dissolution or possible relaxation of the complex. Understanding these 'early' events is crucial for optimalization of the process of transfection. Cationic DNA–dendrimer complexes may initiate cell entry through binding to anionic phospholipids on the cell membrane and trigger either spontaneous endocytosis or direct plasma membrane disruption. The need for an excess of cationic charges over DNA phosphates in the complex supports this hypothesis. Interaction with the plasma membrane can also be achieved with DNA complexes formed with positively charged, high molecular weight diethylaminoethyl (DEAE)-dextran and polyethylenimine (PEI), although both of these compounds are highly cytotoxic (Boussif *et al.*, 1995). Tracing cell entry mechanisms with radiolabeled DNA and/or dendrimer in the complex indicates that the majority of the complexes in most cells are internalized through an energy-dependent endocytosis. Preincubation of cells with inhibitors of cellular metabolism, like sodium azide, or specific inhibitors of endocytosis, like deoxyglucose and cytocholasin B, inhibit the enhanced uptake of the DNA–dendrimer complex regardless of the specific cell type being used (Kukowska-Latallo *et al.*, 1996). In order to be expressed the complexed DNA must reach the nucleus. Elevated expression within the initial 30 min confirmed that translocation to the nucleus took place within 30 min with an advanced uptake up to 3–6 h (Figure 12.3). However, the molecular and cellular events that mediate this translocation remain highly speculative and may differ in various cells, as reflected by the levels of expression. The role of endosome/lysosome escape in this process is thought to be important but is ill defined. Supporting this, transfection can be aided in many cell types with chloroquine which inhibits endosomal acidification. Another potential role for a positively charged dendrimer (with protonable amines) is its ability to act as a weak base and modify the acidification of the endosomal compartment. The DNA release from the complex may, therefore, be the result of an exchange with anionic cytoplasmic ribonucleic acids, proteoglycans, natural polyamines, or nuclear chromatin. Since mitotically-active cells show higher levels of expression of introduced genes, the majority of translocation of exogenous DNA to the nucleus may occur during active cell division. In principle, tracing any uptake mechanism of a cationic polymer–DNA complex is hampered by the fact that probably only a minimal fraction of the DNA that interacts with a cell is involved in observed expression and that the vast majority of the transfection complexes are effectively nonproductive in *in vitro* transfection.

Cell transfection with dendrimers

Upon complexing with DNA, dendrimers can transfect an unusually wide range of adherent and nonadherent cells. This attribute is relatively rare among synthetic transfection reagents. Blood lymphocytes and primary cell lines are notoriously difficult to transfect with commercially available cationic vectors. Dendritic polymers are also superior in transfecting suspension cell lines and, compared with many commercially available cationic liposomes, they have a broader concentration range between transfection and cytotoxicity (Bielinska *et al.*, 1996; Kukowska-Latallo *et al.*, 1996). Dendrimer-mediated transfection of the luciferase gene into Jurkat and U937 (Figures 12.4 and 12.5, respectively), both nonadherent cells of lymphoid lineage, is one to two orders of magnitute higher than that obtained with the commercial lipids, Lipofectamine™ and DMRIE-C™. Without any form of prior activation, expression in Jurkat cells at 18 h post-transfection (Figure 12.4) was maintained at the same level for 36 h and was still present at 72 h (about fivefold lower than at 18 h) post-transfection (data not shown). One of the biggest potential advantages of dendrimers in gene delivery lies in their capability of transfecting a wide range of primary cells. The human primary lung epithelial cell line in its third passage is an example (Figure 12.6). The presence of chloroquine significantly improved expression and the addition of DEAE-dextran was cytotoxic. This latter point is important since the presence of positively charged DEAE-dextran may improve transient transfection with DNA–dendrimer complexes for certain cell lines, but it is cytotoxic for many others and does not allow for stable integration of transfected DNA into the nucleus. DNA–dendrimer complexes are also superior for *in vitro* production of permanently transfected cells, and as such, for *ex vivo* approaches to gene therapy (Kukowska-Latallo *et al.*, 1996).

Figure 12.3 The uptake of plasmid DNA complexed with iodine labeled dendrimer (^{125}I-G7 EDA) at a 1:10 charge ratio. Within 30 min of uptake in the COS-1 fibroblast cell line, complexes, visualized through autoradiography, were present bound to the cell membrane and throughout the cytoplasm (A), and around the perinuclear area (B). The presence of delivered plasmid DNA is also demonstrated by *in situ* staining of the expressed β-galactosidase gene (C).

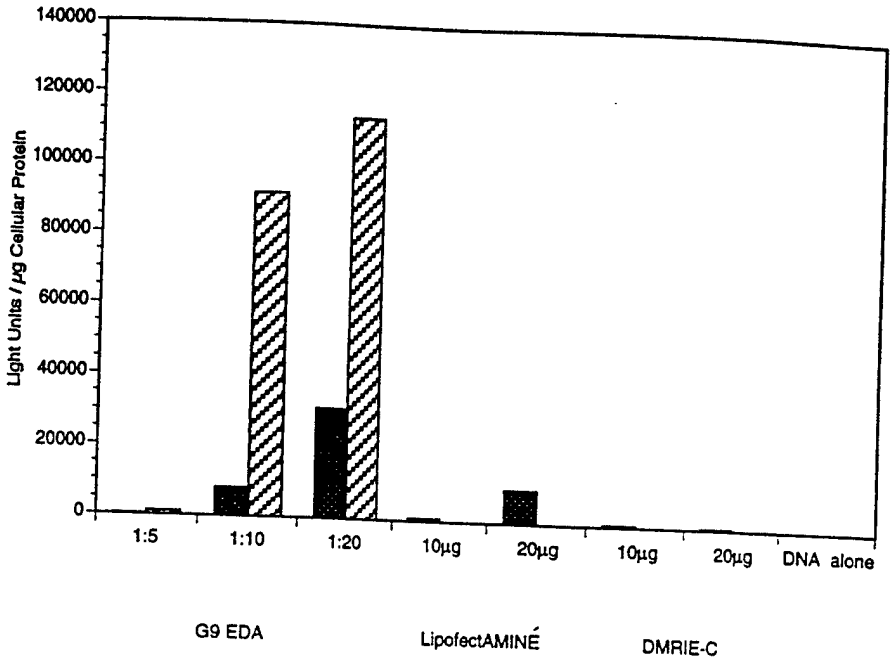

Figure 12.4 *In vitro* transfection of Jurkat human T cell leukemia nonadherent cell line with pCMVLuc plasmid DNA, delivered as a complex with G9 EDA at different charge ratios, was compared with commercially available cationic lipids. Expression of luciferase is one to two orders of magnitute higher than with lipids and is enhanced with addition of 50 μM chloroquine (striped bars) compared with cell culture media (solid bars), suggesting involvement of endosomes in the internalization of the complexes.

Delivery of antisense regulatory nucleic acids using dendrimers

One of the major problems with the use of antisense regulatory nucleic acids is the difficulty in achieving their functional concentrations in cells and subsequent rapid degradation of these molecules by cellular nucleases. The low efficiency of cellular uptake is usually compensated through the use of a high concentration of oligonucleotidesand improvement of their stability by chemical modification of the phosphodiester bond (Crooke, 1993). Polyamidoamine dendrimers function as an effective delivery system for the introduction of regulatory nucleic acids and facilitate the suppression of the specific gene expression (Bielinska *et al.*, 1996). Antisense oligonucleotides or antisense cDNA plasmids can be complexed with the dendrimer and efficiently transfected *in vitro*. Specially developed cell lines with stable expression of a transfected luciferase gene were developed using dendrimers. Delivery of antisense sequences to the luciferase gene resulted in specific inhibition of baseline luciferase activity ranging from 30 to 60% depending on the DNA

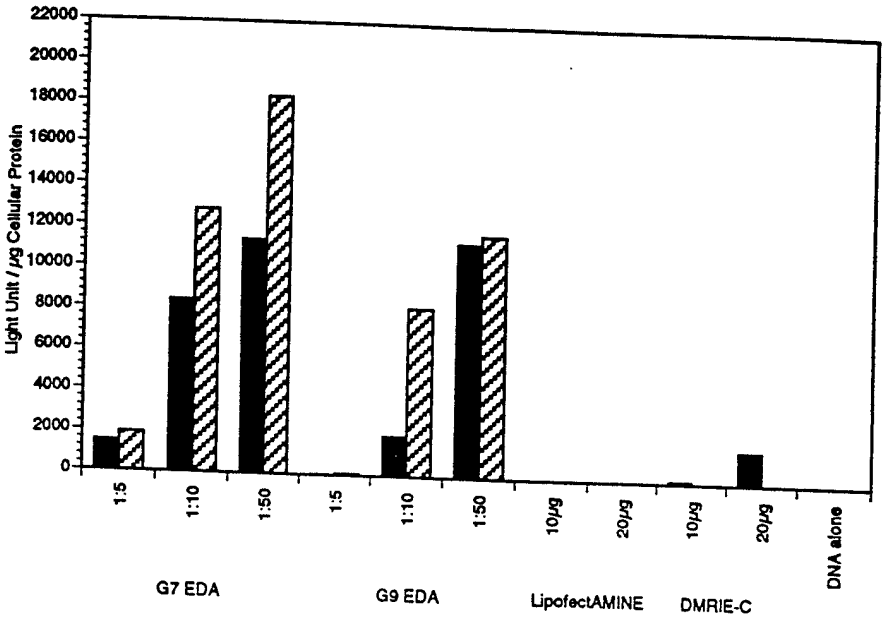

Figure 12.5 Transfection of U937 monocyte-macrophage human histocytic lymphoma cells using two different generations of dendrimers (G7 and G9 EDA) at a wide range of charge ratios and commercial lipid (Lipofectamine™ and DMRIE-C™). The luciferase expression was augmented with 50 μM chloroquine (striped bars).

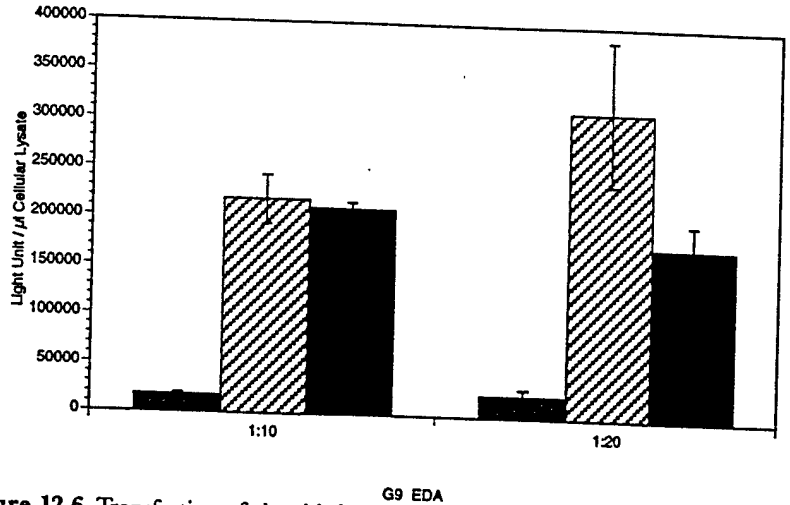

Figure 12.6 Transfection of the third passage of primary human normal small airway epithelial cells (SAEC from Clonetics) with luciferase plasmid DNA complexed with G9 EDA dendrimer at indicated charge ratios. Chloroquine significantly improves expression of the delivered luciferase gene (striped bars) compared with nonsupplemented media (solid bars). Addition of DEAE-dextran (gray bars) did not improve transfection and/or expression and was cytotoxic to the cells.

concentration, type of dendrimer used, and the charge ratio of the DNA–dendrimer complex. Binding of the phosphodiester oligonucleotides to dendrimers also extended their intracellular survival (Bielinska *et al.*, 1996). In contrast to the concentrations of oligonucleotides needed for inhibition reported by others (Bennett *et al.*, 1992; Colige *et al.*, 1993; Goodarzi *et al.*, 1990), we have achieved specific inhibition of targeted gene expression with picomoles of specific oligonucleotides when delivered with dendrimers. Sequence specificity of inhibition by oligonucleotides was not affected by their binding with dendrimers. The dendrimers were not toxic to cells in the concentrations required for gene transfer. Complexing antisense DNA with dendrimers resulted in efficient delivery of complexes that was sequence- and carrier-independent, and could potentially lead to *in vivo* applications of regulatory nucleic acids that are not possible with the currently available delivery techniques (Behr, 1994; Johnson, 1995).

In vivo gene transfer

Trials are currently being carried out to assess the efficacy of *in vivo* gene delivery using dendrimers. Varying amounts of plasmid DNA complexed with different generations of dendrimers have been delivered to mouse and rat lung, either nasally or directly into trachea. Toxicity studies and pathology examination revealed no lung inflammation or pneumonitis. Long-term survival of DNA delivered as a complex with dendrimer was confirmed using polymerase chain reaction (PCR). The PCR amplification was performed with lung homogenate with isolated nucleic acids from the tissue. Plasmid DNA was detected only when plasmid was delivered into the lung as a complex with dendrimer and there was no detectable PCR product in the lung of animals that received plasmid DNA alone (Figure 12.7). Semi-quantitative PCR of plasmid DNA isolated from lung tissue, indicated that complexing of plasmid DNA with dendrimers resulted in up to a 10^5-fold increase in its survival compared with the noncomplexed plasmid DNA. Copurified plasmid DNA remained expressionally active when used as a template in an *in vitro* cell free transcription–translation reticulocyte lysate system (Figure 12.8).

Prospects for the future

In conclusion, our studies outline the ability of Starburst™ dendrimers to mediate the high efficiency transfer of genetic material in a wide variety of eucaryotic cell lines *in vitro*. The lack of toxicity, high transfection efficiency, stability of DNA–dendrimer complexes, and the potential to produce this material under good manufacturing procedure conditions suggest that this transfection method may be useful for *in vivo* applications. In view of the fact that dendrimer–antibody conjugates have already been used experimentally in diagnostic applications, in radioimmunotherapy, and in the imaging of tumors (Wiener *et al.*, 1994; Singh *et al.*, 1994), it is possible that similar forms of antibody-conjugated dendrimers may

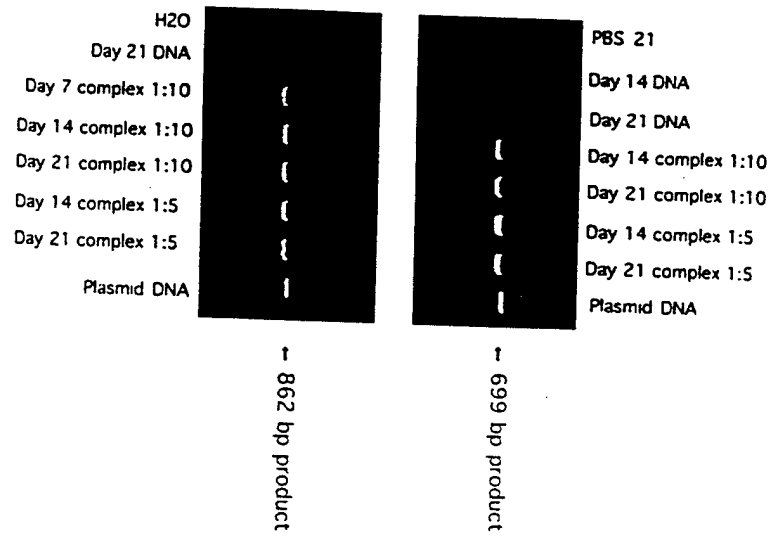

Figure 12.7 The presence of plasmid DNA in samples obtained from rat lungs at 7, 14, and 21 days after nasal delivery of of pCMVβ-gal plasmid DNA complexed with G7 EDA dendrimer at indicated charge ratios. The presence of two different size PCR products (amplified in 30 cycles) identifying different regions of delivered plasmid DNA was compared between animals administered with PBS or noncomplexed plasmid DNA (controls) and the animals that received DNA–dendrimer complexes. Water (left panel, upper lane) and plasmid DNA amplification controls (both panels,bottom lanes) were included.

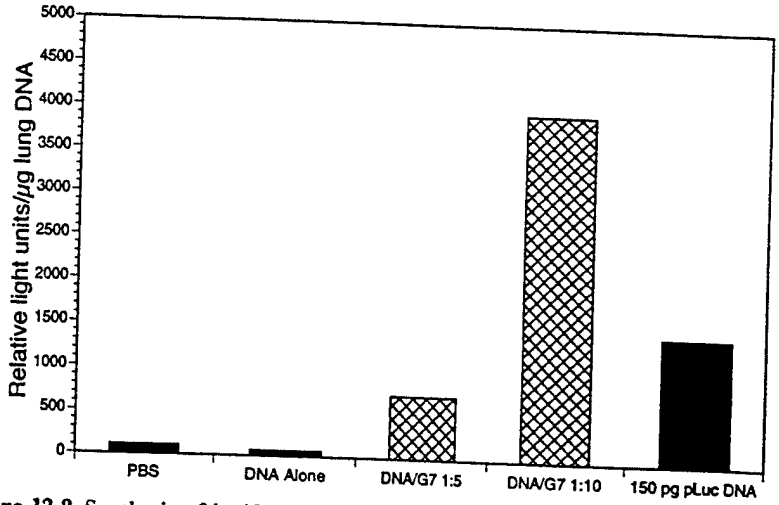

Figure 12.8 Synthesis of luciferase protein in an *in vitro* transcription–translation assay using DNA template copurified with rat lung DNA fraction. The copurified pCMVLuc plasmid remained transcriptionally active whenever it was delivered into the lung as a complex with G7 EDA dendrimer at 1:5 and 1:10 charge ratios, compared with the lungs that received plasmid DNA alone or PBS. Control pLuc plasmid DNA template (150 pg) was included.

be useful in targeted gene delivery *in vivo*. This could enable various therapeutic uses of gene transfer.

Acknowledgment

Starburst is a trademark of Dentritech Corporation.

References

Barth RF, Adams DM, Soloway AH, Alam F and Darby MV. (1994) Boronated starburst dendrimer-monoclonal antibody immunoconjugates: evaluation as a potential delivery system for neutron capture therapy. *Bioconj Chem*, **5**, 58–66.

Behr J-P. (1994) Gene transfer with synthetic cationic amphiphiles: prospects for gene therapy. *Bioconj Chem*, **5**, 382–9.

Bennett CF, Chiang MY, Chan H, Shoemaker JE and Mirabelli CK. (1992) Cationic lipids enhance cellular uptake and activity of phosphorothioate antisense oligonucleotides. *Mol Pharmacol*, **41**, 1023–33.

Bielinska A, Kukowska-Latallo JF, Johnson J, Tomalia DA and Baker JA, Jr. (1996) Regulation of *in vitro* gene expression using antisense oligonucleotides or antisense expression plasmids transfected using starburst PAMAM dendrimers. *Nucl Acids Res*, **24**, 2176–82.

Bielinska AU, Kukowska-Latallo JF and Baker JR, Jr. (1998) The interaction of plasmid DNA with polyamidoamine dendrimers: mechanism of complex formation and analysis of alterations induced in nuclease sensitivity and transcriptional activity of the complexed DNA (submitted).

Boussif O, Lezoualc'h F, Zanta MA, Mergny MD, Scherman D, Demeneix B and Behr J-P. (1995) A versatile vector for gene and oligonucleotide transfer into cells in culture and *in vivo*: polyethylenimine. *Proc Natl Acad Sci USA*, **92**, 7297–301.

Colige A, Sokolov BP, Nugent P, Baserga R and Prockop DJ. (1993) Use of an antisense oligonucleotide to inhibit expression of a mutated human procollagen gene (Coll A1) in transfected mouse 3T3 cells. *Biochemistry*, **32**, 7–11.

Crooke RM. (1993) Cellular uptake, distribution and metabolism of phosphorothioates, phosphodiesters, and methylphosphorothioate oligonucleotides. In: Crooke ST and Lebleu B eds. *Antisense research and applications*. Boca Raton, FL: CRC Press, pp 427–49.

Goodarzi G, Gross S, Tewari A and Watab K. (1990) Antisense oligonucleotides inhibit the expression of the gene for hepatitis B virus surface gene. *J Gen Virol*, **71**, 3021–7.

Johnson LG. (1995) Gene therapy for cystic fibrosis. *Chest*, **107**, 77–83.

Kukowska-Latallo JF, Bielinska AU, Johnson J, Spindler R, Tomalia DA and Baker JR, Jr. (1996) Efficient transfer of genetic material into mammalian cells using starburst polyamidoamine dendrimers. *Proc Natl Acad Sci USA*, **93**, 4897–902.

Remy J-S, Kichler A, Mordvinov V, Schuber F and Behr J-P. (1995) Targeted gene transfer into hepatoma cells with lipopolyamine-condensed DNA particles presenting galactose ligands: a stage toward artificial viruses. *Proc Natl Acad Sci USA*, **92**, 1744–8.

Singh P, Moll F III, Lin SH, Ferzli C, Yu KS, Koski RK, Saul RG and Cronin P. (1994) Starburst dendrimers: enhanced performance and flexibility for immunoassays. *Clin Chem*, **40**, 1845–9.

Tomalia DA, Naylor AM and Goddard WA, III. (1990) Starburst dendrimers: molecular-level control of size, shape, surface chemistry, topology, and flexibility from atoms to macroscopic matter. *Angewandte Chemie* (international edition in English), **29**, 138–75.

Wiener EC, Magnin RL, Gansow OA, Brechbiel MW, Brothers HM II, Tomalia D and Lauterbur PC. (1994) Dendrimer-based metal chelates: a new class of magnetic resonance imaging contrast agents. *Magn Reson Med*, **31**, 1–8.

SUPRAMOLECULAR POLYMERS

EDITED BY
ALBERTO CIFERRI

University of Genoa
Genoa, Italy

Duke University
Durham, North Carolina

MARCEL DEKKER, INC. NEW YORK • BASEL

ISBN: 0-8247-0252-2

This book is printed on acid-free paper.

Headquarters
Marcel Dekker, Inc.
270 Madison Avenue, New York, NY 10016
tel: 212-696-9000; fax: 212-685-4540

Eastern Hemisphere Distribution
Marcel Dekker AG
Hutgasse 4, Postfach 812, CH-4001 Basel, Switzerland
tel: 41-61-261-8482; fax: 41-61-261-8896

World Wide Web
http://www.dekker.com

The publisher offers discounts on this book when ordered in bulk quantities. For more information, write to Special Sales/Professional Marketing at the headquarters address above.

Current printing (last digit):
10 9 8 7 6 5 4 3 2 1

PRINTED IN THE UNITED STATES OF AMERICA

Preface

Contributions from various noncovalent, supramolecular interactions are present in both low molecular weight and polymeric organic materials. Even conventional macromolecules, stabilized by mainchain covalent bonds as originally described by Staudinger, display a variety of supramolecular effects that control their intramolecular conformation and their intermolecular interactions. The selection of systems to be included in a book on supramolecular polymers was therefore a delicate task.

In the early stages of planning the book the tentative title *Supramolecular Polymerizations* was adopted. It was thus intended to restrict the content of the book to the new class of self-assembled polymers that undergo reversible growth by the formation of noncovalent bonds. This class (Part II) is wider than expected: not only mainchain assemblies of hydrogen-bonded repeating units, but also planar organization of S-layer proteins, micellar and related three-dimensional structures of block copolymers may be described as a result of supramolecular polymerization.

The title that was ultimately chosen allowed for the inclusion of polymers conforming to the preceding definition and also the new class of supramolecular polymers that may be stabilized by covalent bonds but nevertheless exhibit *novel* supramolecular features. The latter class (Part III) is exemplified by covalent chains based on 2-concatenane units, dendrimers, monolayers, and some engineered assemblies (Part IV).

Included in the book is a general introduction to supramolecular interactions and assembly processes (Part I) along with two theoretical chapters detailing liquid crystalline phases and micellar-like aggregation, two important driving forces in supramolecular polymerization. Expected developments in supramolec-

ular polymer chemistry leading to functional *materials* and *systems* are highlighted in Part V.

The book focuses on the assembly of synthetic polymers and only relatively simple biopolymers are included. Attempts to control the structure and the growth of supramolecular polymers have been largely empirical. It is hoped that the highlighting in this book of the polymers so far investigated—and of the relevant theoretical mechanisms—will guide the organic chemist in designing chemical units that can be assembled into tailored materials and eventually functional systems.

Several applications as functional materials are already considered in the individual chapters. Hierarchical assembling allows the scaling-up to dimensions exceeding the micrometer range in several instances. Supramolecular polymers include dynamic structures endowed with internal mobility and the potential for storing information. Yet, we are still struggling to learn how to couple these characteristics of supramolecular polymers with their possible functioning as micro-engines allowing, for instance, molecular computing or the motility of some biological systems. A typical case is the long known globular↔fibrous (G↔F) transformation of actin. A basic mechanism for the G→F polymerization has been theoretically described. However, the overall functioning of actin as a system involves a coupling of the association process to a chemical reaction and to additional proteins that control polymerization. Understanding and reproducing coupled mechanisms is a road to future development in supramolecular science and functional systems.

The book was not intended to be a collection of unrelated chapters and efforts were made to achieve at least a partly coordinated outlook. This was made possible by the commitment and patience of the authors. Several discussions followed the preliminary draft, and some of the authors participated in meetings to arrive at a consensus over controversial issues. We were saddened by the premature death of Professor Raymond Stadler shortly after he had confirmed his participation in the book. His symbolic presence and enthusiasm are assured by the contributions of two of his coworkers.

Special thanks are due to Ms. Anita Lekhwani, Acquisitions Editor at Marcel Dekker, Inc., who first saw the importance of the emerging field of supramolecular polymers and insisted that the book should be written. The use of facilities at the Chemistry Departments of both Duke University and the University of Genoa greatly helped the editorial task. The book could not have been written without the encouragement and active cooperation of my wife, Cinzia.

Alberto Ciferri

Contents

Contributors

Volker Abetz Makromolekulare Chemie II, Universität Bayreuth, Bayreuth, Germany

Xavier Arys Unité de Physique et de Chimie des Hauts Polymères, Université Catholique de Louvain, Louvain-La-Neuve, Belgium

Alberto Ciferri Department of Chemistry and Industrial Chemistry, University of Genoa, Genoa, Italy

Perry S. Corbin Department of Chemistry, University of Illinois, Urbana, Illinois

Bernd Fodi Max-Planck-Institute for Polymer Research, Mainz, Germany

Avraham Halperin Departement de Recherche Fondamentale sur la Matiere Condensee, UMR 5819 (CEA-CNRS-Université J. Fourier), SI3M, CEA–Grenoble, Grenoble, France

Reinhard Hentschke Department of Physics, Bergische Universität-Gesamthochschule, Wuppertal, Germany

Wilhelm T. S. Huck Department of Chemistry and Chemical Biology, Harvard University, Cambridge, Massachusetts

Alain M. Jonas Unité de Physique et de Chimie des Hauts Polymères, Université Catholique de Louvain, Louvain-La-Neuve, Belgium

Wolfgang Knoll Department of Materials and Surface Science, Max-Planck-Institute for Polymer Research, Mainz, Germany

André Laschewsky Department of Chemistry, Université Catholique de Louvain, Louvain-La-Neuve, Belgium

Roger Legras Unité de Physique et de Chimie des Hauts Polymères, Université Catholique de Louvain, Louvain-La-Neuve, Belgium

Jean-Marie Lehn Université Louis Pasteur, Strasbourg, and Collège de France, Paris, France

Katja Loos Makromolekulare Chemie II, Universität Bayreuth, Bayreuth, Germany

István Majoros Center for Biologic Nanotechnology, University of Michigan, Ann Arbor, Michigan

Sebastián Muñoz-Guerra Departamento d'Enginyeria Química, Universitat Politècnica de Catalunya, Barcelona, Spain

Fumio Oosawa Aichi Institute of Technology, Toyota-Shi, Japan

Dietmar Pum Center for Ultrastructure Research and Ludwig Boltzmann Institute for Molecular Nanotechnology, Universität für Bodenkultur, Wien, Austria

Françisco M. Raymo Department of Chemistry and Biochemistry, University of California, Los Angeles, California

Jürgen Rühe Max-Planck-Institute for Polymer Research, Mainz, Germany

Margit Sára Center for Ultrastructure Research and Ludwig Boltzmann Institute for Molecular Nanotechnology, Universität für Bodenkultur, Wien, Austria

Masatsugu Shimomura Research Institute for Electronic Science, Hokkaido University, Sapporo, Japan

Uwe B. Sleytr Center for Ultrastructure Research and Ludwig Boltzmann Institute for Molecular Nanotechnology, Universität für Bodenkultur, Wien, Austria

J. Fraser Stoddart Department of Chemistry and Biochemistry, University of California, Los Angeles, California

Donald A. Tomalia Center for Biologic Nanotechnology, University of Michigan, Ann Arbor, and Michigan Molecular Institute, Midland, Michigan

George M. Whitesides Department of Chemistry and Chemical Biology, Harvard University, Cambridge, Massachusetts

Lin Yan Discovery Chemistry, Pharmaceutical Research Institute, Bristol-Myers Squibb, Princeton, New Jersey

Steven C. Zimmerman Department of Chemistry, University of Illinois, Urbana, Illinois

9

Dendrimeric Supramolecular and Supra*macro*molecular Assemblies

Donald A. Tomalia
University of Michigan, Ann Arbor, and Michigan Molecular Institute, Midland, Michigan

István Majoros
University of Michigan, Ann Arbor, Michigan

I. INTRODUCTION

> If all scientific knowledge were lost in a cataclysm, what single statement would preserve the most information for the next generations of creatures? How could we best pass on our understanding of the world? [I might propose:] "All things are made of atoms—little particles that move around in perpetual motion, attracting each other when they are a little distance apart, but repelling upon being squeezed into one another." In that one sentence, you will see, there is an enormous amount of information about the world, if just a little imagination and thinking are applied.
>
> Richard P. Feynman [1]

In this simple quotation, Feynman has perhaps described Nature's ultimate example of a minimalist self-assembly. Most certainly this is not a molecular level self-assembly, but nonetheless atoms serve to remind us that self-organization of fundamental subatomic entities occurred to give us the most basic building blocks of the universe [2]. These self-assembly events were consummated some 10–13 billion years ago and marked a unique moment in time from which *first order* was forever derived from chaos. This was the genesis of the long, unrelenting evolutionary journey to more complex forms of natural matter.

The earliest events involved the assembly of subatomic particles into roughly spherical entities reminiscent of core-shell type architecture. First, lighter elements were formed followed by nuclear synthesis leading to the heavier elements. These discrete, quantized core-shell assemblies of electrons and nuclei were so precise, dependable, and indestructible in chemical reactions that they have functioned as the fundamental building blocks of the universe. Within these elements, Nature successfully organized nuclei and electrons to control atomic space at the subpicoscopic level (i.e., $<10^{-12}$ m) as a function of; size (atomic number), shape (bonding directionality), surface stickiness (valency), and flexibility (polarizability). These variables may, thus, be considered *critical atomic design parameters*—CADPs. This new order set the primordial stage for all evolutionary patterns that followed. These patterns seemed to follow the simple principle: "*order begets order from chaos*" [3–6].

The next phase in this evolutionary sequence involved the natural combination of these reactive elements to produce a bewildering array of simple molecular combinations derived from these core-shell atomic spheroids (i.e., NH_3, CH_4, urea, etc.) followed by the formation of more complex, but yet small molecules that included α-amino acids, nucleic acids, sugars, hydrocarbons, etc. Combinations and permutations of specific CADPs at the atomic level articulated molecular level architectures and incipient properties. One path led to *abiotic* molecular evolution (inorganic chemistry); whereas, the other initiated the *biotic* molecular evolution (organic chemistry), and ultimately life as we recognize it today.

The biotic molecular evolution was defined by the respective CADPs of the combined (atoms) required to produce this new molecular level order. It is now known that within this hierarchical level, new sizes, shapes, surface chemistries (functional groups/nonbonding interactions), flexibilities (conformations), and topologies (architectures) arise. These parameters may be visualized by the various shapes, valencies, and polarizabilities associated with the element carbon in its well-known sp, sp^2, or sp^3 hybridized states. We define these unique features as critical *small molecule design parameters*—CSMDPs. Molecular entities in this domain are generally less than 1000 atomic mass units, thus they occupy space of up to approximately 10 Å (1 nm) in diameter, when normalized as spheroids. They may be thought of as subnanoscale in dimension.

A. Suprachemical Categories and Dimensions

The rich patterns of electronegative and electropositive domains found in these small atom and molecule combinations allowed Nature to devise new rules and strategies for advancement to the next higher levels of ordered complexity by nonbonding interactions (suprachemistry) (e.g., *supramolecular*: "higher in organization or more complex than a molecule; often: composed of many molecules)" [7]. These strategies may be roughly categorized into several major types, namely:

Category I—Supra-atomic (Exo-): those assemblies involving small clusters of metal atoms or elements with subnano and nanoscale dimensions (e.g., quantum dots, etc.);

Category II—Supramolecular (Endo-): those assemblies leading to small and medium-sized supramolecular structure. These examples include primary convergent-type binding compounds (i.e., spheroidal guest–host structures, macrocyclic, carcerands, etc.);

Category III—Supramolecular (Exo-): those assemblies involving amphiphilic monomers that lead to medium-large supramolecular structures. These assemblies tend to function as transport entities, barriers, membranes, and container-type structures (i.e., micelles, liposomes, lipid bilayers, etc.); and

Category IV—Supramacromolecular (Exo-): those assemblies leading to precise, three-dimensional (3D) structure-controlled, noncovalently bound macromolecules. These supra*macro*molecular structures are derived from more complex, but precisely controlled macromolecular structures capable of information storage, expression, amplification, and use as functional/structural building blocks (e.g., protein folding, DNA-histone complexes, DNA expression, etc.).

Figure 1 illustrates these suprachemical categories as a function of dimensions. The objective of this account is to examine abiotic examples and parameters related to larger supramolecular and supra*macro*molecular dendritic structures analogous to those found in Categories II, III, and IV.

B. Progress in the Science of Abiotic Synthesis

Whereas Nature has been evolving the complexity of matter over the past 10 to 13 billion years, mankind formally began its journey directed at the "*science of abiotic synthesis*" only approximately 200 years ago. Beginning with Lavoisier's "*atom hypothesis*," Dalton's "*molecular hypothesis*" followed by the initiation of "*organic chemistry*" with Wöhler's work, the progress of manmade synthetic evolution appears to be in its infancy compared to Nature's evolution [10,11].

Based on the various hybridization states of carbon and other elements in the periodic table, small molecule synthesis has led to at least four major architectural patterns. The major architectural classes may be visualized as described in

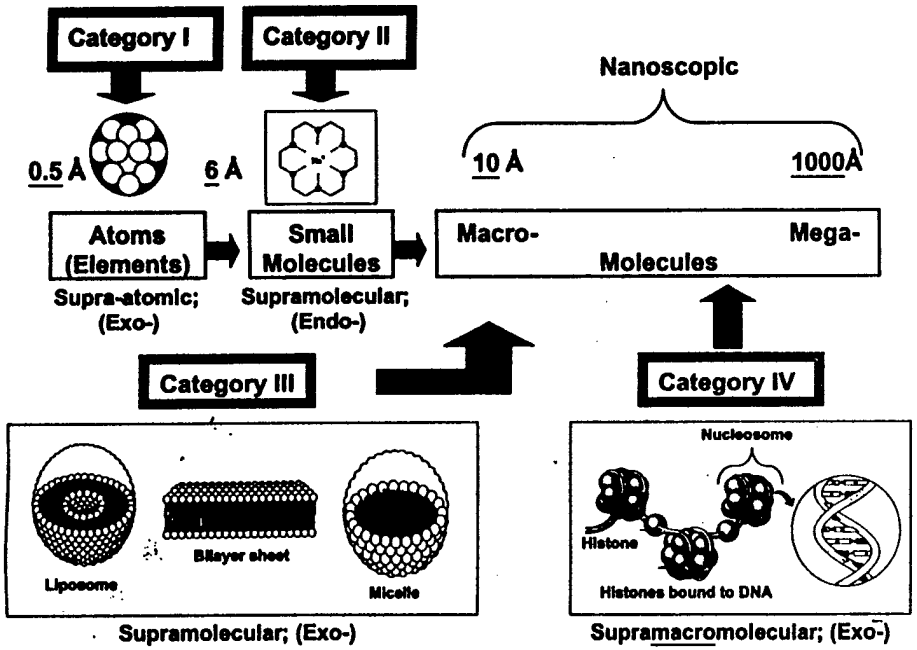

Figure 1 Suprachemistry categories/dimensions.

Fig. 2 and include; (I) Linear, (II) Bridged, (III) Branched, and (IV) Dendritic (cascade) architectures.

C. Progress in the Science of Abiotic Supramolecular Chemistry

> It seemed clear to me now, that the sodium (potassium) ion had fallen into the hole at the center of the molecule. C. J. Pedersen (Aldrichchim. Acta, 4, 1 (1971)).

This simple, but very bold statement made by C. J. Pedersen in the early 1970s literally ushered in the era of supramolecular chemistry based on further elaborations of these basic small molecule architectural classes. J. M. Lehn developed terms to describe two major categories of supramolecular receptors [12]. They are broadly defined as *endo-* and *exo*-receptors. The former present interactive sites that converge on a central locus leading to complexations that are cyclic or

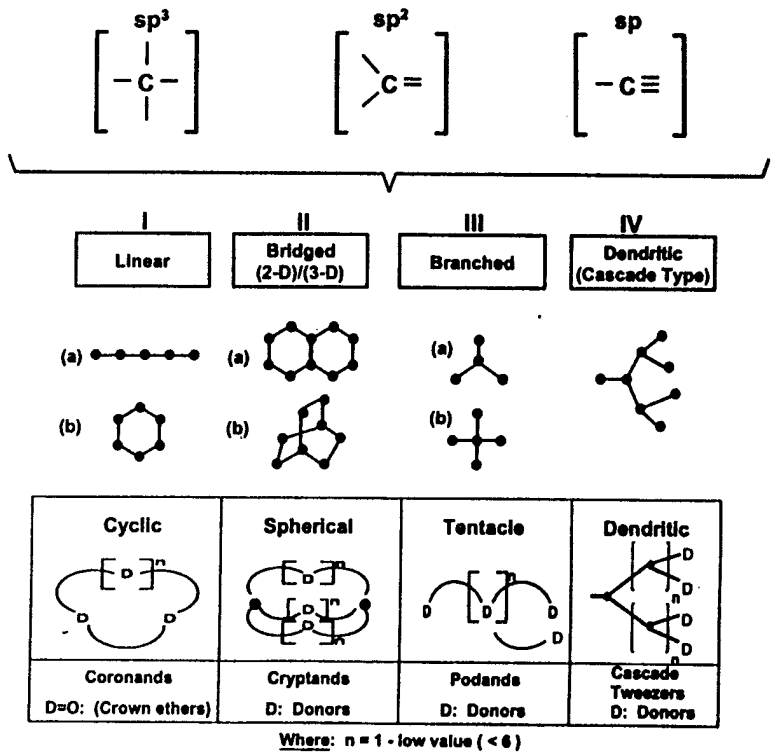

Figure 2 Major small molecule architectures defined as Classes I–IV with comparisons to known donor-type ligands.

severely bent molecules containing holes, clefts, or cavities. These neutral organic ligands are generally referred to as convergent binding molecules. They include small molecule *endo*-receptors such as crown ethers, cryptands, podands, and spherands. This work has been reviewed extensively by many workers [13–19]. *Exo*-complexation typically involves noncyclic molecules containing interactive sites that communicate outwardly. Considerably fewer examples of this type of complexation have been reported.

Recently, however, exciting new reports are appearing that describe the rapid self-assembly of highly ordered linear as well as two- and three-dimensional molecular structure [20]. These strategies usually involve *exo*-recognition among small components to produce tapes [21], squares [22–24], rosettes [25], and other interesting topologies [26–32].

The only topological type in this small molecule area that has not been exploited extensively as a neutral ligand in supramolecular chemistry was the Class IV dendritic (cascade)-type architecture. Vögtle et al. introduced this fourth major small molecule architecture in the late 1970s in a single isolated communication [33]. These low molecular weight dendritic (cascade) molecules served as precursors to macromolecules, which are now recognized as dendrons, dendrimers, and hyperbranched polymers [34,35]. Interest in the supramolecular aspects of dendritic systems has occurred only recently. As described earlier [36], they offer the potential for either *endo* or *exo* complexation and are the focus of this account.

It was only during the past several decades that substantial progress has been made in the use of amphiphilic reagents (monomers) in the construction of nonbonding macro-assemblies. These supramolecular constructs are of the Category II-type and usually lead to entities that are medium to large in dimensions. Amphiphilic reagents used for these constructions are generally derived from Class I (linear) or Class III (branched) small molecule architectures. They include a variety of surfactants, phospholipids, and amphiphilic oligomers as described in Fig. 1. This area has received considerable attention and has been extensively reviewed [37–39].

Many of the reactive linear and branched small molecule reagents were derived during the rich and prolific era of organic chemistry in the 19th century [11]. These developments provided many of the necessary reagents (monomers) upon which H. Staudinger based his work. With these building blocks, Staudinger initiated the synthetic macromolecular evolution some 65 years ago, as he introduced his "macromolecular hypothesis" [40]. This evolution has led to three major macromolecular architectures; namely linear, crosslinked (bridged), and branched types. These architectural classes parallel the major small molecule architectures (Figure 2) and are recognized as traditional polymers [41]. In all cases, these structures/architectures are produced by largely random, uncontrolled polymerization processes. These processes produce polydispersed (i.e., $M_w/M_n > 2–10$) products of many different molecular weights. In general, these are not structure-controlled macromolecular architectures such as one observes in biological systems. However, considerable recent progress has occurred in the areas of living-anionic [42], cationic [43], and radical polymerizations [44,45].

D. Structure-Controlled Macromolecules by Abiotic Synthesis

Structure-controlled abiotic synthesis of macromolecules that mimicked biological polymers was first reported by Merrifield nearly 30 years ago. Abiotic synthesis of poly(peptides) by use of solid phase synthesis was reported as early as 1963 [46]. This synthesis strategy was soon extended to the structure-controlled

synthesis of poly(amides), poly(nucleotides), and poly(saccharides) [47]. Simply stated, the growing chain in all cases is covalently anchored with a cleavable linker to an insoluble substrate. Monomers are sequenced by means of protect/deprotection methods using linear genealogically synthesis schemes [48]. As early as 1979, we discovered simple synthetic strategies that have allowed us to produce structure-controlled macromolecules in ordinary laboratory glassware [49]. These strategies do not require biological components or immobilized substrate reactions. Utilizing traditional organic reagents and monomers such as ethylenediamine and alkyl acrylates, we are now able to routinely synthesize commercial quantities (kilograms) of controlled macromolecular structures with polydispersities of 1.0005–1.10. These new structures are referred to as *dendrons* or *dendrimers*.

Although the mimicry is less elegant and more minimalistic than that found in Nature, these synthetic strategies appear to mimic the four pervasive patterns devised by Nature for the structure control of natural macromolecules such as DNA, RNA, and proteins (Fig. 3).

1. Primary atomic (CADPs) or molecular (CMDPs) information is defined and stored in the initiator core or seed. This information which includes its size, shape, multiplicity (N_c), and chemistry (valency) is presented in an *exo-*

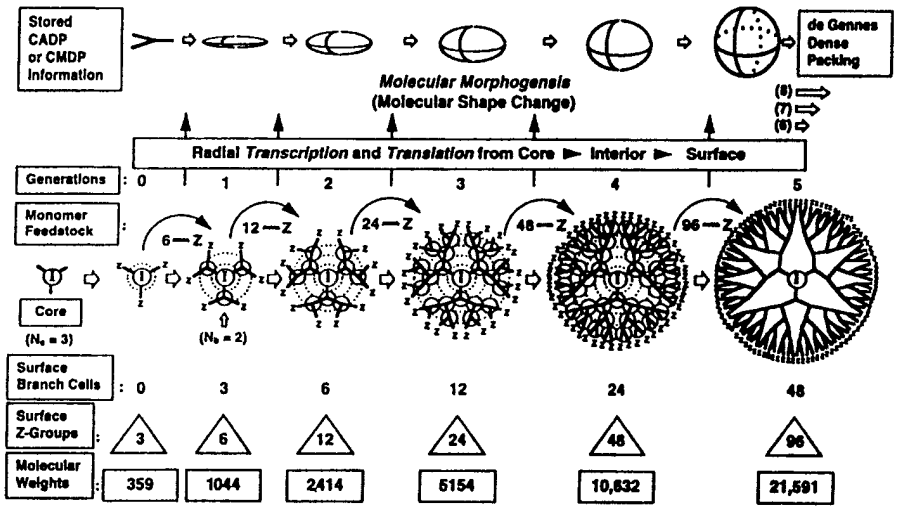

Figure 3 A dendrimer series with core multiplicity ($N_c = 3$) and branch cell multiplicity ($N_c = 2$) illustrating molecular shape changes, surface branch cells, surface Z-groups, and molecular weights as a function of generation.

fashion and communicated to a "template polymerization region," namely, the terminal reactive groups.

2. Appropriate "feedstock monomers" such as acrylates, acrylonitrile, and other organic reagents are defined and adapted to various "template polymerization" schemes. This introduces geometrical amplification at the termini. These amplification values are defined by the multiplicity (N_b) of the branch junctures. Protect/deprotection procedures allow control of complementary chemical reactivities in the template polymerization region. The chemistry is designed to assure high-yield chemical bond formation at each iterative growth stage (generation = G) in an effort to avoid defects or digressions from geometrically ideal branch amplification.

Regioselective control of the template polymerization is obtained by transfer of genetic (i.e., CADP or CMDPs) information through the hierarchy of chemical bond connectivity involved in the dendrimer construction. This includes the following: [initiator core] (*DNA mimic*)—[*transcription*] → [interior branch cells] (*RNA mimic*)—[*translation*] → [surface branch cells] (*ribosome mimic*) → [terminal surface groups (Z)] (*template polymerization region*). In this minimalistic, abiotic core-shell construction, the architectural mimicry of a biological cell is readily apparent by the following comparison: [initiator core] ≡ [biotic cell nucleus], [interior branch cells] ≡ [biotic cell cytoplasm], and [surface branch cells + terminal groups] ≡ [biotic cell membrane].

Self replication of the primary genetic information (i.e., the initiator core) may occur according to a geometrically driven (2^G) amplification process. This specific self-replicating amplification process produces interior branch cells, surface branch cells, and surface functional groups, according to the geometrically progressive values illustrated. These familiar doubling values reflect the well-known (2^G) amplification values associated with biological cell division (mitosis) or DNA amplification (polymerase chain reactions, PCR). For this poly(amidoamine) PAMAM dendrimer family (Fig. 3), initiated from an ammonia core (N_c = 3) with a branch cell multiplicity (N_b = 2), the expected mass values of 359, 1044, 2414, 5154, 10,632 and 21,591 are obtained for generations 0–5, respectively. These values are verified routinely by electrospray or matrix-assisted, laser desorption mass spectroscopy (MALDI) methods. Polydispersity values (M_w/M_n) are obtained ranging from 1.000002–1.005 for this series. Over 50 different dendrimer families possessing compositionally different branch cells (i.e., carbon, nitrogen, silicon, sulfur, phosphorous, metals, etc.) and multiplicity values of N_c = 1–100 and N_b = 2–5 have been synthesized and characterized. Of course there may be some errors or defects (mutations) in these divergent dendrimer constructions just as there are well-known genetic defects and mutations in all biotic genealogically directed processes. This simply adds to the richness of the comparison between these abiotic (cells/organisms) and biotic (cells/organisms).

Biological cells may be thought of as core-shell-like microscale reactors designed to manufacture both structural and functional building blocks (proteins). Similarly, dendrimers may be thought of as nanoscale core-shell models with certain analogies to biological cells. In each case, core-shell characteristics and growth patterns are determined by a central library of information, which flows from the respective cores to the shell-like surfaces [48]. The major differences between the two systems are (a) scaling and (b) the mode of information transfer.

II. THE DENDRITIC STATE

Dendritic architecture has been widely recognized as a fourth major class of macromolecular architecture [50,51]. The signature for such a distinction is the unique repertoire of new properties manifested by this class of polymers. New properties and applications for this polymer class have been reviewed elsewhere [34,52]. Within the realm of macromolecular structure, dendritic architecture may be viewed as an intermediary architectural state that resides between linear (thermoplastic) structures and crosslinked (thermoset) systems [53]. As such, the dendritic state may be visualized as advancement from a lower order to a higher level of structural complexity [54,55]. Furthermore, recent developments in the synthetic control of macromolecular structure now suggest these transitions may involve various levels of structural control. In fact, these transformations may occur via statistical (A), semi-controlled (B), or Controlled (C) pathways. It is widely recognized that dendrons/dendrimers constitute a significant subclass of dendritic polymers and represent a unique combination of very high structural complexity, together with extraordinary structural control. The focus of this account is confined to the dendritic supramolecular and supra*macro*molecular aspects of assembling those entities indicated in the boxed area of Fig. 1. Furthermore, a cursory examination of the supramolecular properties of these dendritic structures is made as they relate to nanotechnology and issues of theoretical interest.

The assembly of reactive monomers [49], branch cells [14,52], or dendrons [56] around atomic or molecular cores to produce dendrimers according to divergent/convergent dendritic branching principles is well demonstrated [57]. Such systematic filling of space around cores with branch cells as a function of generational growth stages (branch cell shells) to give discrete quantized bundles of mass has been shown to be mathematically predictable [58]. Predicted theoretical molecular weights have been confirmed by mass spectroscopy [59,60] and other analytical methods [61]. In all cases their growth and amplification is driven by the general mathematical expressions shown in Fig. 4.

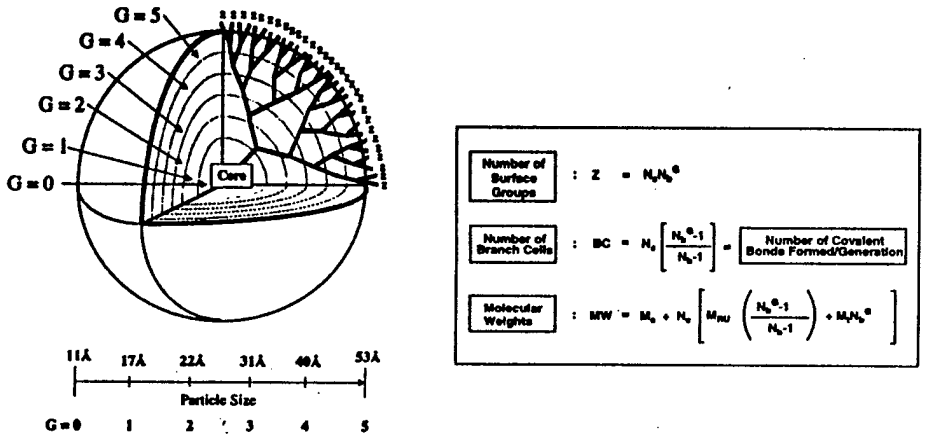

Poly(amidoamine) PAMAM; (NH_3 Core) Dendrimers

Figure 4 Core-shell dendrimer architecture with mathematics defining number of surface-groups (Z), number of branch cells (BC), theoretical molecular weights (MW), dimensions (Å) as a function of generation (G), branch cell multiplicity (N_b), core multiplicity (N_c), and core molecular weight (M_c).

A. A Comparison of Traditional Polymer Science with Dendritic Macromolecular Chemistry

It is appropriate to compare covalent bond formation in traditional polymer chemistry with that in dendritic macromolecular chemistry. This allows one to fully appreciate the implications and differences between the two areas in the context of supramolecular polymerization. Covalent synthesis in traditional polymer science has evolved around the use of reactive modules (AB-type monomers) that can be engaged in multiple covalent bond formation to produce single molecules. Such multiple bond formation is driven either by chain reaction or poly(condensation) schemes. Staudinger first introduced this paradigm in the 1930s by demonstrating that reactive monomers could be used to produce a statistical distribution of one-dimensional molecules with very high molecular weights (i.e., $>10^6$ daltons). These covalent synthesis protocols underpin the science of traditional polymerizations. As many as 10,000 or more covalent bonds can be formed in a single chain reaction of monomers. Although megamolecules with nanoscale dimensions may be attained, relatively little control can be exercised to precisely manage critical molecular design parameters such as: sizes, atom positions, covalent connectivity (i.e., other than linear topologies), or molecular shapes [43,44].

These polymerizations usually involve AB-type monomers based on substituted ethylenes, strained small ring compounds, or AB-type monomers that may undergo polycondensation reactions. The chain reactions may be initiated by free radical, anionic, or cationic initiators. Multiple covalent bonds are formed per chain sequence wherein the average lengths are determined by monomer to initiator ratios. Generally, polydispersed structures are obtained that are statistically controlled. All three classical polymer architectures (namely, Class I—linear, Class II—crosslinked (bridged), and Class III—branched topologies can be prepared by these methods, keeping in mind that simple introduction of covalent bridging bonds between polymer chains (Class I-type) is required to produce Class II crosslinked (thermoset) type systems [53].

In the case of dendron/dendrimer syntheses, one may view those processes leading to those structures as simply sequentially staged (generations), quantized polymerization events. Of course, these events involve the polymerization of AB_2 monomer units around a core to produce arrays of covalently bonded branch cells that may amplify up to the shell saturation limit as a function of generation.

Mathematically, the number of covalent bonds formed per generation (reaction step) in a dendron/dendrimer synthesis varies as a power function of the reaction steps (Fig. 5). This analysis shows that covalent bond amplification occurs in all dendritic strategies. This feature clearly differentiates dendritic processes from covalent bond synthesis found in traditional organic chemistry or polymer chemistry. Polymerization of AB_2 or AB_x monomers leading to hyperbranched systems also adheres approximately to these mathematics, however, in a more statistical fashion.

It is interesting to note that this same mathematical analysis may be used to predict the amplification of DNA by PCR methods or the proliferation of biological cells by mitosis as a function of generation. This comparison is described later.

B. Dendrimer Synthesis Strategies

Beginning in 1979 [35,49,62–67], certain major strategies have evolved for dendrimer synthesis. The first was the divergent method, wherein growth of a dendron (molecular tree) originates from a core site (root) (Fig. 6.) During the 1980s, virtually all dendritic polymers were produced by construction from the root of the molecular tree. This approach involved assembling monomeric modules in a radial, branch-upon-branch motif according to certain dendritic rules and principles [50]. This divergent approach is currently the preferred commercial route used by worldwide producers such as Dendritech (U.S.A), DSM (Netherlands), and Perstorp (Sweden).

A second method which was pioneered by Fréchet et al. in 1989 is referred to as the "convergent growth process" and proceeds in the opposite direction

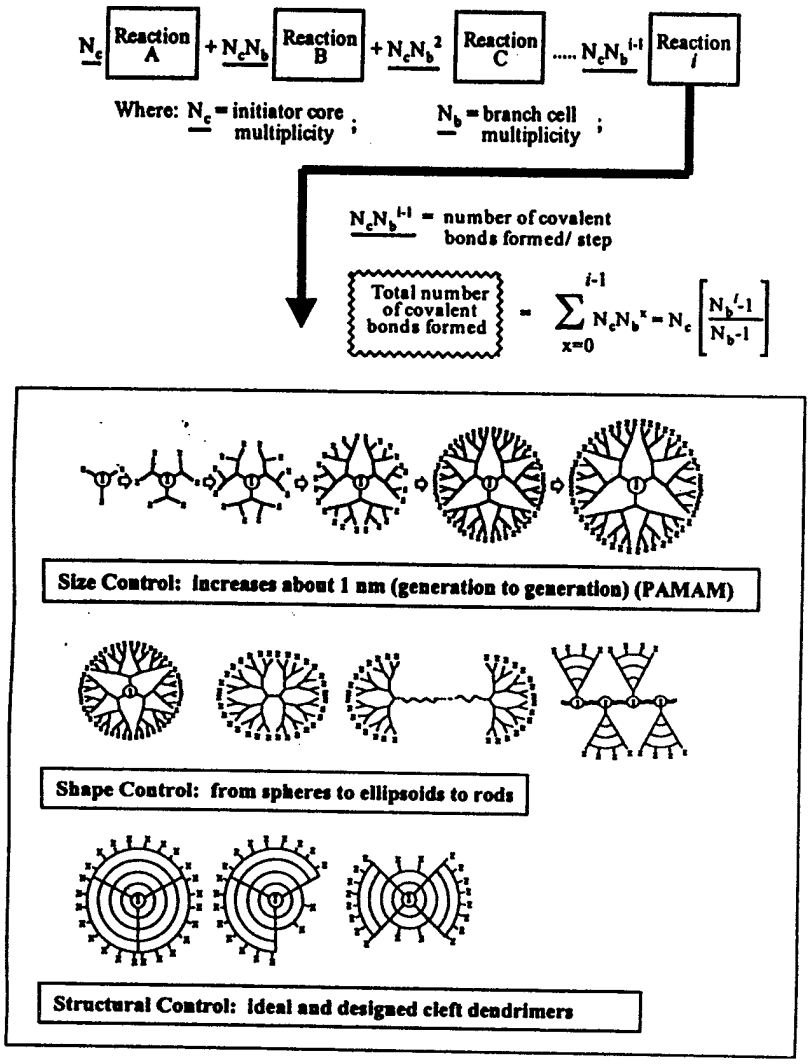

Figure 5 Dendritic macromolecular chemistry.

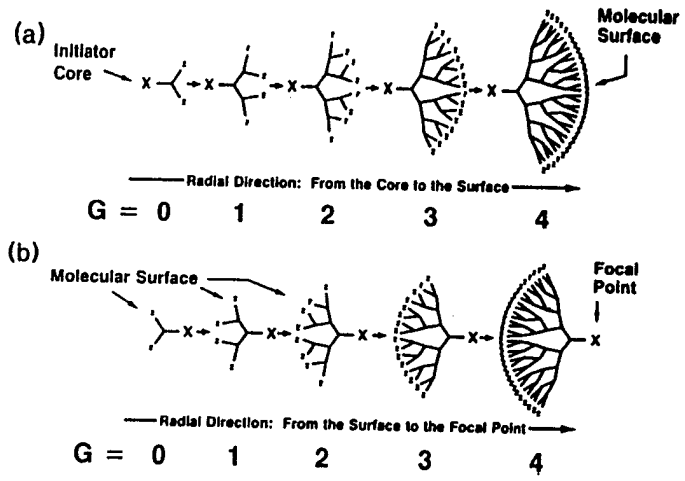

Figure 6 Two principal synthetic methods for building up hyperbranched dendritic macromolecules: (a) divergent and (b) convergent methods.

inward from what will become the dendrimer molecular surface to a focal point (root). In this matter, the latter results in formation of a single dendron, so that in order to obtain a multidendron structure one additional step is required (i.e., an anchoring reaction). In this reaction, several dendrons are connected via a covalently coupling reaction with a multifunctional core to yield the desired dendrimer product. Using these two major synthetic strategies, over 100 compositionally distinct dendrimer families have been synthesized and are reviewed elsewhere [14,35].

C. A Comparison of Divergent Abiotic Synthesis with the Biotic Strategy

Dendrimers may be thought of as nanoscale information processing devices. It is now well recognized that they possess the facility for transcribing and translating their core information into a wide variety of dimensions, shapes, and surfaces by organizing abiotic monomeric/branch cell reagents [48]. Furthermore, these transcription and translational events are accompanied by mathematically defined dendritic amplifications. The syntheses may be thought of as sequence staged, quantized polymerizations orchestrated to the amplification patterns dictated by the core (N_c) and branch cell (N_b) multiplicities. Presently, there appears to be very little limitation to the linear or branched polymerization

units that may be used for these constructions. The limitations are determined primarily by the ability to control regiospecific reactivity of these construction units. Over 100 different types of polymerizable units have been used to make at least that many different compositional dendrimer families. These reactive monomeric reagents are processed by terminal group directed transcription into precisely defined peripheral assemblies. Such assemblies of polymerizable units organized in the terminal group region constitute well-defined shells (generations) [68]. These self-assembled shells are frozen genealogically by covalently fixing (translation of) these organized arrays.

Phenomenologically speaking, these molecular level events are reminiscent of those that occur during biotic protein synthesis. Within biotic cells, the objective is to provide a micron-sized compartment (reactor) for the synthesis and amplification of a requisite population of structural and functional proteins—the building blocks of life. These steps involve the dynamic transfer of information through space within the cell by specific carrier molecules (i.e., RNA, etc.). This journey begins with a supramolecular transfer of information in the nucleus (core) and terminates with a supramolecular-codon transfer of this information at the ribosome sites. These supramolecular events are covalently fixed as linear, genealogically directed sequences catalyzed by polymerases to produce the primary structure of proteins. Similarly, within the nanoscale environs of a dendrimer the information journey begins at the core of the dendrimer. Information such as shape, size, multiplicity, and directionality manifested at the dendrimer nucleus is transferred by means of presumed supramolecular events, followed by covalent bond formation at the terminal groups of the dendrimer construct. These informational parameters are processed by molecular level events that are dauntingly analogous to those that occur in biological cells. It should be apparent that the phenomena of transcription, translation, and amplification of this information has occurred unimolecularly within the space occupied by the dendrimer. Documentation of this information transfer is ultimately frozen and amplified at each generational level (G = 1–5) in the form of dendritic covalent connectivity.

Although these comparisons of information transfer phenomena have been made among vastly different dimensional scales the analogies appear to be remarkably consistent. Biotic cells manufacture precise protein building blocks either for structural or functional purposes. Similarly one may view the parallel products of dendrimeric growth as both structural (i.e., interior branch cells) and functional (i.e., surface branch cells) to the dendrimer. It should be noted that the final dendrimer products possess dimensions [i.e., poly(amidoamine) (PAMAMs)] that scale very closely to many important life-supporting protein building blocks, as illustrated in Fig. 48. However, the subtle shape and regiospecific chemistry control that Nature has mastered has yet to be attained with dendrimer constructs.

D. Supramolecular Aspects of the Classical Divergent Dendrimer Synthesis

1. The "All or Nothing" Observation

The divergent synthesis process has been the objective of much speculation and curiosity. Questions often asked are the following. Does the controlled generational growth of a dendrimer have any supramolecular characterizations? Is it an example of *exo*-molecular recognition and self-assembly, followed by covalent bond formation? The answer at this time is very likely. However, the evidence at this time is indirect and not unequivocal. Undoubtedly, the amphiphilic nature, the complementary shapes of the termini and the reagents, as well as the processing conditions will determine the degree of supramolecular character one might expect in these transformations.

First, the molecular recognition character at the terminal groups is largely determined by the complementary reactivities (communication) between the reagents and these terminal sites. The question remains—is there any evidence for enhanced or catalytic reactivity at these termini, which might suggest preorganization followed by covalent bond formation. The strongest evidence in support of this contention is the so-called "all or nothing reactivity" of dendrimer surfaces which has been observed in our laboratory, as well as Meijer's laboratory (Eindhoven University) with certain amphiphilic reagents. This observation is made routinely when allowing amphiphilic fatty acid chlorides to react with primary amine terminated dendrimers in the presence of an acid acceptor.

When using substoichiometric amounts of a fatty acid chloride in the presence of triethylamine with either amine terminated poly(amidoamine) PAMAM or poly(trimethyleneamine) POPAM-type dendrimers one observes only fully unreacted and fully reacted dendrimer products as illustrated in Fig. 7. This observation may be interpreted as a manifestation of regiospecific self-assembly, fol-

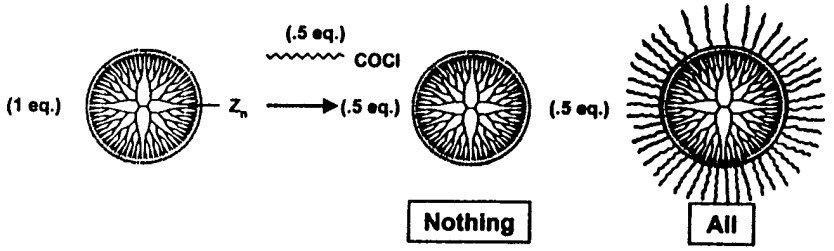

Figure 7 Reaction of substoichiometric amounts of acid chloride reagents with dendrimers to produce the "all or nothing" phenomena.

lowed by covalent amide bond formation, since the reactions are performed under kinetically favored mild conditions (i.e., 25–30°C). Alternatively, one might invoke some unidentified catalytic neighboring group effect. This catalytic effect may favor very rapid complete modification of those dendrimer surfaces that are initially substituted. However, very recent work by Froehling [222] supports the self-assembly hypothesis. When these same reactions were performed with fatty acids under thermodynamically driven (i.e., 130–150°C), azetroping conditions, a statistical distribution of substituents was observed in all cases. This is in complete contrast to the "all or nothing" reaction products, which are invariably obtained under milder, more kinetically driven conditions.

2. Sterically Induced Stoichiometry (SIS)

It was interesting to note that when these authors attempted to amidate higher generation poly(propyleneimine) (PPI) dendrimers under these same conditions, they observed regiospecific positional preference for single substitution at the available amine dyad termini. This observation is in complete agreement with the so-called "sterically induced stoichiometry" (SIS) hypothesis we have proposed previously [36,48,69]. This phenomenon is uniquely related to the size of a proposed surface modification reagent and the tethered congestion conditions that a dendrimer manifests at its surface. This becomes significant especially at higher generations. It was first predicted in 1983 [70], and occurs as a manifestation of de Gennes dense packing. As indicated in this experimental example, these congestion phenomena can affect dendrimer surface substituent patterns and reaction rates. We describe later how this congestion phenomenon literally determines the shell saturation levels for the supramolecular polymerization of dendrimers into core-shell tecto(dendrimers).

3. Dendrimer Structure Ideality—A Signature for Self-Assembly and for de Gennes Dense Packing

Further evidence to support the role of self-assembly in divergent dendrimer synthesis can be found in the construction of poly(amidoamine) PAMAM dendrimers. First, ideality and fidelity of structure is usually a signature of a self-assembly event. This is a universal observation throughout biological systems. In all cases, nearly ideal PAMAM structures are obtained *only* under mild conditions favoring such organizational events as a prerequisite to bond formation [71]. Attempts to impose more severe reaction conditions (i.e., reaction temperature >40°C dramatically reduces the ideality of dendrimer structures even in the early generations. Under mild, kinetically favorable reaction conditions, however, nearly ideal dendrimer structures are obtained up to the onset of de Gennes dense packing. Observation of ideal structure is consistent with amplification predictions based

on core and branch cell multiplicities as well as observed mass defects by mass spectral analysis.

In order to better understand the parameters that cause sterically induced defects in dendrimer synthesis it is appropriate to review the contributing events. First, normal divergent growth occurs precisely as an ideal molecular structure consistent with molecular weights that predictably obey geometrical mathematics, as described earlier. It should be noted that the experimentally determined radius of a dendrimer molecule increases in a linear fashion as a function of generation, whereas the terminal groups amplify according to geometric progression laws. Therefore, ideal dendritic growth cannot extend indefinitely. Such a relationship produces a critical congestion state at some generational level. This creates a significant dilemma at a reacting dendrimer surface as a result of inadequate space to accommodate all of the mathematically required new monomer/branch cell units. This congested generational growth stage is referred to as the de Gennes dense packed state [70]. At this stage, the dendrimer surface has become so crowded with terminal functional groups that it is sterically prohibited from reacting completely to give ideal branching and dendrimer growth. The de Gennes dense packed state is the point in dendritic growth wherein the average free volume available to the reactive surface groups decreases below the molecular volume required for the transition state of the desired reaction to extend ideal branching growth to the next generation. Nevertheless, the onset of the de Gennes dense packed state in divergent synthesis does not preclude further dendritic growth beyond this point; however, it does mean that there will be notable mass defect digressions from ideality.

(a). Dramatic Changes in Dendrimer Container Properties Coincidental with de Gennes Dense Packing. We have previously described the dramatic influence that core multiplicity (N_c) and branch cell multiplicity (N_b) manifested on the onset of de Gennes dense packing [35,36]. As shown in Figs. 8a,b, it can be seen that for ammonia and ethylenediamine (EDA) core PAMAM dendrimers, respectively, nearly ideal molecular weight masses are observed by mass spectroscopy up to generations 5 and 4, respectively. It should be noted, a systematic pattern of mass defects is observed at a critical generation in each case, due to the sterically induced stoichiometry (SIS) induced by the de Gennes dense packing phenomenon [35,36]. For example, in the case of ammonia core ($N_c = 3$; $N_b = 2$) dendrimer mass defects are not observed until generation = 5 (Fig. 8a). At that generation, a gradual digression from theoretical masses occurs for generations =5–8, followed by a substantial break (i.e., $\Delta = 23\%$) between G = 8 and 9. This discontinuity in shell saturation is interpreted as a signature for de Gennes dense packing. It should be noted that shell saturation values continue to decline monotonically beyond this breakpoint down to a value of 35.7% of theoretical saturation at G = 12. A similar mass defect trend is noted for the EDA core,

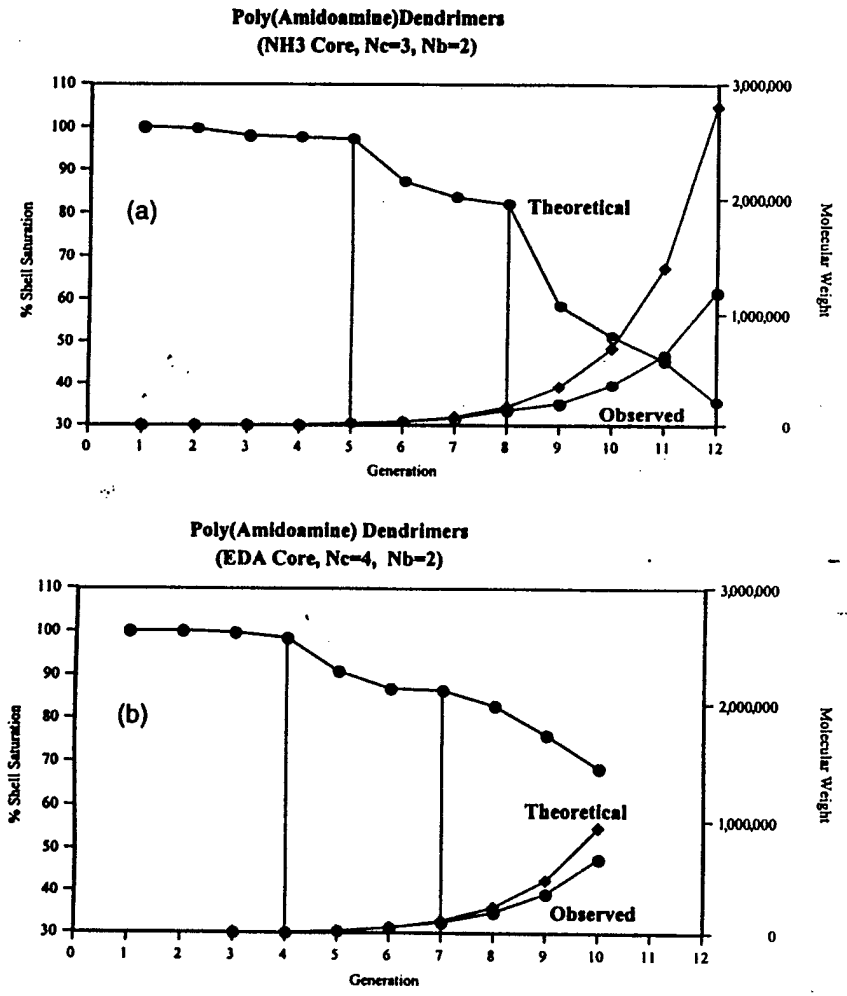

Figure 8 Shell saturation level (%), theoretical molecular weights, and observed molecular weights (mass spectroscopy) as a function of generation for (a) NH_3 core (N_c = 3, N_b = 2) and (b) EDA core (N_c = 4, N_b = 2) poly(amidoamine) PAMAM dendrimers.

PAMAM series (N_c = 4; N_b = 2); however, the shell saturation inflection point occurs at least one generation earlier (i.e., G = 4–7) (Fig. 8b) for the higher multiplicity EDA core. This suggests that the onset of de Gennes dense packing may be occurring between G = 7 and 8. These latter data are completely consistent with metal ion probe experiments [72]. It has been shown that the interior of hydroxyl terminated (EDA core) PAMAM dendrimers G = 1–6 is completely accessible to Cu^{++} hydrate. However, attempts to drive Cu^{++} .6 H_2O (metal ion hydrate) into the interior of G = 7–10 did not occur even under forcing conditions. Subsequent treatment of these respective Cu^{++} as a function of G = 1–10 (chelated) solutions with hydrogen sulfide manifested three different behaviors as a function of generation. Copious precipitates were obtained from Cu^{++}/G = 1–3. In contrast, completely soluble solutions were obtained for Cu^{++}/G = 4–6. Finally, a totally different precipitate was obtained for Cu^{++}/G = 7–10. TEM analysis of the three sets of metal/dendrimer combinations confirmed that G = 4–6 dendrimers had incarcerated copper sulfide and were functioning as *host container* molecules to the copper sulfide guest aggregation. Similar analysis of the last set indicated G = 7–10 were functioning as *surface scaffolding* with virtually no metal incorporation into the interior. This clearly defines a congestion periodicity pattern, as illustrated in Fig. 9, and reveals a unique pattern of dendrimer/metal ion relationships as a consequence of generational surface congestion. Obviously, these metal ion probe experiments are consistent with and support the mass spectral de Gennes dense packing signature hypothesis.

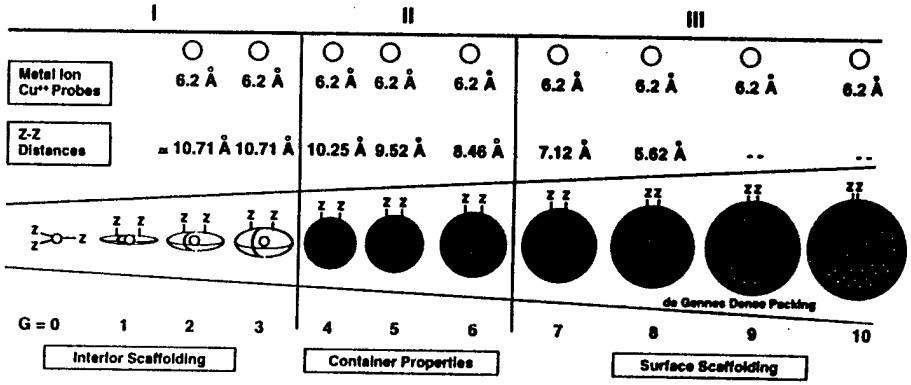

Figure 9 Periodic congestion patterns for a PAMAM EDA core (N_c = 4, N_b = 2) dendrimer series (G = 0–10) defining (I) interior scaffolding, (II) container-like properties, and (III) surface scaffolding properties when combined with an aqueous Cu^{+2} probe.

In summary, it is readily apparent that these abiotic, amplified genealogically directed polymerizations of AB_2 monomers have many things in common with biological systems. For example, certain biological processes, such as polymerase chain reactions PCR [73] or cell mitosis [8,9] may be thought of as analogous examples of amplification, but at much larger dimensional scales than are found in dendrimers. Most importantly, branch cell amplification and DNA amplification may be viewed as special examples of supramolecular directed polymerization leading in each case to very highly controlled macromolecular structures.

E. Strategies for the Supramolecular Assembly of Components to Produce Dendrimers

One of the major themes in biological systems is the noncovalent assembly of large structures from smaller components. Self-assembly is usually rapid, requires minimized energy for synthesis, and guarantees reproducible construction of complex products with high fidelity [8,9]. The presumed supramolecular construction of dendrimers from its constitutional components provides prime examples of abiotic supramolecular polymerizations to give well-defined structures with notable complexity. More recent developments in this area may be broadly categorized into those involving the supramolecular assembly of dendron components and those involving the assembly of subdendron units or branch cells.

1. Supramolecular Assembly of Dendrimers Based on Focal Point Functionalized Dendrons

This construction strategy evolved from the pioneering work of Zimmerman et al. reported in 1996 [74]. Their approach involved the hydrogen bond directed aggregation of Fréchet-type dendrons, which were terminated with two isophthalic diacid moieties at their focal point. In appropriate solvents, these assemblies were stable enough to be characterized by size exclusion chromotoraphy (SEC), laser light scattering (LLS), and vapor pressure osmometry (VPO). Dendrons as high as generation = 4 could be self-assembled by this process (Fig. 10).

Fréchet and coworkers [221] have recently described a similar self-assembly of benzyl ether dendrons, possessing carboxylic acid substituents at their focal points by metal–ligand coordination around a core of trivalent lanthanide metals (e.g., Er, Eu, or Tb). These self-assembled dendrimers were isolated by using ligand exchange reactions to produce structures derived from metal–ligand ionic interactions as shown in Fig. 11. As a consequence, these self-assembled dendrons served as a dendritic shell, which shielded the lanthanide atoms from one

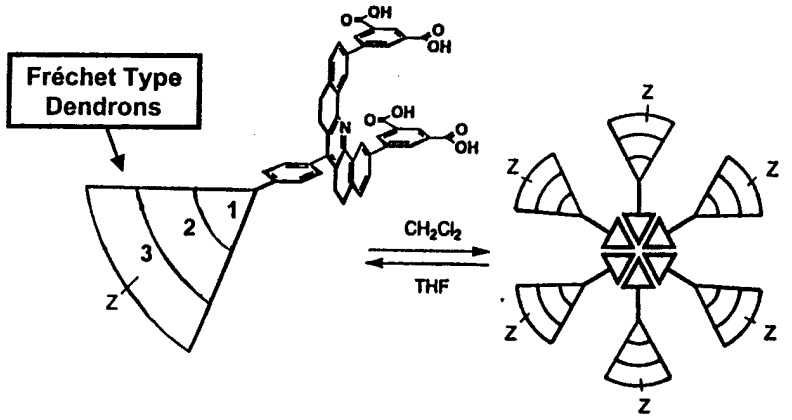

Figure 10 The self-assembly of a hexameric aggregate of wedgelike dendrons that are functionalized at their focal points by two isophthalic acid moieties. (From OA Matthews, Prog Polym Sci, 28, 1998. With permission from Elsevier Science.)

another. It was significant to note that these dendritic structures produced a substantial decrease in the rate of self-quenching (an energy transfer process) between metal atoms. This effect has been referred to as a *site isolation phenomenon.* The importance of this effect was clearly demonstrated as one progressed from lower to higher generations, wherein, the dendrimers exhibited vastly enhanced luminescence activity over the lower generation dendrimers.

2. Supramolecular Assembly of Dendrimers Based on the Assembly of Branch Cells

Numerous examples have been reported describing the use of hydrogen bonding between complementary groups to induce self-assembly [56,75]. Another approach is to use metal-induced coordination chemistry as the driving force in the assembly process. Metal-based coordination-driven methodology allows the rapid facile formation of discrete structures with well-defined shapes and sizes. Metal–ligand dative bonds are stronger than hydrogen bonds and have more directionality than other weak interactions such as π–π stacking, electrostatic hydrophobic/hydrophilic interactions, and even hydrogen bonding. One metal–ligand interaction can therefore replace several hydrogen bonds in the construction of supramolecular species. Perhaps the earliest work reported in this area was that described by Balzani et al. [76–82]. Referred to by Balzani as the "complexes as ligands and complexes as metals" strategy, the synthesis involved the divergent assembly of dendrimer structures as described in Fig. 12.

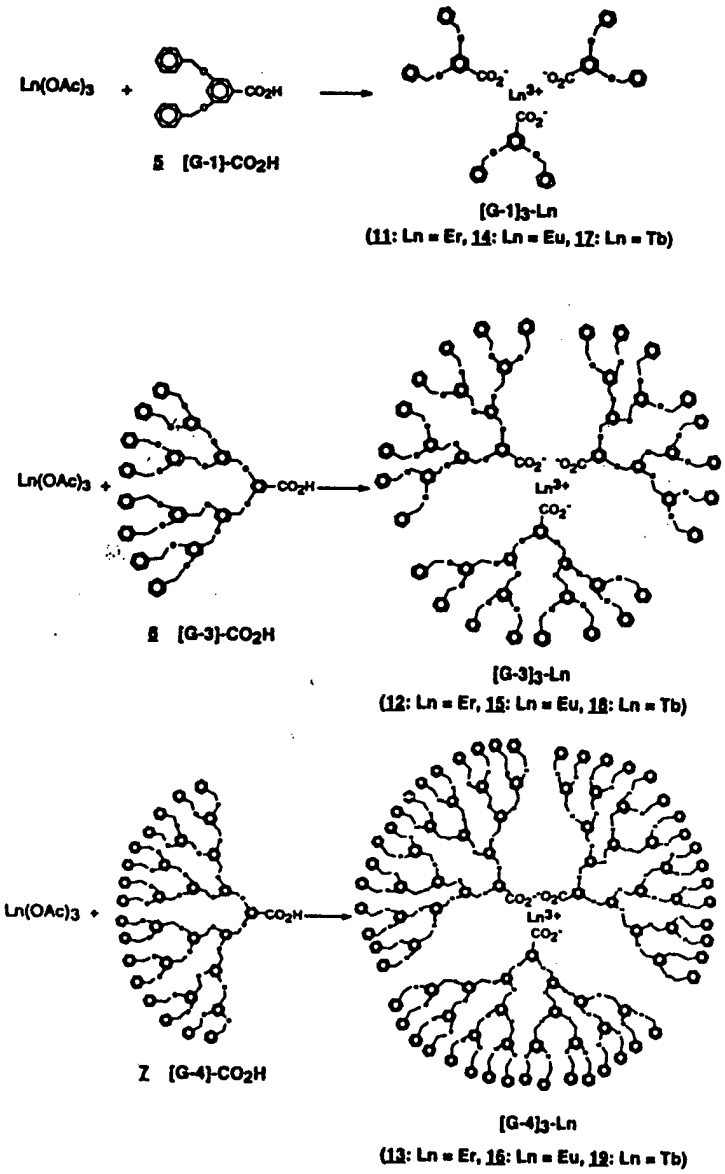

Figure 11 Self-assembly of focal point functionalized dendrons around metal cations according to Fréchet et al. (JMJ Fréchet et al. Chem Mater 10:287, 1998. Copyright 1998 American Chemical Society.)

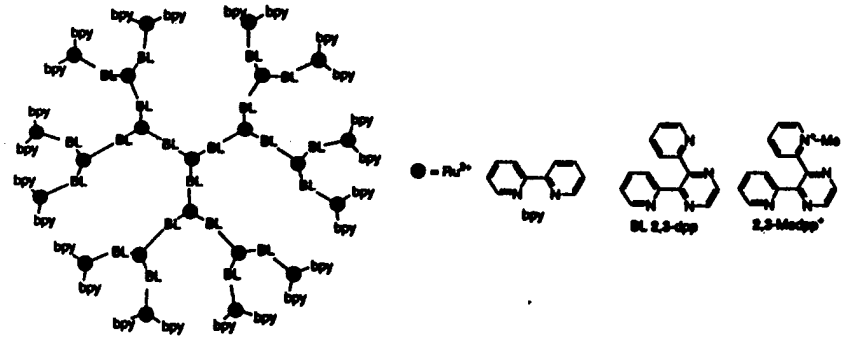

Figure 12 Dendritic ruthenium complex reported by Balzani and coworkers. (Courtesy Chem Rev 97:1706, 1997. Copyright 1997 American Chemical Society.)

In a similar fashion, Puddephatt and coworkers [83–85] described the use of platinum coordination chemistry involving a convergent strategy. By this method, they reported the synthesis of a generation = 4 dendrimer containing up to 28 coordination centers.

Perhaps the only true, reversible coordination, self-assembly for the synthesis of dendritic systems is that described in a series of papers by Reinhoudt and coworkers. They first reported the reversible assembly of hyperbranched spheres from palladium-substituted compounds by replacing a labile, coordinating nitrile ligand with a kinetically stable moiety located on an AB_2 monomer [86,87]. Subsequently, they used a combination of hydrogen bonding and noncovalent coordination chemistry to construct a unique rosette-type structure [88]. More recently, this group reported related chemistry that allows either a divergent or convergent approach [88] to dendrimer synthesis [89,90]. This strategy involves first the synthesis of three basic building units as described in Fig. 13. The controlled divergent assembly requires first the core unit containing three Pd—Cl pincer complexes, which are activated by removing chloride ion with $AgBF_4$. Subsequent addition of three equivalents of nitrile containing building block 2 yields a first generation metallo(dendrimer) possessing nitrile ligands coordinated to the palladium centers. Using this concept, they were able to synthesize metallodendrimers up to generation 5 [87]. They also described [90] the synthesis of building unit 3 with pyridine instead of nitrile ligand and were able to use this intermediate for the preparation of more stable metallodendrimers, due to the stronger coordination of pyridine ligands to the palladium centers.

The convergent route (Fig. 13c) begins with the synthesis of dendrons using building block 2 as a carrier unit and building block 3 as a building unit. The three dendrons were coupled to a trifunctional core 1 to form the dendrimer structure. Figure 13c illustrates a dendron (DG_2 and DG_3) constructed via controlled

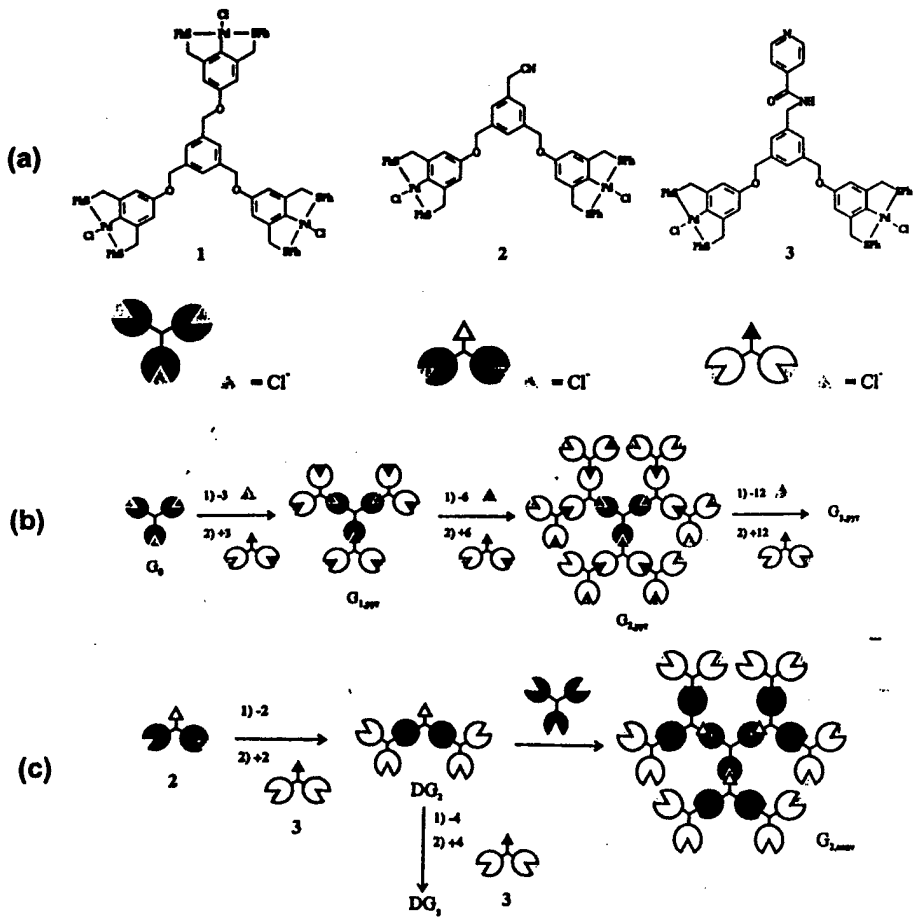

Figure 13 Self-assembly of Pd contained metallodendrimers using (a) building blocks 1–3 (b) divergent method, and (c) convergent method according to Reinhoudt et al. (Courtesy J Am Chem Soc 120:6242; 6243, 1998. Copyright 1998 American Chemical Society.)

convergent assembly. Activation of 2 with $AgBF_4$ and subsequent addition of two equivalents of 3 gave DG_2 after coordination of the pyridine ligands. Reiterating these steps led to higher generation metallodendrons. Evidence for the formation of all of these metallodendrimers was obtained by IR, H^1 NMR, ESMS, and MALDI-TOF mass spectrometry.

III. SUPRAMOLECULAR AND SUPRA*MACRO*MOLECULAR CHEMISTRY OF DENDRIMERS

In the very first papers published [62–67] it was apparent from electron microscopy data presented that dendritic architecture would offer rich possibilities in the area of supramolecular chemistry. It was virtually impossible to observe individual dendrimer modules due to their great propensity to form clusters or aggregates even when sampled from very dilute solutions. Similar observations were made by Newkome, as he published his early work on the related arborols [91]. In contrast, samples from more concentrated solutions displayed breathtaking dendritic arrays of microcrystallites upon drying [62,63]. Recent work by Amis et al. [92] using cryo-TEM and other methods has shown that dendrimers exhibit a great propensity to self-organize even in solution.

In the same early publications [62–67], the reported observation that copper sulfate could be solubilized in organic solvents with ester terminated PAMAM dendrimers to produce deep blue transparent chloroform solutions offered very early evidence for the unique *endo*-receptor (i.e., unimolecular inverse micellar) properties of these macromolecules. These properties are discussed in the following section.

A. The Dualistic Role of Dendrimers as Either *Endo*- or *Exo* Receptors

The field of dendritic supramolecular chemistry is young. As recently as three years ago fewer than a half dozen papers could be found on the subject [93]. Since that time, this field has expanded dramatically. As early as 1990, we commented extensively on the dualistic property of dendrimers [36]. At that time, it was noted that dendrimers could function as unimolecular *endo*-receptor-type ligands manifesting noncovalent chemistry reminiscent of traditional regular or inverse micelles or liposomes. Furthermore, it was noted that dendrimers also exhibited a very high propensity to cluster or complex in an *exo*-fashion with a wide variety of biological polymers (i.e., DNA proteins) or metals. In the following sections, we describe nonexhaustive samplings of recent work illustrating the supramolecular and supra*macro*molecular behavior of dendrimers that connects them to all three categories of suprachemical types observed in biological systems (Fig. 1).

B. Dendrimers as Unimolecular Nanoscale Cells or Container Molecules

1. Evolution of Abiotic Container Molecules—From Carcerands/Carceplexes to Dendrimers/Dendriplexes

The abiotic evolution of "container-type" molecules may be traced from the original synthesis of cubane [94], pentaprismane [95], and dodecahedrane [96].

These platonic solids are all closed surface compounds; however, their interiors are too small to host organic or inorganic compounds. It was not until 1983 that Cram et al. [97] reported a container-like hydrocarbon referred to as carcerand that was large enough to host simple organic compounds, inorganic ions, or gases [97]. This discovery has led to a vast array of small container-type molecules, which have been extensively reviewed [98]. Quite remarkably, this was approximately the same time that ester terminated PAMAM dendrimers were noted to dissolve and incarcerate copper salts to produce "blue chloroform" solutions due to their unimolecular, inverse micelle properties. This observation was publicly reported in 1984–1985 [62,63], during the same year that Smalley, Curl, and Kroto et al. described the first synthesis of buckminsterfullerene [99]. Of course, it is well known that "bucky balls" will host a variety of metals. Thus, it is apparent that the emergence of container molecules has followed the systematic enhancement of the organic host structure dimensions as illustrated in Fig. 14.

(a). Incarceration of Zero Valent Metals and Metal Compounds. Very recently, a novel and versatile method has been reported for the construction of stable, zero-valent metal quantum dots, using dendrimers as well-defined nanotemplate/containers. The concept involves the use of dendrimers as hosts to pre-organize small molecules or metal ions, followed by a simple in situ reaction that immobilizes and incarcerates these nanodomains (Fig. 15) [72,100]. The size, shape, size distribution, and surface functionality of the dendritic nanocomposites are determined and controlled by the architecture. Dendrimer-based nanocomposites display unique physical/chemical properties as a consequence of the atomic/molecular level interactions between the guest and host components within the dendrimer as well as the dendrimer interaction with various solvents and media.

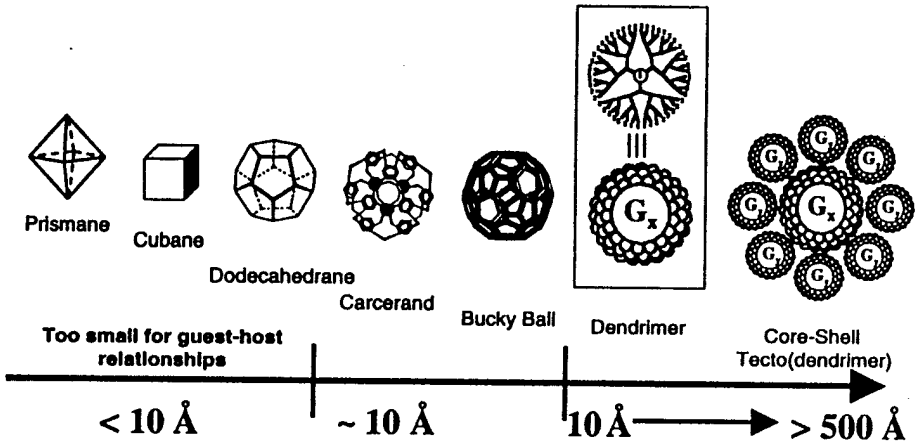

Figure 14 Evolution of abiotic container molecules as a function of dimensions and complexity.

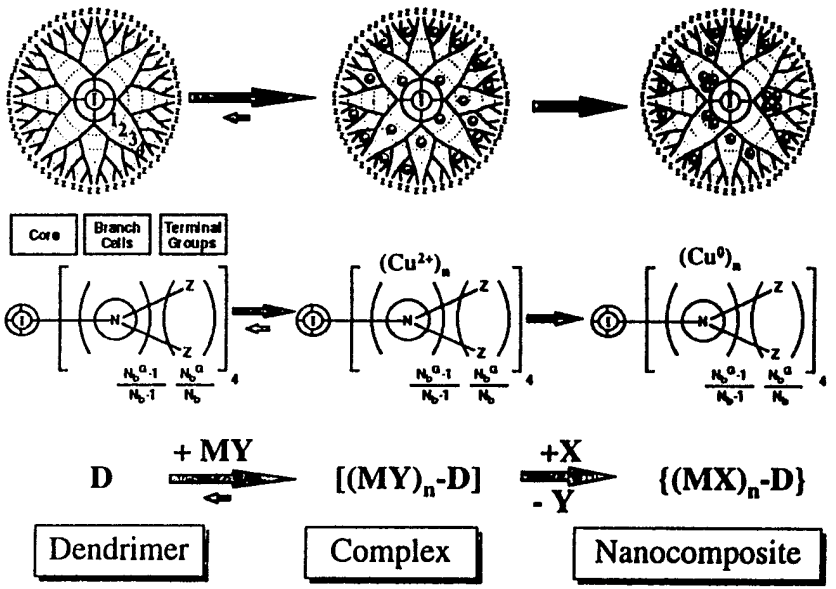

Figure 15 Construction of dendrimer nanocomposites by reactive encapsulation. Y (Cu^{+2}) denotes ligands after complex formation. X (Cu^0) represents zero valent metal incarcerated within the dendrimer interior after reduction. (Courtesy J Am Chem Soc 120:7355, 1998. Copyright American Chemical Society.)

Preparation of stable, zero valent metallic copper solutions were demonstrated in either water or methanol [72]. After complexation within various surface modified poly(amidoamine)(PAMAM) dendrimers, copper(II) ions were reduced to zero valent metallic copper thus providing a bronze, transparent dendrimer–metal nanocomposite soluble in water. Solubility of the metal domains is determined by the surface properties of the dendrimer host molecules; however, their solutions still display characteristic optical properties associated with metal domains. Both aqueous and methanolic solutions of copper clusters were stable for several months in the absence of oxygen. Similar work and results were also reported by Crooks et al. [101].

More recent work describing SAN characterization of copper sulfide PAMAM dendrimer nanocomposites [102] and extensions to silver and gold-

based dendrimer nanocomposites have been reported [103]. This latter work confirms and demonstrates the periodic container properties described in Fig. 9.

(b). Incarceration of Organic Compounds, Unimolecular Encapsulation, the Dendritic Box. In another elegant study, Meijer and coworkers [104,105] skillfully enhanced an earlier concept for producing artificial cells by modifying dendrimer surfaces to induce "unimolecular encapsulation" behavior [36]. They referred to this new construction as the "dendrimer box." Surface-modifying generation = 5, poly(propylene imine) (PPI) dendrimers [104] with 1-phenylalanine or other amino acids [106] induced dendrimer encapsulation by forming dense, hydrogen-bonded surface shells with almost solid-state character. Small guest molecules were captured in such dendrimer interiors and were unable to escape even after extensive dialysis [105]. The maximum number of entrapped guest molecules per dendrimer box was directly related to the shape and size of the guests, as well as to the number, shape, and size of the available internal dendrimer cavities. For example, 4 large guest molecules (e.g., Bengal Rose, Rhodamide B, or New Coccine) and 8–10 small guest molecules (e.g., p-nitrobenzoic acid, nitrophenol, etc.) could be simultaneously encapsulated within these PPI dendrimers containing 4 large and 12 smaller cavities (Fig. 16). Quite remarkably, this dendrimer box could also be opened to release either all or only some of the entrapped guest molecules [105]. For example, partial hydrolysis of the hydrogen-bonded shell liberated only small guest molecules, whereas total hydrolysis (with 12N HCl; 2 h at reflux) released all sizes of entrapped molecules.

2. Mimicry of Classical Regular Micelles

Based on qualitative evidence, Newkome et al. first hypothesized the analogy between dendrimers and regular micelles in 1985 [91]. Simultaneously, Tomalia

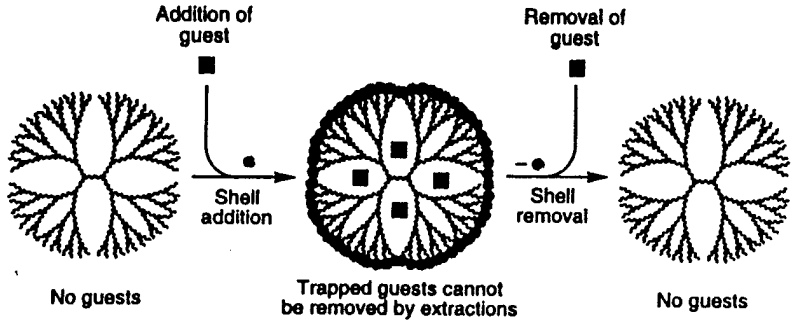

Figure 16 Principle of the dendritic box. (From OA Matthews, Prog Polym Sci, 28, 1998. With permission from Elsevier Science.)

et al. reported the direct observation of sodium carboxylated PAMAM dendrimers by electron microscopy in 1985 [62–67] and 1986 [107] which experimentally supported the fact that dendrimers clearly possessed topologies reminiscent of regular classical micelles. At that time, it was also noted from electron micrographs that a very high population of individual dendrimers possessed hollowness presumably due to the peripheral stacking association of terminal head-groups. This was experimentally confirmed [108] by noting the importance of branch cell symmetry as a requisite for interior void space. Such interior hollowness is observed in essentially all symmetrically branched dendrimers, but does not appear to exist in asymmetrically branched dendrimers such as those described by Denkewalter et al. [109–110]. Furthermore, experimentally determined hydrodynamic dimensions [108], shape confirmations, and comparisons of dendrimer termini (surface areas) as a function of generation with traditional micelle head-groups added further support to this hypothesis in 1985 to 1987 [107,108,113]. This unique dualist property of micelle topology and interior void space normally associated with liposomes was noted by Tomalia et al. in 1989 [114]. Subsequent nmr studies and computer-assisted simulations by Goddard et al. in 1989 [115], molecular inclusion work by Newkome et al. [116] in 1991, as well as extensive photochemical probe experiments by Turro et al. [117–120], have now unequivocally demonstrated the fact that symmetrically branched dendrimers may be viewed as unimolecular cells (nanoscale container molecules). Depending on the nature of their surface groups and interiors these dendrimers will manifest behavior reminiscent of either traditional regular or inverse micelles, however, with unique differences and advantages.

3. Mimicry of Classical Inverse Micelles

The first examples and observed dendritic inverse micelle properties were noted in the initial papers on poly(amidoamine) dendrimers published in 1984 to 1985 [62–67]. At that time, it was observed that methylene chloride or chloroform solutions of the methyl/alkyl ester modified dendrimers readily extracted copper ion (Cu^{+2}) from water into the organic phase. Beautiful "blue chloroform" solutions were obtained that were completely transparent and did not scatter light. It was assumed that the copper ions had been chelated into the interior and were being compatibilized by the more hydrophobic sheathing of the dendrimer surface groups. Variations of this work were both patented [121] and ultimately published [122], wherein PAMAM dendrimers were hydrophobically modified with alkyl epoxides and used to extract metal ions into toluene, styrene monomer, or a variety of other hydrophobic solvents.

Meanwhile, other examples of unimolecular dendritic, inverse micelles have been reported by Meijer et al. [123] and DeSimone et al. [124]. In the latter case, surface perfluorinated *dendri*-PPI dendrimers were used that have a high

affinity for liquid CO_2. Thus, the hydrophilic dendrimer core provides a favorable environment for hydrophilic guests such as ionic methyl orange. Thus while the $-CO_2$-philic dendrimer shell allows the micelle to dissolve in CO_2, the ionic dye can be effectively transferred from a water layer into liquid CO_2.

C. Dendrimers as Nanoscale Amphiphiles

1. Dendritic Architectural and Compositional Copolymers

Perhaps one of the most elegant and complex examples of an *architectural copolymer* [125] that was constructed by both self-assembly and covalent synthesis is that reported by Stoddart et al. [126,127]. Stoddart and coworkers prepared a series of rotaxanes with dendritic stoppers using a "threading approach" (Fig. 17). Within this single rotaxane structure possessing dendritic stoppers one finds all three architectural types are represented. Although no amphiphilic properties were reported for this system, it has been shown that both compositional as well as architectural dendritic copolymers do manifest interesting amphiphilic properties leading to self-assembly processes.

It is very well known that the general area of traditional amphiphilic structure-property relationships can be broadly divided into two major types, namely, small molecule surfactants and amphiphilic block copolymers (see Chapter 3). Each of these classes has been the subject of extensive studies [37,128–131]. A detailed examination of the influence that increasing head/tail sizes and shapes have on the nature of aggregation has been limited to traditional structures. Such structures have included only low molecular weight surfactants, possessing

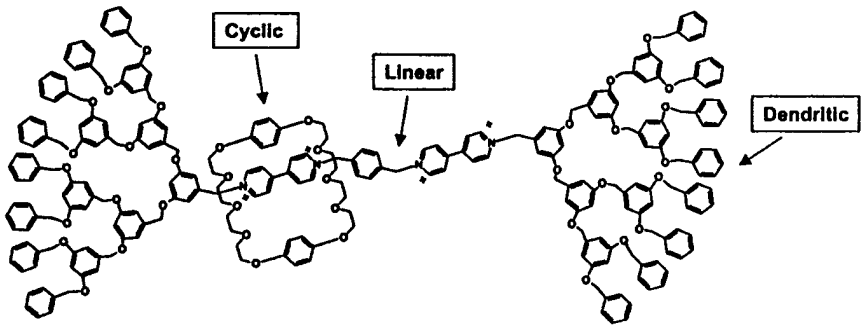

Figure 17 A rotaxane with dendritic stoppers. An example of a dendritic-linear-cyclic architectural copolymer. (Courtesy Chem Rev 1701, 1997. Copyright 1997 American Chemical Society.)

compact polar head-groups/tail, or classical linear, block copolymers (see Chapter 3).

With the advent of dendritic synthesis, the precise construction of nanoscale sizes and shapes has allowed the synthesis of new larger dimensioned amphiphilic structures. Perhaps the first well-documented example of dendrimers exhibiting *exo*-receptor, supramolecular behavior was that reported by Friberg et al. in 1988 [132]. It is well known that one may evolve a rich variety of lyotropic mesophases by merely coordinating the relative sizes of the amphiphilic components of a system (i.e., hydrophobic head-groups versus hydrophobic tail). This was accomplished by combining a G = 2, poly(ethyleneimine) (PEI) dendrimer (hydrophilic head-group) with octanoic acid (hydrophobic tail) to give a lamellar liquid-crystalline assembly. In effect, a nanoscale amphiphile was constructed in situ by the acid–amine reaction between octanoic acid and G = 2 *dendri*-PEI—$(NH)_{12}$ to produce an amphiphilic salt.

Additional examples of dendritic-type surfactants were reported in the early patent literature as hydrophobic core functionalized PAMAM dendrons [35,133]. For example, when the core was a 12 carbon chain, the first two generation PAMAM dendrons exhibited hydrocarbon solubility (TMF). However, beyond generation two, the amphiphilic dendrons were water-soluble. This demonstrates the effect one observes as the hydrophilic head-group is amplified through the HLB crossover point. The result is a dendron possessing a dominant hydrophilic head-group, which undoubtedly engulfs the tethered hydrocarbon core in aqueous medium. Many of these products were useful as amphiphilic reagents to produce novel Starburst® dendrimer-type micelles [133]. Among the many interesting properties exhibited by these micelles was the ability to sequester hardness ions (i.e., Mg^{+2}, Ca^{+2}, etc.) thus manifesting self-building surfactant properties within unimolecular structures.

Later extensions of this general concept were reported by Chapman, et al. [134] and Fréchet [52] wherein they reversed the amphiphilic components to produce a functionalized dendron possessing a hydrophobic head and a hydrophilic tail. The Chapman dendritic amphiphiles were derived from alkylene oxide tails and BOC terminated, Denkewalter-type dendritic heads. The Fréchet amphiphiles were obtained by attaching poly(ethylene oxide) to the focal point of a hydrophobic poly(ether) dendron as illustrated in Fig. 18 [135,136].

Nearly simultaneously, Fréchet et al. pioneered [52] the synthesis and development of a new type of amphiphilic dendrimer wherein the unimolecular architecture was differentiated. In these instances, Fréchet demonstrated that his poly(ether) dendrimers derived via convergent synthesis could be either homogeneously terminated or differentiated into hydrophobic and hydrophilic hemispheres, as illustrated in Fig. 19. These dendrimers could be oriented at an interface, as illustrated, or under the influence of an external stimulus. Indeed amphiphilic dendrimers form monolayers at the air–water interface and such den-

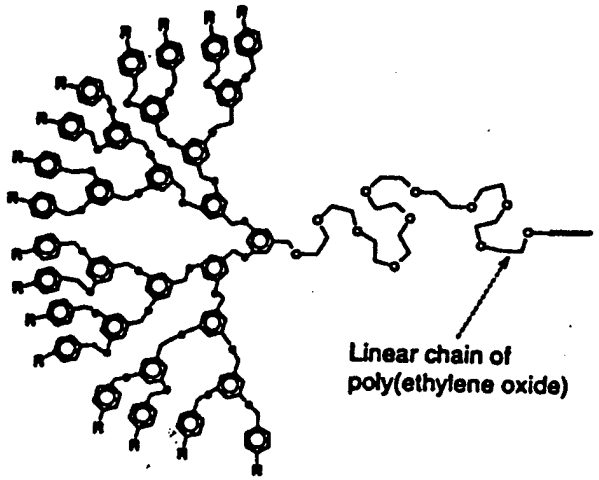

Figure 18 Hybrid dendritic linear polymer obtained by attaching poly(ethylene oxide) to the focal point of structure G-4.

drimers [137] are useful in forming interfacial liquid membranes or in stabilizing aqueous–organic emulsions. A dendrimer constructed from two segregated types of chain ends (i.e., half electron dominating and half electron withdrawing) can be oriented in an electrical field and has been shown to exhibit very large dipole moments [138].

One of the most comprehensive examinations of dendritic nanoscale amphiphiles involved structures that mimicked traditional surfactants. This work was reported in a thesis by van Hest and Meijer [93]. In this study, extensive hydrophobic tails were precisely constructed by the living anionic polymerization of styrene, followed by termination with a primary amine function. Dendronization of these amine functionalized poly(styrenes) produced focal point functionalized, hydrophobically substituted PPI dendrons, as illustrated in Fig. 20. More specifically, the living polystyrene anion is terminated with ethyleneoxide, thus providing a hydroxyl terminated poly(styrene) with molecular weights between 3000 and 5000 and a polydispersity <1.05. In a phase-transfer reaction the addition of acrylonitrile to the alcohol, followed by a (Raney Co/H_2) hydrogenation yields the primary amine terminated poly(styrene). Subsequent dendrimer construction is performed by the sequential Michael addition of acrylonitrile and heterogeneously catalyzed hydrogenation to form a variety of super amphiphiles with different sized nanoscale head-groups.

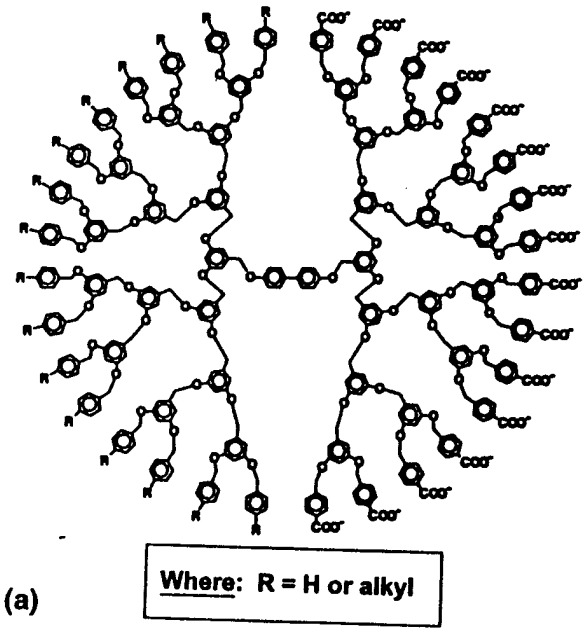

Figure 19 (a) Amphiphilic dendrimer obtained by hemispherical functionalization of half the terminal groups with carboxylic anions; (b) liquid membrane of amphiphilic dendrimer at the interface between water and an immiscible organic solvent.

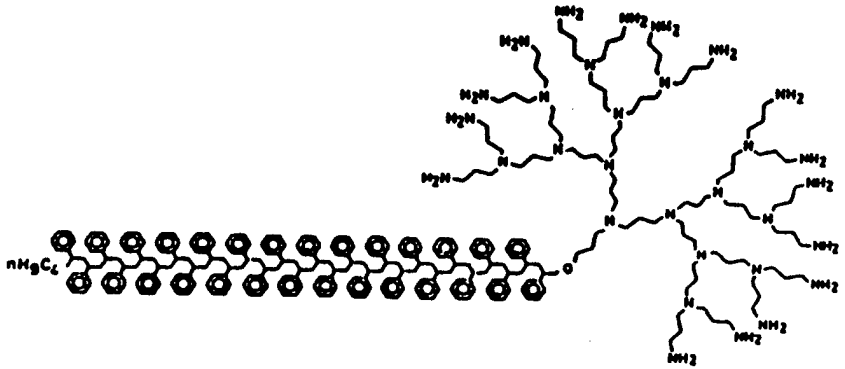

Figure 20 *Linear*-poly(styrene), focal point functionalized poly(propyleneimine) (PPI) dendrons; G = 4.0.

These new architectural copolymers derived from both linear and dendritic architectures exhibited very profound properties as nanoscale amphiphiles. In general, as one increases the head-group size from PS-*dendri*-PPI-$(NH_2)_4$ to PS-*dendri*-PPI-$(NH_2)_{32}$, the aggregation topologies change from planar bilayers to vesicles to rodlike micelles and finally to spherical micelles. Since only the head-group size and not the chemical composition of the amphiphilic structure is being changed, this study offers excellent proof for the validity of the Israelachvili et al. theory [131,139,140] of shape-dependent aggregation behavior.

Changing the head-group functionality from primary amine terminated to either carboxylic acid or quaternary amine terminated, produced amphiphilic behavior, which was very rational in the context of traditional theory. A major difference in all cases was the substantially larger dimensions of the aggregates compared to those obtained from traditional small molecule amphiphiles. In fact, one might visualize these dendritic amphiphiles as amplified forms of their traditional analogues. Aggregates and assemblies derived from these linear, dendritic architectural copolymers are roughly five times the size of those obtained from traditional surfactant molecules.

One of the earliest examples demonstrating the self-assembly of dendrimers based on inherent amphiphilic characters was that reported by Newkome et al. [141]. It was found that *dendri*-poly(amidoalcohols); G = 1–2 attached to various alkyne and hydrocarbon cores (Fig. 21) produced thermally reversible gels in aqueous solutions. It was postulated that formation of these rod-shaped aggregations was driven by a combination of hydrogen bonding of the hydroxyl terminal groups and the hydrophobic bonding of the core substituents in an orthogonal fashion. Various helical morphologies were proposed to account for the extraordinarily large diameters (i.e., ≅ 600 Å) that were observed by electron microscopy [116]. It is quite likely that multiples of these rod aggregates may have self-assembled much as has been observed recently for covalently fixed, linear-dendritic architectural polymer rods reported recently by Tomalia et al. [125].

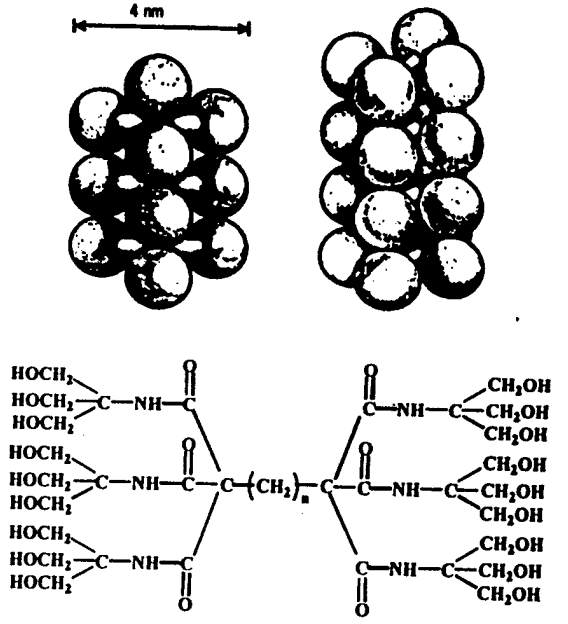

Figure 21 Molecular rods derived from micellarization of Starburst® poly(amidoalcohols).

D. Dendrimers as Nanoscale Scaffolding

1. Dendritic Rods and Cylinders

(a). Congestion Induced Morphogenesis (Shape Control). Cylindrical rod-shaped dendrimer assemblies were first synthesized by Tomalia et al. as early as 1987 [35,36,142]. These structures represent some of the first examples of hybridized dendritic architecture. Since they possess a linear polymeric core and dendritic arms, they are called *architectural copolymers.* This work was recently

reported in detail [125]. The method involved the divergent dendronization of *linear* poly(ethyleneimine) (PEI) cores (see Scheme 1). These cores, which had DPs of ≅ 100–500, were dendronized by iterating with standard PAMAM chemistry from the active hydrogens on the backbone of the *linear* poly(ethyleneimine) (PEI). The first step involved the reaction of methyl acrylate followed by an excess of ethylenediamine to give first generation monodendrons along the PEI backbone. Reiteration of these steps led to the development of higher generations (G = 1–4). These final products were characterized by FTIR, C^{13} NMR, SEC, HPLC, MALDI-TOF MS, and transmission electron microscopy. Electron microscopy of sodium carboxylated forms of G = 1–3 revealed nondescript random coil topologies. However, as the G = 3 structure was advanced to the next generation (G = 4), a remarkable congestion-induced shape change occurred to produce rigid, rodlike cylinders as determined by electron microscopy. The rod diameters varied between 25–32 Å with lengths ranging between 500–3000 Å. Furthermore, additional supra*macro*molecular assembly appeared to be occurring to give parallel clusters of the rods (Fig. 22).

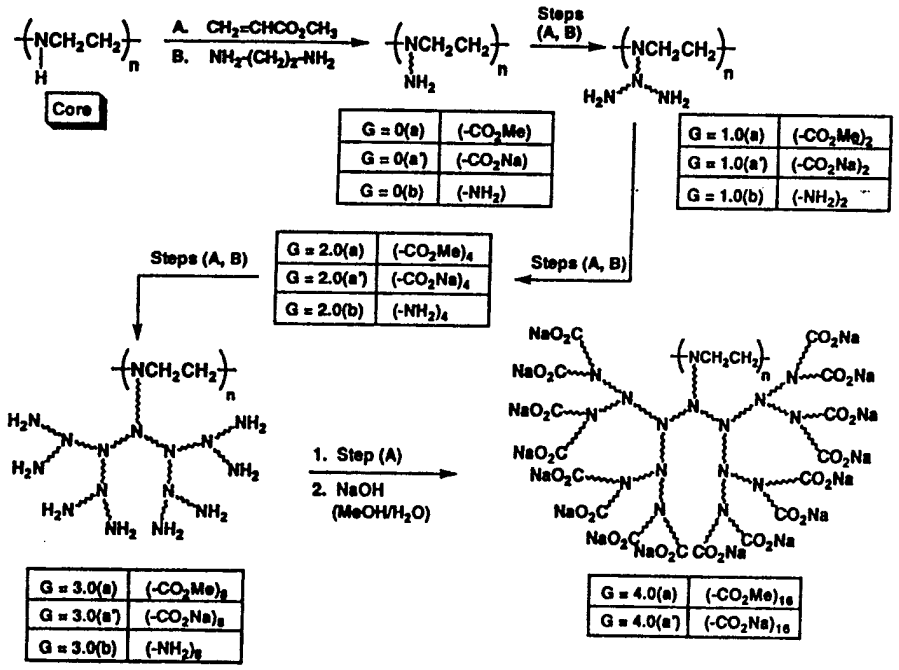

Scheme 1 Dendronization scheme for conversion of *linear* poly(ethyleneimine) cores to *dendri*-poly(amidoamine) hybrids. (Courtesy of J Am Chem Soc 1998, 120 (11), 2679. Copyright 1998 American Chemical Society.)

As early as 1996, Schluter et al. [143] reported their first efforts to synthesize linear-dendritic architectural copolymers [144]. In general, their approaches involved some general strategies. The first method involved the synthesis of a linear core, followed by the coupling of preformed dendrons to produce the architectural copolymers. The second method involved the synthesis of dendrons possessing polymerizable functionality at their focal points. These dendritic macromonomers were then polymerized to give a polymeric mainchain with pendant dendrons. In each case, linear-dendritic architectural copolymers would be obtained. They would be expected to exhibit rodlike or cylindrical properties if the backbone core possessed a high degree of polymerization and the dendritic component were highly congested.

With the first method, Schluter et al. [145,146] utilized the Suzuki reaction to produce a poly (p-phenylene)-type backbone possessing reactive *ortho*-hydroxy-methyl substituents. These substituents were subsequently used to couple a variety of Fréchet-type monodendrons along the backbone as described in Fig. 23. In general, the lower generations (i.e., G = 1) coupled with linking efficiencies as high as 95%. However, coupling efficiencies for G = 2 or 3 decreased dramatically (i.e., 50–60%) unless appropriate 2-hydroxyethyl spacers were introduced to relieve steric problems [145].

The second approach involved the covalent attachment of Fréchet-type monodendrons (i.e., G = 1–3) to appropriate polymerizable reagents such as styrenes [143,146] or methacrylates [144] (Fig. 24). Suitable radical catalysts were used to polymerize these dendritic macromonomers into structures that were observed to be cylindrical rodlike architectures [144,146,147].

Percec and coworkers [148] utilized a similar strategy for the conversion of perfluorinated alkylene functionalized 3,4,5-trihydroxy benzoic acid-type dendrons into methyl methacrylate functionalized dendritic macromonomers. Characterization of the resulting linear-dendritic architectural copolymers involved DSC, X-ray diffraction, and thermal optical polarized microscopy. It was concluded that the self-assembly of the pendant dendritic mesogens forced the linear backbone into a tilted, helical ribbon-type structure. The self-assembly behavior was largely controlled by the multiplicity, composition, and molecular weights of the pendant dendritic mesogens.

Using a variation of this dendritic macromonomer method, Percec et al. [149,150] synthesized a variety of dendritic 7-oxanorbornene macromonomers and polymerized them with ROMP catalysts [150] as shown in Fig. 25, as well as with free radical or anionic catalysts. Yields were dependent upon the route used. Products were characterized by DSC, ^{13}C-NMR, and X-ray scattering. It was proposed that the resulting structures were mesogen-assembled supramolecular columns possessing single chain helicity.

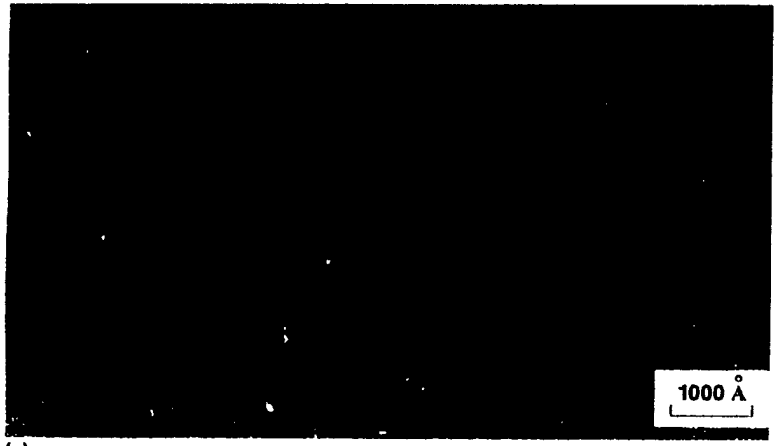

(a)

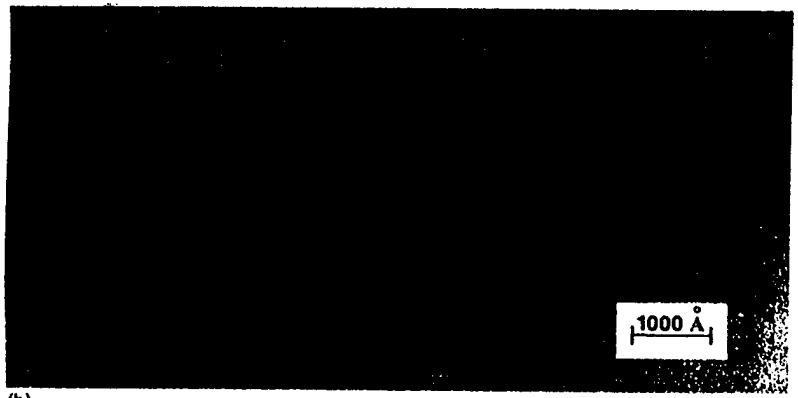

(b)

Figure 22 (a) Electron micrograph (TEM) of *linear* poly(ethyleneimine) (PEI) core; *dendri*-poly(amidoamine) PAMAM; G = 4(a); Z = $(-CO_2Na)_{16}$; N_c = 300–500 (Note: self-organization of dendrimer rods into parallel arrays). (b) Electron micrograph (TEM) of ammonia (NH_3) core; *dendri*-poly(amidoamine) PAMAM; G = 4(a); Z = $(-CO_2Na)_{48}$; N_c = 3 (Note: self-organization of dendrimer spheroids into clusters). (Courtesy J Am Chem Soc 120:2679, 1998. Copyright 1998 American Chemical Society.)

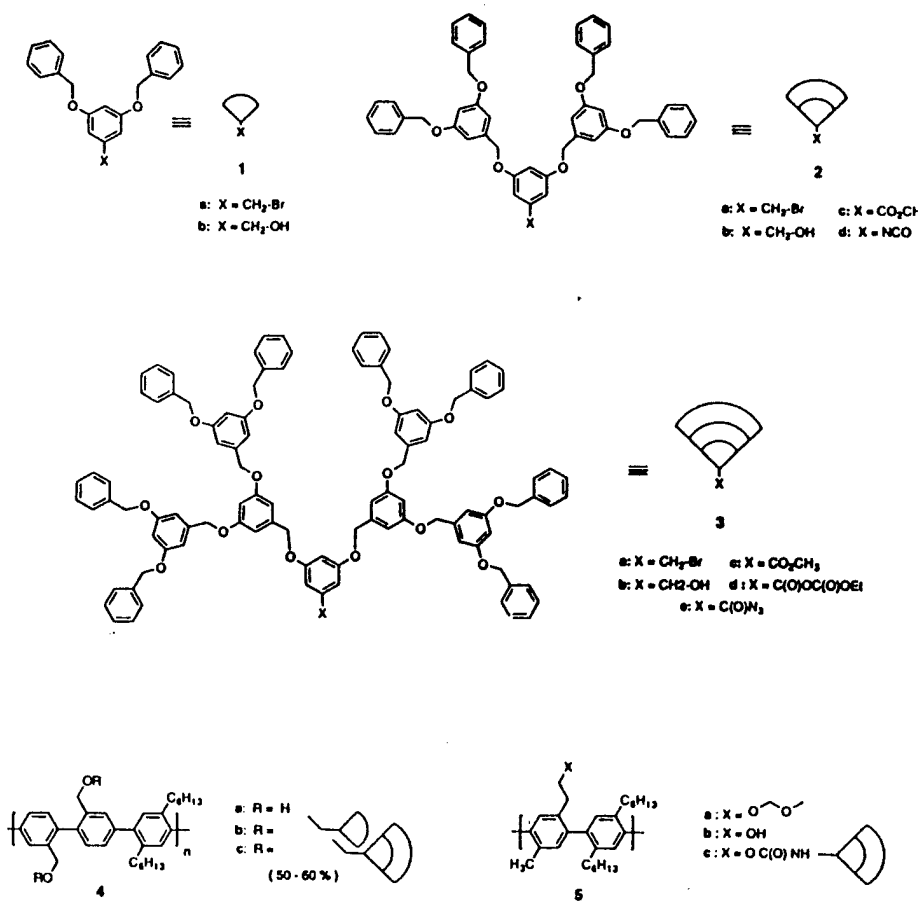

Figure 23 Fréchet-type monodendrons (Generations 1, 2, and 3) possessing various reactive groups at the focal point. Rod-shaped, dendritic-linear architectural copolymers obtained by coupling respective dendrons to linear poly(*para*-phenylene) (PPP) backbone. (Courtesy J Am Chem Soc 119:3297, 1997. Copyright 1997 American Chemical Society.)

(b). Dendrons as Mesogens—Dendromesogens. In addition to mainchain and sidechain liquid-crystalline polymers based on linear polymeric architecture, it was apparent as early as 1992 that new displays of mesogens presented on alternate architectures were possible. At that time, Ringsdorf et al. [151] and Percec et al. [152–155] pioneered extensive work in the area of dendritic mesogens. In general, this activity involved the examination of liquid-crystalline properties for

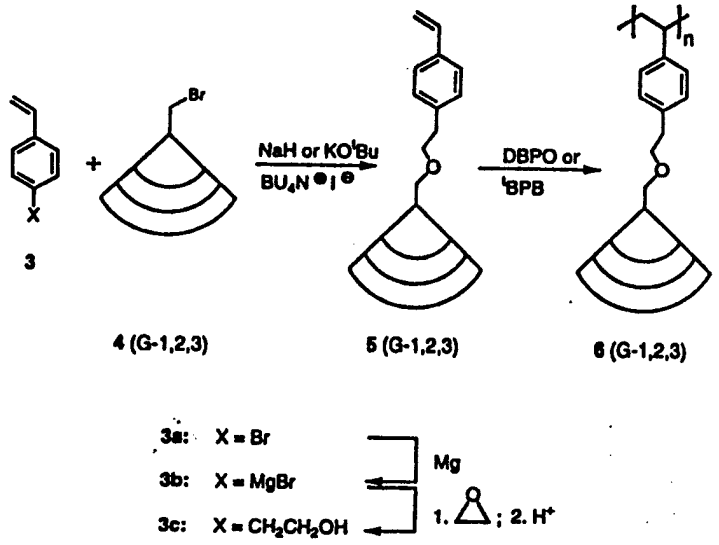

Figure 24 The synthetic sequence to macromonomers 5 (G-1,2,3) carrying dendritic fragments of the first (G-1), second (G-2), and third (G-3) generation and corresponding polymers 6 (G-1,2,3). (Courtesy Macromol Rapid Commun 17:519, 1996. With permission of Wiley-VCH Verlag GmbH, Germany.)

both hyperbranched and dendron-type architecture. For example, Percec et al. [156,157] synthesized low generation perfluorinated dendrons possessing a 15-crown-5-ether at their focal point. These unique structures were found to self-assemble into cylinders and ultimately into hexagonal columnar supramolecular arrays as illustrated in Fig. 26.

More recently, Lattermann et al. [158] described the attachment of mesogens to the terminal groups of poly(propyleneimine) dendrimers as a function of generation (i.e., G = 0–4). These new structures were referred to as *dendromesogens*. The authors noted that for the lower generations (i.e., G = 0–3), hexagonal columnar mesophases (Col_h) were observed. As the mesogen-induced congestion maximized at G = 4, mesomorphism disappeared and it was hypothesized that the dendromesogen transformed into a globular structure. These observations appear to parallel those of Tomalia et al. [125] and Percec et al. [159].

(c). Quasi-Equivalence of Dendritic Surfaces (Coats). An emerging direction in polymer chemistry is biomimicry of biological structures by using appropriate polymeric architectures, building blocks, and functionality. Quasi-equivalent building blocks or subunits are defined as chemically identical subunits, which may control their shape by switching between different conformational states

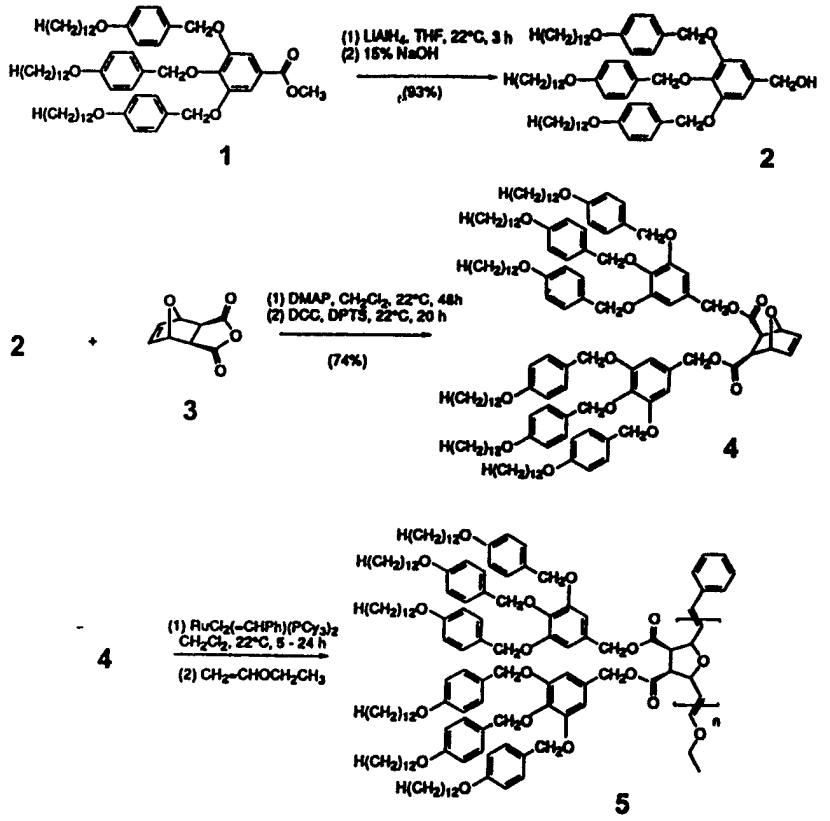

Figure 25 Synthesis of 7-oxanorbornene macromonomer derived from two (G-1) dendrons followed by ROMP polymerization into a linear dendritic hybrid architecture. (Courtesy of Macromolecules 1997, 30(19):5786. Copyright 1997 American Chemical Society.)

during the process of self-assembly [160,161]. Classic biological examples include the flat-tapered and conical protein subunits that are required for sheathing the nucleic acid component of a tobacco mosaic virus (TMV). By comparing very similar protein subunits it is apparent they will assume conical-type conformation to provide an appropriate sheathing for the protection of genetic material in an icosahedral virus, respectively [162]. In the former case, flat-tapered proteins self-assemble in the presence of a nucleic acid to generate rodlike viruses which have a helical symmetry. The cylindrical shape of this assembly induces a helical conformation to the nucleic acid (for example, a classic rodlike virus: TMV). On other hand, icosahedral viruses are approximated by a spherical shape

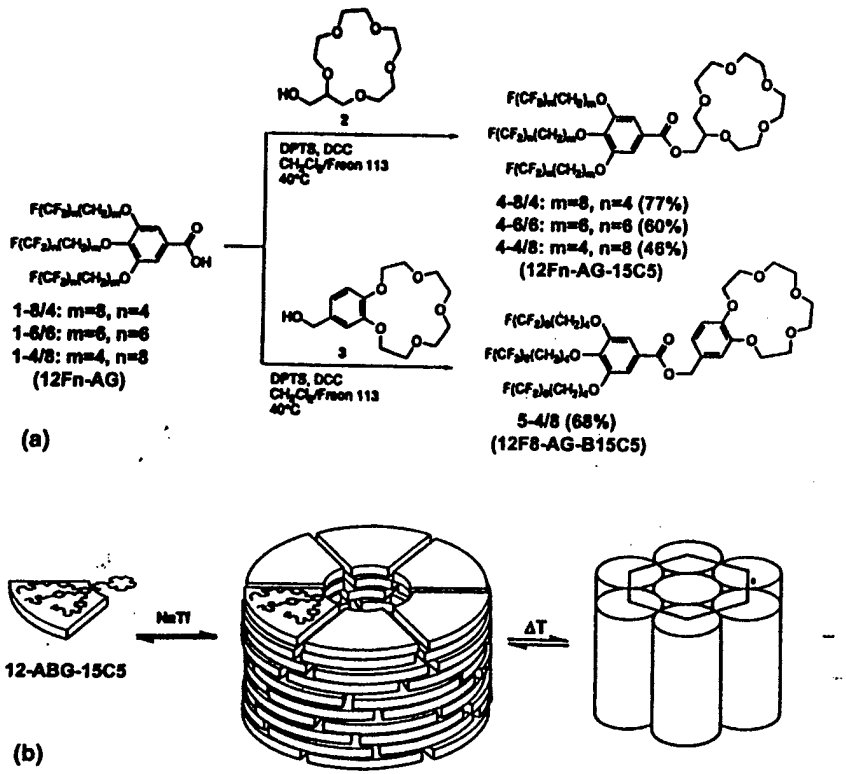

Figure 26 (a) Synthesis of monodendritic building unit with 15-crown-5 ether in the focal point; (b) self-assembly of cylindrical building blocks into a hexagonal columnar supramolecular architecture. (Courtesy J Am Chem Soc 118(41):9858, 1996. Copyright 1996 American Chemical Society.)

and are constructed from cone-shaped proteins. In the case of icosahedral viruses the nucleic acid adopts a random-coil conformation.

Using totally abiotic dendron subunits, Percec et al. [159,163] built structures that adapted either the shape of a rodlike virus with helical symmetry or an icosahedral virus with cone-shaped symmetry. Figure 27 outlines each of these viruses and their respective abiotic mimics.

In several seminal papers, Percec et al. [157,159] reported the demonstration of abiotic quasi-equivalency by controlling the degree of polymerization of various polymerizable dendrons described earlier. For example, 12 second-generation conical monodendrons (DP = 12) produced a spherical dendrimer

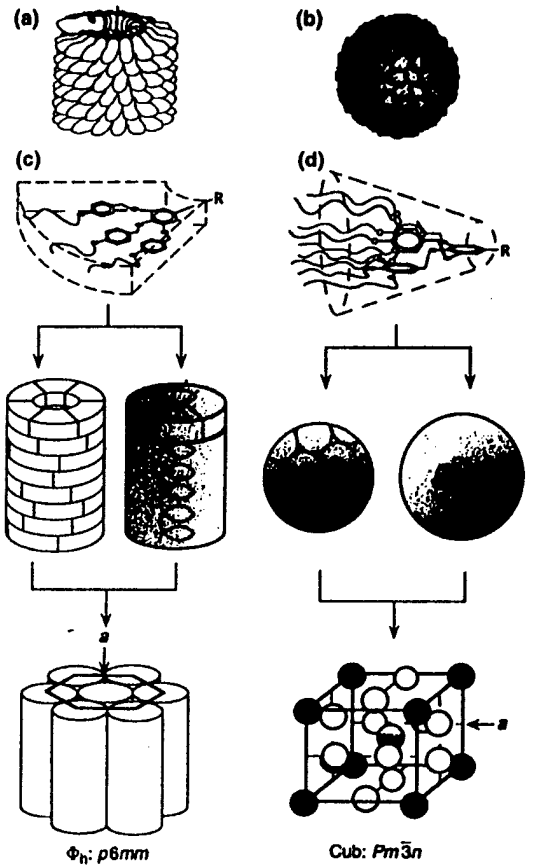

Figure 27 Quasi-equivalency of natural and synthetic supramolecular systems with cylindrical and spherical shapes: (a) tobacco mosaic virus, (b) icosahedral virus; synthetic analogue of (a) and (b) have been self-assembled from (c) tapered and (d) conical monodendrons. (Courtesy of Nature 1998, 391, 8, 161. Copyright 1998 Macmillan Magazines Limited.)

which results from self-organization into a cubic Pm3n three-dimensional (3-D) liquid-crystalline (LC) lattice. The attachment of methacrylate (12G2-AG-MA) or styrene (12G2-AG-S) monomer moieties to the dendron followed by radical initiation yields spherical (DP < 20) or cylindrical (DP > 20) polymers depending on the degree of polymerization (DP). The spherical polymers self-organize into the same cubic (Pm3n) 3-D lattice while the cylindrical ones self-assem-

ble into a p6 mm columnar hexagonal (Fig. 28) (2-D liquid-crystal lattice). Furthermore, Percec found that the radical polymerization of the styrene or methylacrylic functionalized dendrons exhibited a very dramatic self-acceleration in polymerization kinetics. These kinetics are presumably enhanced by the unique self-assembly events that accompany these polymerizations [164]. As illustrated in Fig. 28, the principles for the design of such macromolecular structures are outlined.

2. Hypervalency/Hypercooperativity

Biological systems have long exploited the advantages of multivalent recognition events in the development of *exo*-supramolecular and supra*macro*molecular structures. Most notable is the power of multivalent hypercooperative binding associated with biological cell adhesion processes. It is now well recognized that this biological strategy is very versatile and ubiquitous. In the case of carbohydrate recognition at cell surfaces the preferred recognition mode is to involve many polyvalent soft recognition events that are geometrically optimized to provide hypercooperativity as opposed to single isolated events with harder recognition parameters. The power of this concept is illustrated in Fig. 29, eloquently described by Kiessling and Pohl [165], and further elaborated upon more recently by Whitesides et al. [166]. Simply stated, once a ligand has attached itself to a cell at one site, it suffers a smaller entropy loss by binding at neighboring sites. Mimicry of these biological adhesion parameters can be exquisitely modeled and tested with dendrimeric systems. Although a substantial number of linear, poly (valent) polymeric architectures [e.g., poly(acrylamides), etc.] have been tested with some success [167–170], efforts toward the use of dendrimer technology to create multivalent ligands for these purposes are in their infancy.

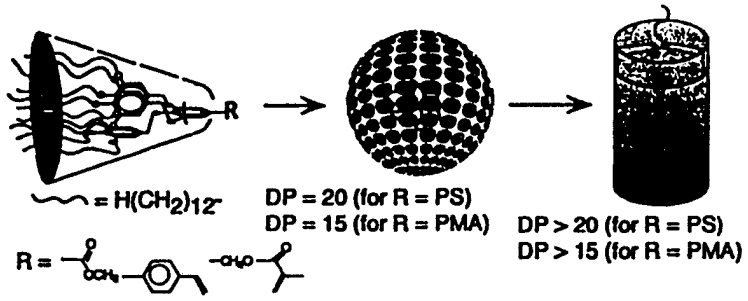

Figure 28 Scheme describing conversion of dendritic macromonomers to either spheroidal or cylindrical architectures depending on the degree of polymerization (DP). (Courtesy of J Am Chem Soc 1997, 119, 12978. Copyright 1997 American Chemical Society.)

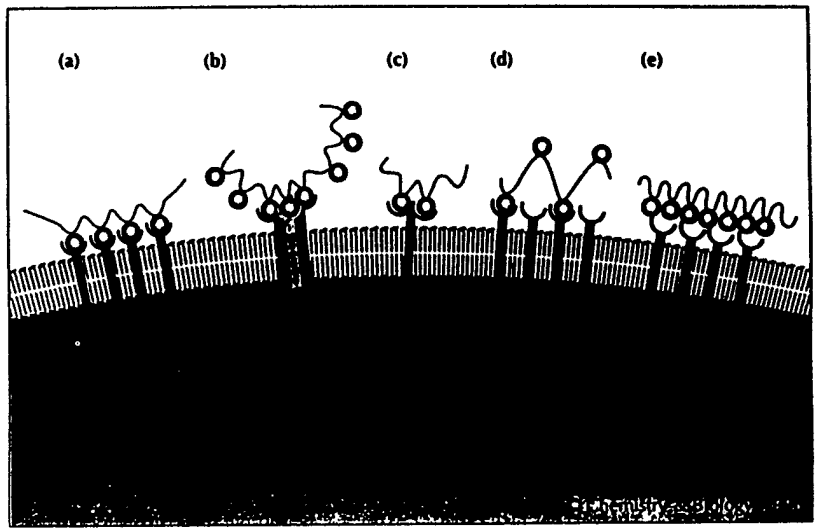

Figure 29 Specific recognition in multivalent interactions. Cells can use several strategies to bind to a multivalent ligand: (a) forming a cluster of many monovalent receptors on a small area of the cell surface; (b) using oligomeric receptors; or (c) using receptors with more than one saccharide-binding site. In all such systems, multivalent saccharide ligands bind more tightly to the cell than their monovalent counterparts. For a divalent ligand, the free energy of binding to a multivalent receptor array will be greater than the sum of the contributions of each individual site. This primarily results from the fact that once the ligand has attached itself to a cell by one site, it is closer to the second site and will suffer a smaller entropy loss by binding to it. Multivalent ligands with incompatible relative orientations (d) or spacing (e) of the saccharide units in the multivalent array will not bind tightly. (Courtesy of Chemistry & Biology 1996, 3(2):72. Copyright Current Biology Ltd., London.)

(a). Glyco(dendrimers). While searching for inhibitors of influenza virus hemagglutinin, Roy et al. [171–173] pioneered the synthesis and use of carbohydrate-substituted dendrimers, using solid-phase methodology to synthesize sialic acid decorated dendrimers. These dendrimers, containing 2, 4, 8, or 16 sialic acid residues, all inhibited the agglutination of erythrocytes by influenza virus (which is caused by hemagglutinin-mediated crosslinking of the erythrocytes) in the micromolar concentration range. (See Fig. 30.)

Very recent work in the Tomalia–Baker group [174] has shown that certain classes of dendritic architecture offer distinct advantages as scaffolding for presenting C-sialoside groups. For example, use of dendrigraft architecture [175] as

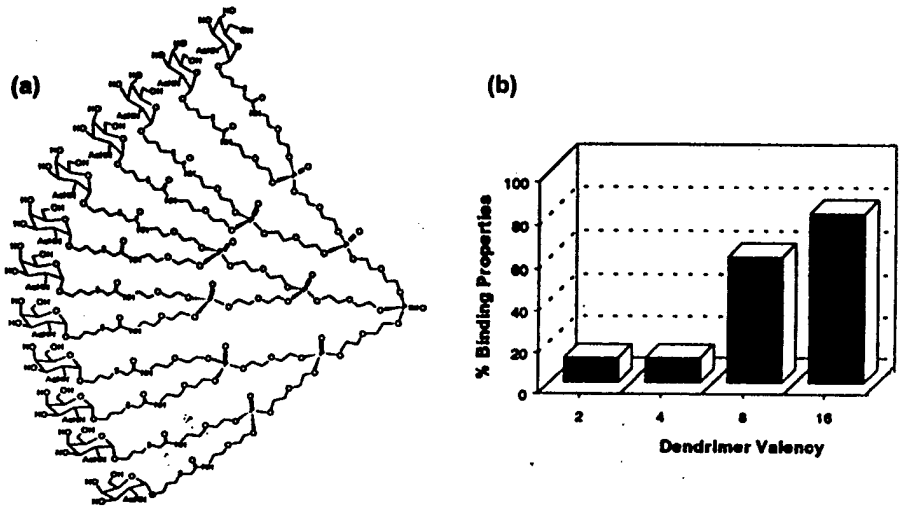

Figure 30 (a) Structure of phosphotriester GalNAc glycodendrimer. (b) Enzyme-linked lectin assays (ELLA) of L-lysine-based sialic acid dendrimers used as coating antigens in microtiter plates and detected with horseradish peroxidase labeled wheat germ agglutinin (HRPO-WGA). Binding activity as a function of dendrimer valency. (Courtesy of Polymer News, 1996, 21(7), 230. Copyright Gordon and Breach Publishers, Switzerland.)

scaffolding for the presentation of sialic acid groups was found to be more than 1000 times more effective than the corresponding linear architecture for the inhibition of influenza A viruses (see Fig. 31).

E. Dendrimers as Nanoscale Tectons (Modules)

1. Two-Dimensional Dendritic Assemblies

The self-assembly of dendrimers in two dimensions has been studied at both the air–water interface [i.e., Langmuir–Blodgett (LB) films] as well as at the air–bulk solid interface [i.e., self-assembled monolayer (SAM) films].

(a). At the Air–Water Interface [LBs]. Some of the earliest work was reported by Fréchet et al. in 1993 [176]. It involved the examination of LB films derived from the spreading of amphiphilic hydroxyl functionalized poly(arylether) dendrons as a function of generation level (i.e., G = 1–5) (Fig. 32). There was a strong dependence of the isotherm on molecular weight (generation level). The lower generations (i.e., G = 1–4) exhibited an increase in surface pressure through the liquid expanded phase (LE) followed by a peaked collapse transition, indicating a nucleation and growth event leading to a liquid condensed phase

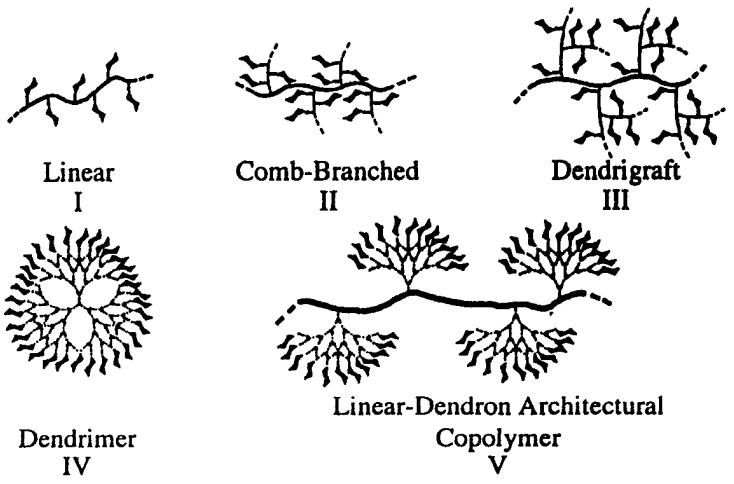

Figure 31 Model representations of sialic-acid-conjugated polymeric inhibitor subunits used to inhibit viral infection. Structures are not drawn to scale. (Courtesy of Bioconjugate Chemistry 1999, (10)2. Copyright 1999 American Chemical Society.)

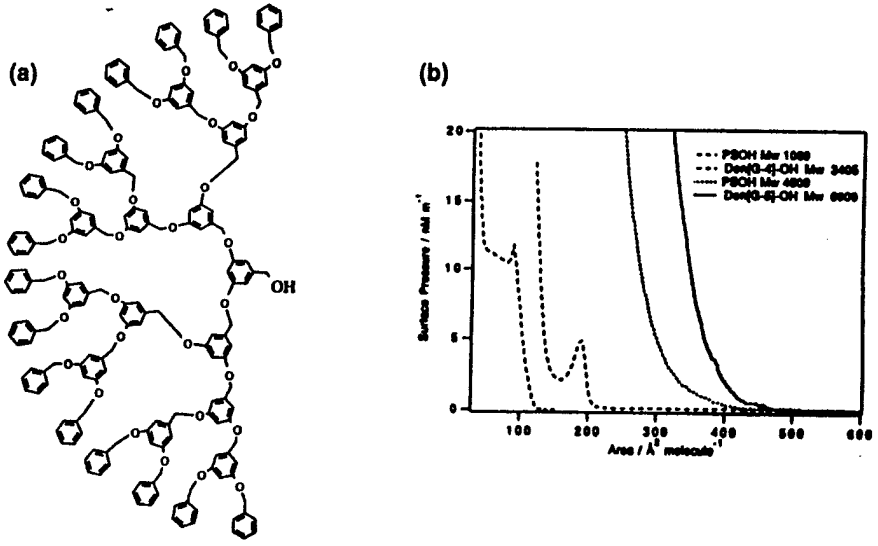

Figure 32 (a) Fourth generation [G=4] dendron, based on 3,5-dihydroxy benzyl alcohol core. (b) Isotherms of [G=4] and [G=5] dendrons showing differences due to compression rate and pause time before compression. (Courtesy of J Phys Chem 1993, 97, 294. Copyright 1993 American Chemical Society.)

(LC). A sharp transition in behavior occurred in progressing from G = 4 to 5. Advancement from G = 4 to 5 caused envelopment and isolation of the hydrophilic dendrimer focal point group from the water phase, thus proceeding directly to the condensed solid phase. In summary for generations 1–4, the dendrimers behave as classical surfactant molecules on a Langmuir trough. The isotherms of G = 5–6, however, manifest nonsurfactant behavior, once again reflecting the surface congestion-induced properties known for higher-generation dendrimers. Compression of the fourth generation poly(ether) dendrimer results in the formation of a stable bilayer. In this bilayer the dendrimers are compressed laterally in respect to the surface normal, producing an ellipsoid shape that is twice as high as it is broad (Fig. 33). Neutron-scattering studies on analogues with perdeuterated end-groups indicate that the terminal benzyl groups are located at the top of the lower layer [177]. More stable monolayers were formed when oligo(ethylene glycol) tails were used as core functionality [178,179].

Very interesting amphiphilic behavior at the air–water interface was observed by van Hest and Meijer [93] for hydrophobe (focal point) modified poly(propyleneimine) (PPI) dendrons [i.e., poly(styrene)-*dendri*-PPI $(NH_2)_n$, where n = 2,4,8]. These dendritic amphiphiles were essentially a reverse version of the Fréchet examples (see above). Only PS-*dendri*-PPI-$(NH_2)_n$ with n = 8 and 16 (i.e., G = 3 and 4) exhibited normal pressure-area isotherms. The lower generations (i.e., G = 1 and 2) all displayed isotherm curves indicating they transitioned directly to solid-state behavior.

Poly(propylene imine) dendrimers functionalized with hydrophobic alkyl chains (palmitoyl chains or alkyloxyazobenzene chains) assembled into stable monolayers at the air–water interface [122,180]. In the assemblies, the dendrimers adopted a cylindrical amphoteric shape in which the ellipsoidal dendritic moiety acted as a polar head-group and the alkyl chains arranged in a parallel fashion to form an apolar tail (Fig. 33b). This representation is based on the observation that the molecular area of a dendritic molecule increases linearly with the number of end-groups in this molecule.

Amphiphilic PAMAM dendrimers comparable in design to those reported

Figure 33 (a) Compressed dendrimer Langmuir bilayer; (b) dendrimer Langmuir monolayer.

for the poly(propylene imine) dendrimers have been studied at the air–water interface by Tomalia et al. [122]. The PAMAMs with aliphatic core groups of varying lengths (6, 8, 10, and 12 carbon atoms) also display the linear behavior between the molecular area at the compressed state and the number of end-groups per molecule. Tomalia et al. explain their findings in a model in which the lower generations are asymmetric like the poly(propylene imine) dendrimers, while the higher generations act as hydrophobic spheroids floating on the air–water interface. Since no indication for the latter behavior is found, it is proposed here that the amphiphilic PAMAM dendrimers of high generations when disposed on air–water interfaces, are also highly distorted with all aliphatic end-groups pointing upwards (Fig. 33b).

Most notable was the fact that it was shown that metal-loaded (Cu^{+2}) dendrimers can be readily organized into two-dimensional layers. Langmuir isotherms obtained for both unloaded and metal-loaded dendrimers in this series differed substantially from those observed by Fréchet. It was reassuring to note that radii measurements obtained from limiting area Langmuir–Blodgett film studies compared very favorably with radii determined by size exclusion chromatography measurements.

(b). At the Air–Bulk Phase Interface (SAMs). Very early observations [51,181] indicated the amine terminated PAMAM dendrimers exhibited tenacious adhesion to a variety of substrates. Early indications were that they formed SAMs on glass, silicon, or metal surfaces (i.e., gold, etc.). In a pioneering effort by Mansfield [182], it was predicted that dendrimers would exhibit various deformation modes on surfaces depending on generation and adsorption strength. This Monte Carlo simulation considered the adsorption of dendrimers on a surface at different interaction strengths. The calculations showed a flattening of the dendrimer shape with increasing adsorption strengths. As reflected in the "phase" diagram (Fig. 34), the mode of adsorption of the dendrimers is dependent on adsorption strength and on the generation number (higher-generation dendrimers have more interaction sites per molecule and, therefore, these dendrimers have a better chance to be adsorbed).

A wide variety of dendrimer adhesion modes have been defined experimentally that are beginning to fulfill the Mansfield predictions. They vary from self-assembled monolayers to multilayer assemblies as described in Fig. 35. Perhaps one of the first published works to clearly demonstrate the ability to construct mono/multilayers was reported by Regen and Watanabe [183]. They fabricated multilayers by repetitive activation with K_2PtCl_4 on a silicon wafer surface possessing primary amine groups, followed by deposition of PAMAM dendrimer, illustrated in Fig. 35(d). Reiteration of this sequence produced film thicknesses that were shown by elipsometry to increase linearly as a function of the number of cycles performed. After 12–16 cycles, multilayers with a thickness close to

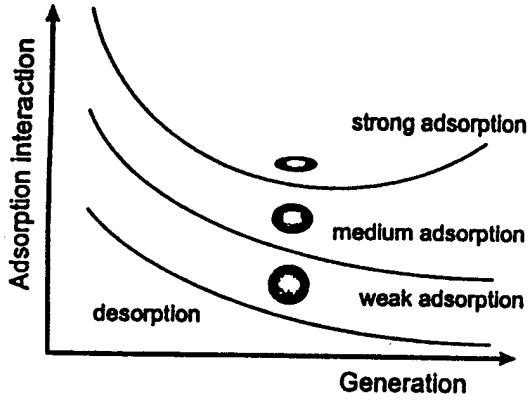

Figure 34 A "phase diagram" that shows how the shape of dendrimers in adsorbed monolayers depends on the strength of the adsorption interaction and the dendrimer generation. The data are based on calculations by Mansfield. (From Ref. 182.)

80 nm were obtained by using G = 8 or 6 PAMAM dendrimers, respectively. The elemental composition was confirmed by photoelectron spectroscopy (XPS)- which both demonstrates the incorporation of PAMAM dendrimers as well as the necessity of the Pt^{+2} as a requisite component in the growth cycle.

An interesting type of dendrimer deformation has been reported by Crooks

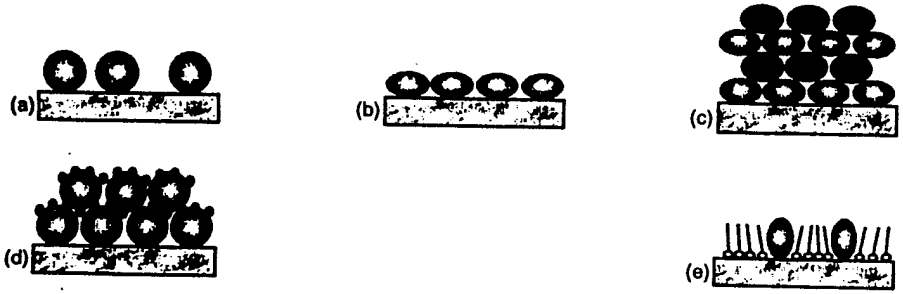

Figure 35 Schematic representation of the different modes of adsorption of dendrimers on surfaces: (a) adsorbed noninteracting dendrimers; (b) adsorbed dendrimers with surface-interacting end-groups; (c) interacting multilayer dendrimer films; (d) multilayer dendrimer films with ionic shielding; (e) mixed monolayer.

et al. [101,184,185]. Monolayers of PAMAM dendrimers adsorbed on a gold surface flatten due to multiple Au-amine interactions, but subsequent submission of alkanethiols to the surface results in a mixed monolayer in which the PAMAMs acquire a prolate configuration due to the shear exerted by the thiols (Fig. 35e). The shear originates from the stronger thiol–Au interaction as compared to the amine–Au interaction (see Chapter 10). If the adsorption time of the dendrimer monolayer is rather short (45 s instead of 20 h), exposure to hexadecanethiol results in piling up of the dendrimers to vacate the surface in favor of the thiols [101,184,185]. Eventually, this leads to complete desorption of the dendrimers from the surface.

Tsukruk et al. [186–188] reported on the alternating electrostatic layer-by-layer deposition of PAMAM dendrimer up to generation G = 10. This concept is illustrated in Fig. 35c. First an amine terminated dendrimer is adsorbed onto a SiO_2 surface followed by a carboxylic acid terminated dendrimer that deposits on top of a full generation. The cycle is repeated and multilayers are formed. They measured the layer thickness and found it to be below the theoretical one, which also supports the elastic deformation of dendrimer to obtain the most favorable energy balance. Molecular dendrimer dimensions follow scaling laws as a function of molecular weight of dendrimer with exponent of 0.27 (for spheres it is 1/3). Cast and spin-coated films exhibit large sensitivity toward conditions used during their formation. Thermal annealing can change dendrimer shape from oblate toward spherical. Change in surface characteristics (post- or pre-functional group modification) can largely influence the quality and properties of SAMs. Phase diagrams based on molecular modeling define the correlations among generation number, interaction strength, and shape (i.e., at strong interactions PAMAM G = 4 on Au dendrimer will be oblate on a surface, but at strong repulsion ($C_{16}SH$, PAMAM G = 8 on Au) dendrimer will be prolate. With weak interactions (G-0, G-2) dendrimer can retain sphere-like shapes.

Perhaps one of the most remarkable breakthroughs concerning dendrimeric SAMs is that reported recently by Fréchet et al. [189,190]. They have demonstrated that monolayers of dendritic polymers can be prepared by covalent attachment to a silicon wafer surface (Fig. 36a). These ultrathin polymer films can serve as effective resists for high-resolution lithography using the scanning probe microscope. These dendrimer films may be patterned using the SPL to create features with dimensions below 60 nm. Although very thin, the dendrimer films are resistant to an aqueous HF etch, allowing the production of a positive tone image as the patterned oxide relief features are selectively removed.

The patterned oxide relief features can be selectively removed under aqueous hydrofluoric acid (50:1, 60 sec) etching conditions resulting in a pattern transfer of raised oxide relief features into positive tone images. Figure 36b is a two-dimensional AFM image of the same patterns (from Fig. 36c) after etching

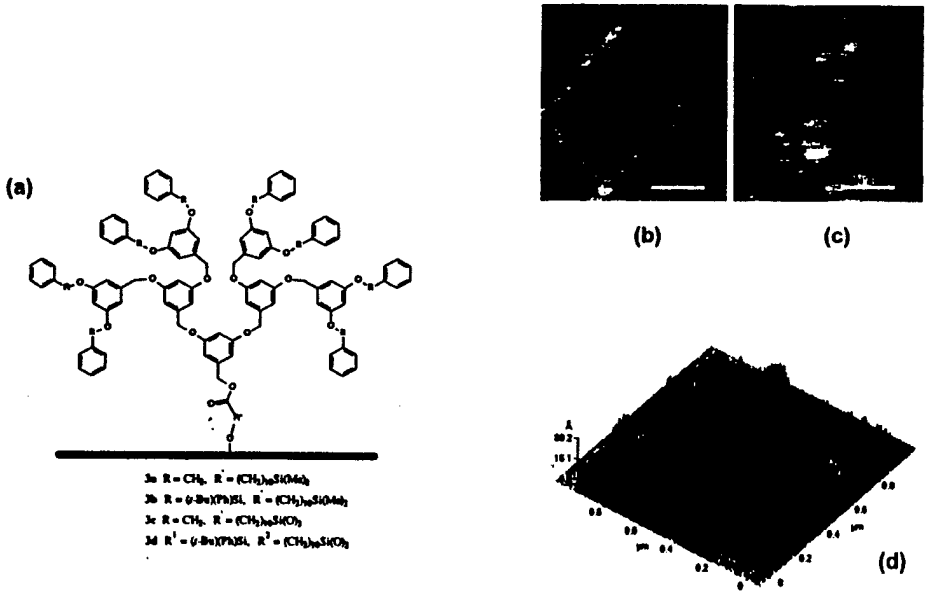

Figure 36 Covalent attachment of dendritic monolayers to a silicon wafer surface. (Courtesy of Cur Opinion in Colloid & Interface Sci, T Emrick, JMJ Fréchet, "Self-Assembly of Dendritic Structures," 4, 1999 with permission from Elsevier Science.)

the wafer for 60 sec in 1M HF. The dark regions represent depressions approximately 2 nm deep into the silicon. Under these conditions, the dendrimer monolayer clearly resists the etch as evidenced from the lack of any line broadening or pitting in the unpatterned regions.

2. Three-Dimensional Dendritic Assemblies

(a). Statistical Structures. Earlier work by Tomalia et al. [55] has shown that dendrimers may be used as reactive (modules) building blocks to construct statistical three-dimensional covalent networks and gels. In contrast to traditional crosslinked networks [60], within the dendrimer networks one is able to observe conserved order in the form of unique topological features which have been seen in electron micrographs of the dendrimer system. Examples of linear, bridged, radially bridged, and macrocyclic bridged topologies were observed as shown in Fig. 37. Several of these topological types (i.e., linear and cyclic) are remarkably reminiscent of those that are obtained by noncovalent self-assembly of proteins.

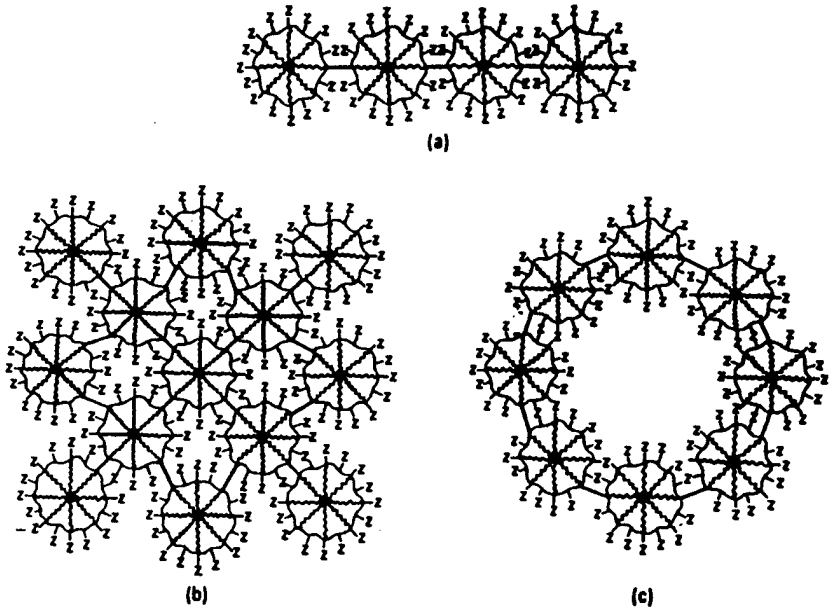

Figure 37 Bridged dendrimer types: (a) linear bridged, (b) radial bridged, (c) macrocyclic bridged.

However, virtually no reports have appeared concerning the self-assembly of dendrimers by noncovalent electrostatic methods until recently. Aida et al. [191] have reported the electrostatically directed assembly of prophyrin core dendrimers to produce large infinite aggregates as illustrated in Fig. 38. Energy transfer constants were obtained and used to determine distances between acceptors and donors as it was demonstrated that communication occurred between those domains.

Self-assembled, three-dimensional dendritic network structures possessing critical π-type surface groups have been reported to exhibit unique electrical conducting properties. Miller and coworkers [192] observed unusually high conductivities (i.e., 18 s/cm at 90% humidity) for generation = 3 PAMAM dendrimers surface-modified with cationically substituted naphthalene diimides (Fig. 39). In all cases, the conductivity was electronic and isotropic. Near-infrared spectra showed the formation of extensive π-stacking, which presumably favored electron hopping via a three-dimensional network.

Similarly, Wang and coworkers [193] reported that hyperbranched dendritic structures possessing poly(3-alkylthiophene) arms self-assemble into thin

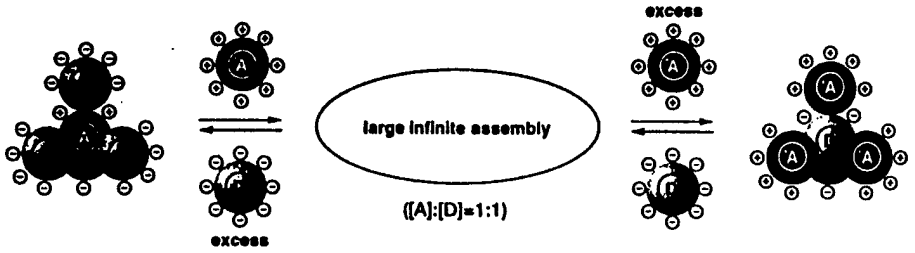

Figure 38 Schematic representation of the electrostatic interaction between negatively and positively charged dendrimer electrolytes. D represents a donor and A an acceptor in energy transfer. (Courtesy of Angew Chem Int Ed 1998, 37(11) 1533. Copyright Wiley-VCH Verlag GmbH, Weinheim, Germany.)

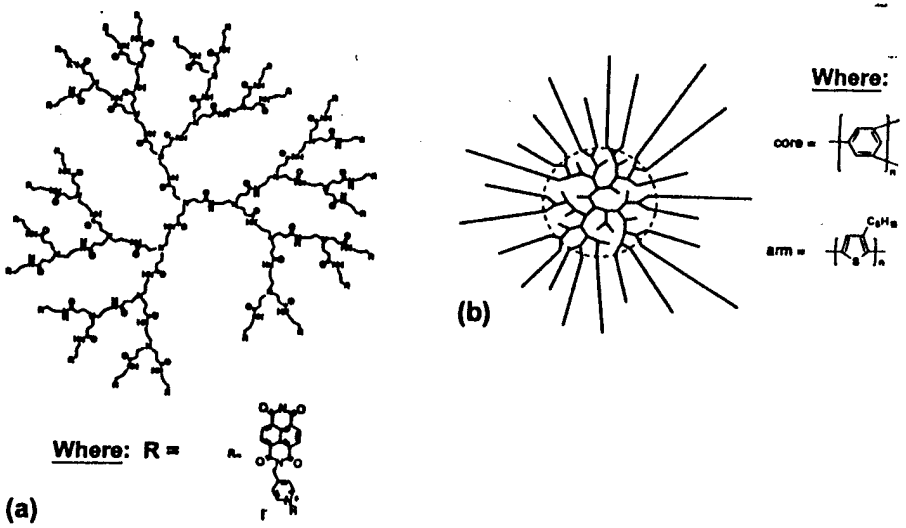

Figure 39 Examples of electrically conducting (a) dendrimeric and (b) hyperbranched star polymers. (Courtesy of J Am Chem Soc 1997, 119, 1006 and (b) 11106. Copyright 1997 American Chemical Society.)

films with morphological features, as well as electrical and optical properties that reveal a surprising degree of structural order. Typical conductivities varied between 42–65 s/cm.

(b). Structure Controlled Core-Shell Tecto(dendrimers). Core-shell architecture is a very recognizable concept in the lexicon of science. Beginning with the first observations by Galileo concerning the heliocentricity of the solar system [194] to the planetary model first proposed by Rutherford [1] and expounded upon by Bohr [195], such architecture has been broadly used to describe the influence that a central focal point component may exercise on its surrounding satellite components. Such has been the case recently at the subnanoscale level. Rebek et al. [196] have described the influence that a guest-molecule may have on self-assembling components that are directed by hydrogen-bonding preferences and the filling of space. It was shown that hydrogen-bonding preferences combined with spatial information such as molecular curvature can be used to self-assemble a single core-shell structure, as shown in Fig. 40 at the subnanoscopic level.

At the nanoscale-dimensional level it was shown by Hirsch et al. [197] that [60]-fullerenes could be used as a core tecton to construct a core-shell molecule with T_h-symmetrical C_{60} core and an extraordinarily high branching multiplicity of 12.

As described earlier, the assembly of reactive monomer [49] branch cells [14,52] around atomic or molecular cores to produce dendrimers according to divergent/convergent dendritic branching principles is well demonstrated [57]. The systematic filling of molecular space around dendrimer cores with monomer units or branch cells as a function of generational growth stages (dendrimer shells) to give discrete quantized bundles of mass has proven to be mathematically predictable [58]. This generational mass relationship has been demonstrated experimentally by mass spectroscopy [59,60] and other analytical methods [61,92]. These synthetic strategies have allowed the systematic control of molecu-

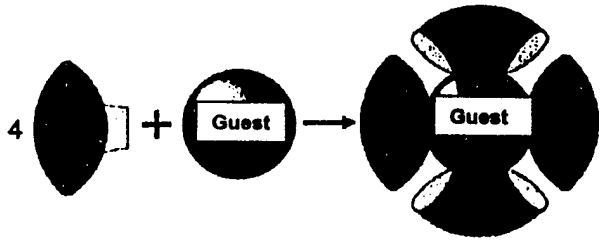

Figure 40 Self-assembly of a core-shell structure involving hydrogen bonding and complementary shape preferences according to Rebek et al., Ref. 196.

lar structure as a function of size [92], shape [125], and surface/interior functionality [36]. Such synthetic strategies have allowed construction of dendrimeric structures with dimensions that extend well into the lower nanoscale regions (i.e., 1–30 nm).

Since the very first reports on dendrimers in 1984 [62–67], we have proposed the use of these entities as fundamental building blocks for the construction of higher complexity structures on numerous occasions [35,58,198]. Early electron microscopy studies [55] and other analytical methods [61] indicated that the supra*macro*molecular assembly leading to formation of dimers, trimers, and other multimers of dendrimers occurred almost routinely; however, these were largely uncontrolled events.

Recent studies have shown that poly(amidoamine) PAMAM dendrimers are indeed very well-defined, systematically sized spheroids [92] as a function

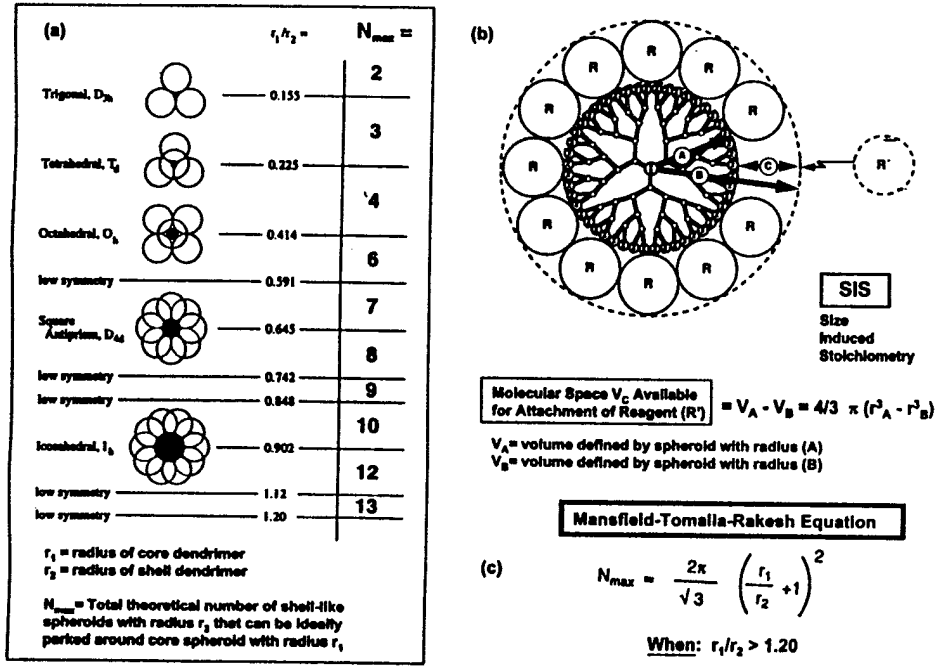

Figure 41 (a) Symmetrical properties for core-shell structures where $r_1/r_2 < 1.20$. (b) Sterically induced stoichiometry (SIS) based on respective radii (A) and (B) of dendrimers. (c) Mansfield–Tomalia–Rakesh equation for calculation of maximum shell filling when $r_1/r_2 > 1.20$.

of generation level. Furthermore, evidence has been obtained by SANS studies to show that these PAMAM dendrimers behave as originally described by de Gennes and Hervet [70]. The terminal groups remain largely at the periphery and are *exo*-presented with virtually no backfolding [68,199,200].

Anticipating the use of these nanoscale modules in a variety of construction operations we examined the random parking of spheres upon spheres [201]. From this study, it was rather surprising and pleasing to find that at low values of radii ratios (i.e., <1.2), absolutely beautiful symmetry properties appeared as illustrated in Fig. 41. However, at higher radii ratios, the mathematics resolved

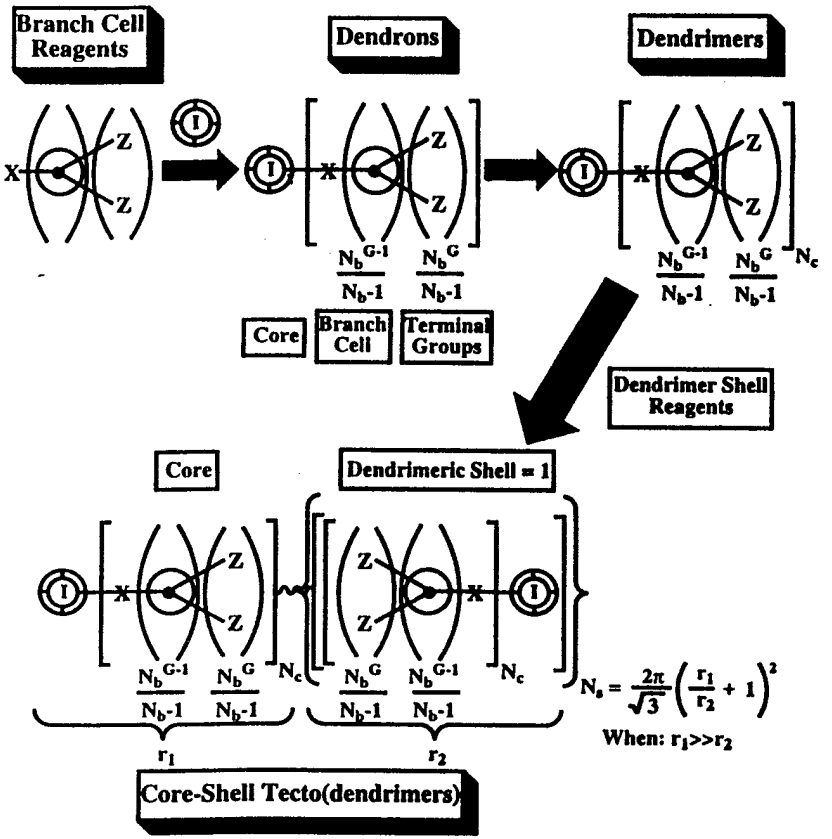

Figure 42 Empirical formulas for branch cells, dendrons, dendrimers, and core-shell tecto(dendrimers), where N_b = branch cell multiplicty; N_c = core multiplicty; G = generation; r_1 = radius of core dendrimer; r_2 = radius of shell dendrimer.

into the following Mansfield–Tomalia–Rakesh general expression. From this relationship, it is possible to calculate the number of spheroidal dendrimers one could possibly place in a shell around a core dendrimer as a function of their respective radii (Fig. 42).

Inspired by these derived values for shell filling around a central dendrimer core, we devised several synthetic approaches to test this hypothesis. The first method involved the direct covalent reaction of a dendrimer core with an excess of dendrimer shell reagent; referred to as the (a) Direct Covalent Method. The second method involved self-assembly by electrostatic neutralization of the dendrimer core with excess shell reagent to give the (b) Self-Assembly with Sequential Covalent Bond Formation Method. These strategies are described in Section IV. In each case, relatively monodispersed products are obtained. We call these new dendritic architectures *core-shell (tecto)dendrimers.*

IV. ASSEMBLY OF DENDRIMERS INTO PRECISE CORE-SHELL TECTO(DENDRIMERS)

A. Direct Covalent Method

This route produces partially filled shell structures and involves the reaction of a nucleophilic dendrimer core reagent with an excess of electrophilic dendrimer shell reagent as illustrated in Fig. 43 [54,202].

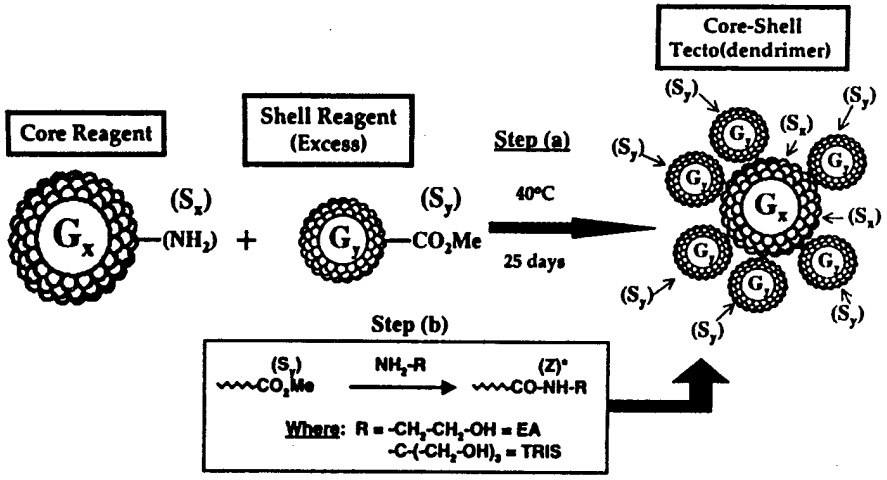

Figure 43 Synthetic scheme for core-shell tecto(dendrimers), where Z = surface functionality after reaction with R-type reagents.

Various poly(amidoamine) PAMAM dendrimer core reagents (i.e., either amine or ester functionalized) were allowed to react with an excess of appropriate PAMAM dendrimer shell reagents. The reactions were performed at 40°C in methanol and monitored by FTIR, ^{13}C NMR, SEC, and gel electrophoresis. Conversions in Step (a) (Fig. 43) were followed by the formation of shorter retention time, and higher molecular weight products using size exclusion chromatography (SEC). Additional evidence was gained by observing the loss of migratory band associated with the dendrimer core reagent present in the initial reaction mixture, accompanied by the formation of a higher molecular weight product, which displayed a much shorter migratory band position on the electrophoretic gel. In fact, the molecular weights of the resulting core-shell tecto(dendrimer) could be estimated by comparing the migratory time of the core-shell product (polyacrylamide) gel electrophoresis (PAGE) results (Table 1), with the migration distances of the PAMAM dendrimers (e.g., G = 2–10) used for their construction [61].

It was important to perform capping reactions on the surface of the resulting ester terminated core-shell products in order to pacify the highly reactive surfaces against further reaction. Preferred capping reagents were either 2-amino-ethanol or *tris*-hydroxymethyl aminomethane.

The capping reaction, Step (b) (Fig. 43), was monitored by following the disappearance of an ester band at 1734 cm^{-1}, using FTIR. Isolation and characterization of these products proved that they were indeed relatively mono(dispersed) spheroids as illustrated by AFM in Fig. 44. It was very important to perform the

Table 1 Analytical Evidence for Core-Shell Tecto(dendrimers)

$X;[(Y)(Z^*)]_n$	G4[(G3); $(EA)]_n$	G5(G3); $(TRIS)]_n$	G6(G4); $(TRIS)_n$	G7(G5); $(TRIS)_n$
Theoretical shell sat. levels(n)	9	15	15	15
Observed shell sat. levels(n*)	4	8–10	6–8	6
Percent theoretical shell sat. levels	44%	53–66%	40–53%	40%
MALDI-TOF-MS (MW):	56,496	120,026	227,606	288,970
PAGE (MW):	58,000	116,000	233,000	467,000
AFM: Observed dimensions:	25 × 0.38 nm (D,H)	33 × 0.53 nm (D,H)	38 × 0.63 nm (D,H)	43 × 1.1 nm (D,H)
CALC. (MW):	56,000	136,000	214,000	479,000

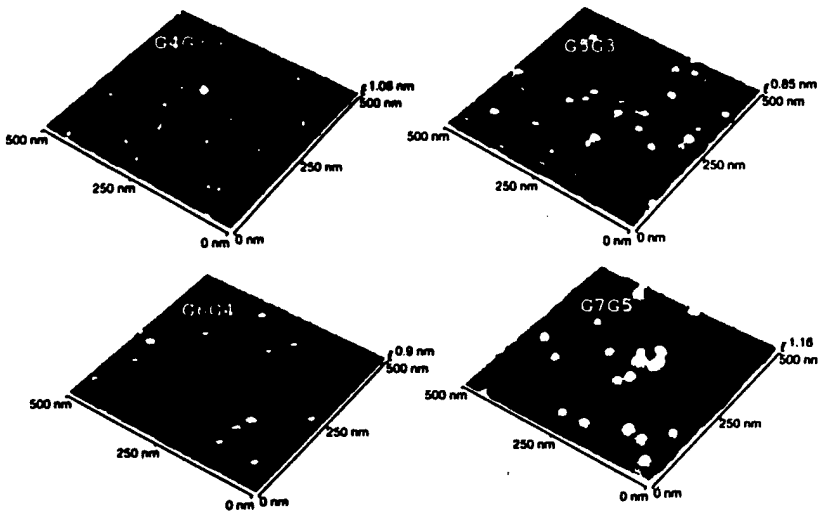

Figure 44: AFM images of core-shell tecto(dendrimer) PAMAMs. (Courtesy of PMSE, 1999, 80, 6. Copyright 1999 American Chemical Society.)

AFM analysis at very high dilution to avoid undesirable core-shell molecular clustering. In spite of these efforts, a small amount of clustering was still observed.

A distinct core-shell dimensional enhancement was observed as a function of the sum of the core-shell generation values used in the construction of the series (e.g., G4/G3, <G5/G3, <G6/G4, and <G7/G5). This is in sharp contrast to nondescript polydispersed dendrimer cluster/gel formation observed for 1:1 reaction ratios described in our earlier work [55].

Molecular weights for the final products were determined by MALDI-TOF-MS or PAGE. They were corroborated by calculated values from AFM dimension data (Table 1 and Fig. 44). These values were found to be in relatively good agreement within this series (Table 1).

Calculations based on these experimentally determined molecular weights allowed the estimation of shell filling levels for respective core-shell structures within this series. A comparison with mathematically predicted saturated shell structures reported earlier [201] indicates these core-shell structures are only partially filled (i.e., 40–66% of fully saturated values, see Table 1).

Functional groups differentiated clefts produced on the surfaces of these unique partially filled tecto(dendrimer) core-shell structures suggest rich possibilities for catalytic sites and other novel surface modifications that are presently under examination in our laboratory.

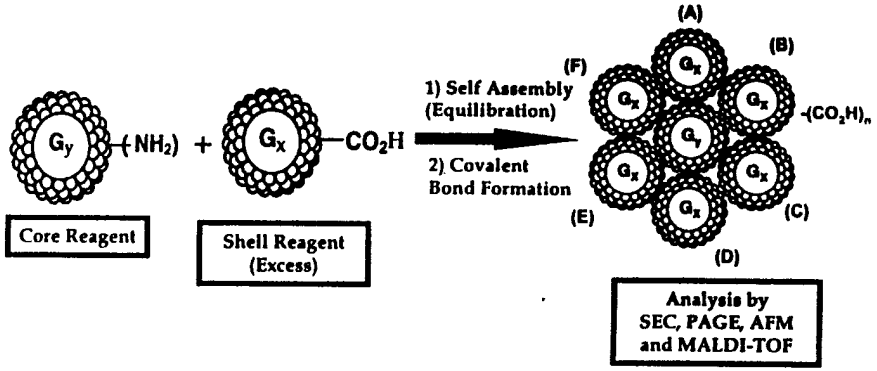

Figure 45 Self-assembly of core and shell dendrimers by charge neutralization (1) followed by covalent bond formation (2).

B. Self-Assembly with Sequential Covalent Bond Formation Method

The chemistry used in this approach involved the combination of an amine terminated dendrimer core with an excess of carboxylic acid terminated shell reagent dendrimer (Fig. 45) [203]. These two charge-differentiated species were allowed to equilibrate and self-assemble into the electrostatically driven core-shell tecto (dendrimer) architecture followed by covalent fixing of these charge-neutralized dendrimer contacts with carbodiimide reagents. Reactions were readily monitored

Table 2 Comparison of % Shell Filling as a Function of Core and Shell Dendrimers, Using the Supramolecularly Assisted Method Followed by Covalent Bond Formation

Core reagent	Shell reagent	Observed no. of parked dendrimers by mass spec.	Ideal no. of parked dendrimers[a]	Shell filling (%)
G5	G3)-COOH	10	12	83
G6	G3)-COOH	13	15	87
G7	G3)-COOH	15	19	79
G7	G5)-COOH	9	12	75

[a] Calculated using Mansfield–Tomalia–Rakesh equation for the maximum parking problem

$$N_{max} = \frac{2\pi}{\sqrt{3}}\left(\frac{r_1}{r_2} + 1\right)$$

Source: Ref. 201.

by SEC, gel electrophoresis, AFM, and MALDI-TOF mass spectroscopy. As might be expected, preliminary data show that the self-assembly method provides for more efficient parking of the dendrimer shell reagents around the core to yield very high saturation levels as shown in Table 2. Our present experimentation indicates that this method should allow the the assembly of additional shells in a very systematic fashion to produce precise nanostructures that transcend the entire nanoscale region (1–100 nm) [219].

V. OVERVIEW, PRESENT APPLICATIONS, DENDRITIC NANODEVICES

A. Overview of the Dendritic State

In summary, rheological (fluidity) investigations in our laboratories indicate that dendrimers behave like soft spherical bodies surrounded by relatively hard surface shells (i.e., like core-shell type entities) [204]. According to this emerging picture, the interiors of dendrimers may be deformable or rigid depending on the character of the monomers used in construction. The interiors may contain cavities, voids, and well-defined space capable of accommodating many small guest molecules such as solvents, dyes, and oligomers (intermediates between monomers and polymers). Guest molecules may enter or exit the dendrimer depending on their size and shape.

On the other hand, dendrimer surfaces appear to be impenetrable to other dendrimer molecules or natural and synthetic macromolecules, especially at higher generations. Dendrimers can thus be envisioned as unimolecular containers for encapsulations [36] or so-called dendrimer boxes [104]. Potential uses may include molecular delivery agents, transport vehicles, unimolecular micelles, molecule ball bearings, interphase catalysts, flow regulators in fluids, and highly monodispersed "dwarf latexes" for coatings, etc. If applications in these areas can be realized, the future of dendrimers and other polymers is very bright indeed.

Another fascinating area of dendrimer applications is based on their high surface functionality. No other class of synthetic or natural compounds contains so many reactive terminal groups per molecule as do the dendrimers. This provides major directions for possible exploitation. First, dendrimers can be modified in various ways with reagents of small molecular weight. It is thus possible to produce dendrimers with so-called *exo*-modified or differentiated surfaces. For example, attachment of catalytic or biological receptor sites suggests many possible applications. Furthermore, the dendrimer interiors may be modified in many yet specific ways. Interior differentiated dendrimers with different combinations

of radial layers or segments may be prepared by using different dendrons or parts of dendrons in their construction. Incarceration of zero valent metals or their salts (i.e., iron, copper, silver, palladium, platinum, or cadmium sulfide, etc.) suggest many uses as catalysts, magnetic dendrimers, and quantum dots.

Equally significant, is the possibility of using the dendrimer surface reactivity to open a new branch of synthetic chemistry, namely, *nanoscopic chemistry.* This would involve using dendrimers as building blocks for the preparation of even larger compounds with nanoscopic and microscopic dimensions [58,205, 206]. Such megamolecules could result from reactions between dendrimers, as described in Section IV. B, or with appropriate biological macromolecules yielding covalently bonded nanoscopic structures with hybridized architectures (i.e., linear, branched, crosslinked, or dendritic types) [125]. Of course, this present account describes the numerous possibilities based upon various molecular recognition and noncovalent bonding processes, which include both supra- and supra*macro*-molecular interactions.

Perhaps most exciting is the emerging role that dendritic architecture is playing in the role of commodity polymers. Recent reports by Guan et al. [207] have shown that ethylene monomers polymerize to dendrigraft poly(ethylene) at low pressures. This occurs when using late transition metal or Brookhart-type catalyst (Fig. 46). Furthermore, these authors also stated that small amounts of dendrigraft poly(ethylene) architecture may be expected from analogous early transition metal–metallocene catalysts.

B. Dendritic Nanodevices

Abiotic–biotic hybrids composed of dendritic polymers and natural biopolymers have already found application as nanodevices. In many instances, these dendritic nanodevices are used in abiotic–biotic molecular recognition events involving suprachemistry. One prime example is the conjugation of poly(amidoamine) dendrimers to IgG antibodies for use in diagnostic immunoassay [208]. In that work, the architecturally precise dendrimers act as a replacement for a secondary antibody by spacing the primary antibody away from the solid phase. The replacement of a secondary binding antibody dramatically reduces lot rejections in manufacture and minimizes nonspecific interactions between analytes and the immobilized antibodies. In this nanodevice, the dendrimer acts both as an antibody replacement in contact with the solid phase as well as a macromolecular spacer to hold the antibody away from the solid phase.

Dendrimers have also found application as carriers of genetic materials into cells [209,210,220]. In this usage, the dendrimers can be thought of as a histone mimetic. With appropriately charged surface groups the polycationic dendrimers form a supra*macro*molecular complex with the polyanionic nucleic acid biopolymer. This dendrimeric nanodevice transports the genetic material across cell

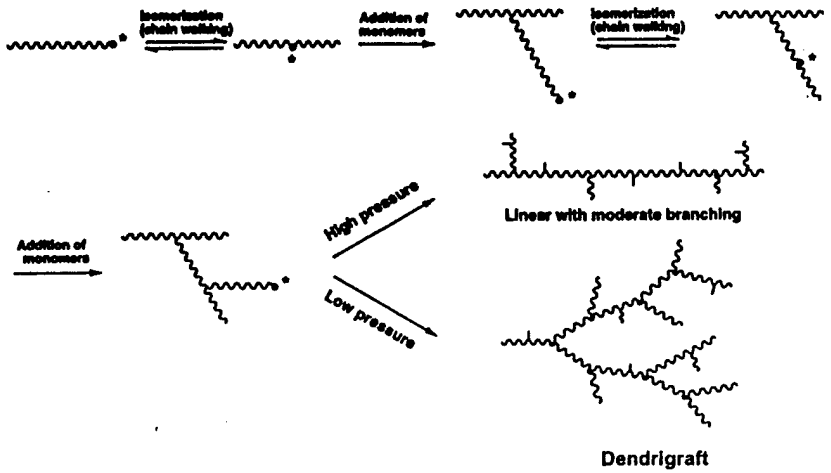

Figure 46 (a) Condensation polymerization of AB_2 monomers to give a hyperbranched polymer. Condensation of each monomer increases the active site from one to two. (b) "Self-condensing" polymerization of vinyl monomers to give a hyperbranched polymer. Addition of a new monomer increases the active site from one to two. (c) Proposed new approach to make hyperbranched polymer. The active site isomerizes to the internal backbone, and addition of monomers leads to branching.

membranes wherein the DNA is eventually incorporated into the cellular expression machinery to generate protein.

Dendrimer-based nanodevices have also found application in magnetic resonance imaging [211]. Dendrimer–chelate conjugates have been prepared that are extraordinarily robust complexes of gadolinium ions. The size of the dendrimer–gadolinium complexes allows sufficiently long residence times in the bloodstream for appropriate imaging studies. Furthermore, the nuclear relaxation parameters are dramatically enhanced when compared to conventional MRI contrast systems. Higher complexity conjugates have been prepared with target directors to introduce biotic molecular recognition functionality into these conjugates [211].

Dendritic polymers may also have application in the delivery of anticancer agents [212]. Dendrimers have been shown to selectively deliver a high payload of traditional chemotherapeutic agents, such as cisplatin, to a tumor [213]. Blood vessels in tumors have a higher permeability and poorer lymphatic drainage than vessels in normal tissue. This enhanced permeability and retention effect (EPR effect) allows selective delivery of a drug to a tumor, and has been demonstrated with nondendritic polymer–antitumor agent conjugates [213].

Dendrimer–saccharide conjugates are unique nanodevices in their ability to tightly bind lectins and other proteins with specific saccharide recognition capabilities [174]. The multivalency of dendrimer surfaces allows for a cooperative binding effect. Where single saccharide-receptor interactions are relatively weak, the multiplicity of poly(valent) interactions introduced by conjugating a

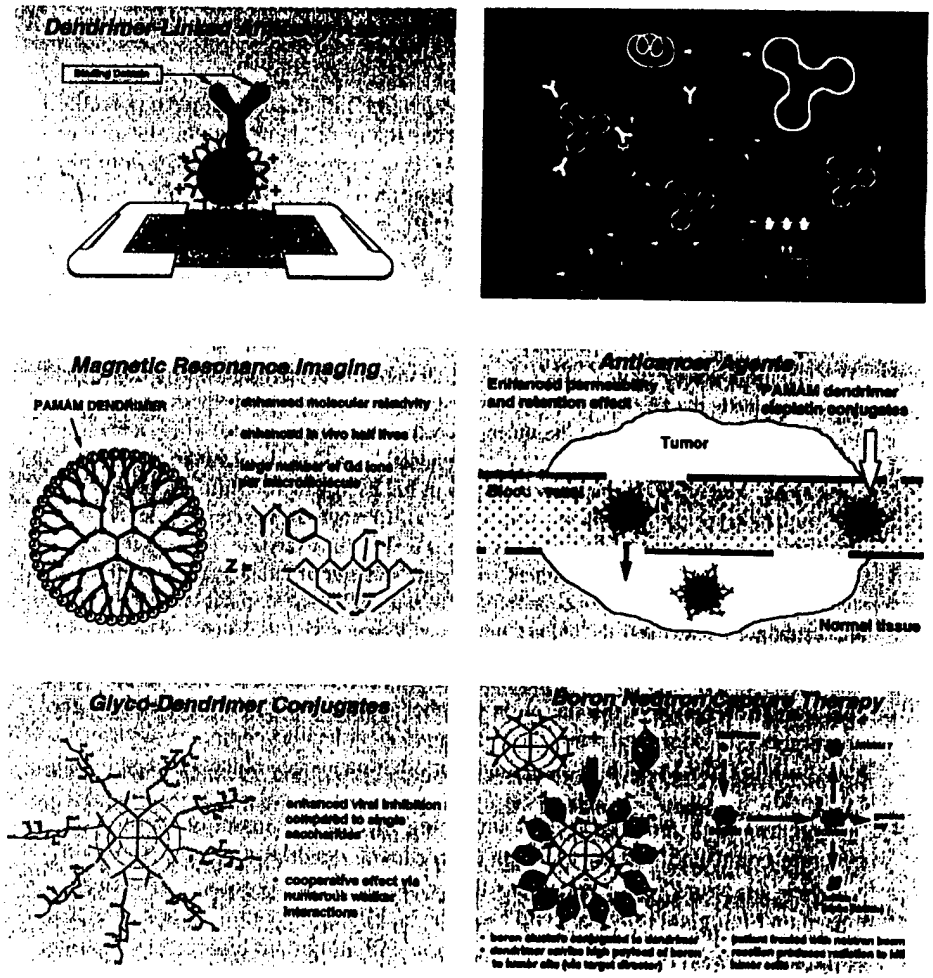

Figure 47 Some current nanobiological devices utilizing dendritic polymers.

large number of sugars onto a single dendrimer particle yields a cooperative unimolecular binding event that is thermodynamically much more favorable.

Dendritic polymers offer the potential to serve as amplifiers in a variety of applications. Researchers in boron neutron capture therapy have investigated the potential of dendrimers to deliver a large payload of boron to tumor sites by conjugating a large number of boron clusters to the surface of a dendrimer [214]. When irradiated with a neutron beam, the high cross-section of boron captures sufficient energy to produce a secondary radiation of sufficient energy to damage cells in the immediate vicinity of the boron. Again, conjugates with higher specificity can be prepared by introduction of target receptors [21].

Although many of the above examples are in the early stages of development, they have clearly demonstrated concepts that illustrate the current potential for dendrimers in a variety of nanodevices, many of them supramolecular or supra*macro*molecular in nature. Figure 47 is a pictorial summary of some of these nanobiological devices. Further information on the individual concepts may be found in the literature [34,215,216].

VI. THE FUTURE/CONCLUSIONS

> Nature is a very strange affair, and the strangeness already encountered by our friends the physicists are banalities compared to the queer things being glimpsed in biology, and the much queerer things that lie ahead.
>
> As these turn up . . . they will inevitably change the way the world looks. And when this happens, the view of life itself will also shift; old ideas will be set aside; the look of a tree will be a different look; the connectedness of all the parts of nature will become a reality for everyone, not just the mystics, to think about; painters will begin to paint differently; music will change from what it is to something new and unguessed at; poets will write stranger poems; and the culture will begin a new cycle of change.
>
> Lewis Thomas, 1985

This quotation conveys the daunting prophesies that may be expected from the convergence of supramolecular and supra*macro*molecular chemistry with nanoscale building blocks such as dendrimers or other nanoscale objects in the biological world.

It was both remarkable and surprising to find that many of these abiotic structure-controlled macromolecules (dendrimers, dendrigrafts, etc.) possess topologies, functions, and dimensions that scale very closely to a wide variety of important biological polymers and assemblies. Figure 48 compares poly(amidoamine) dendrimers as a function of generation with important biological structures that are both conserved and essential for life in the plant, as well as the animal, kingdom. History has shown that the introduction of traditional synthetic polymer

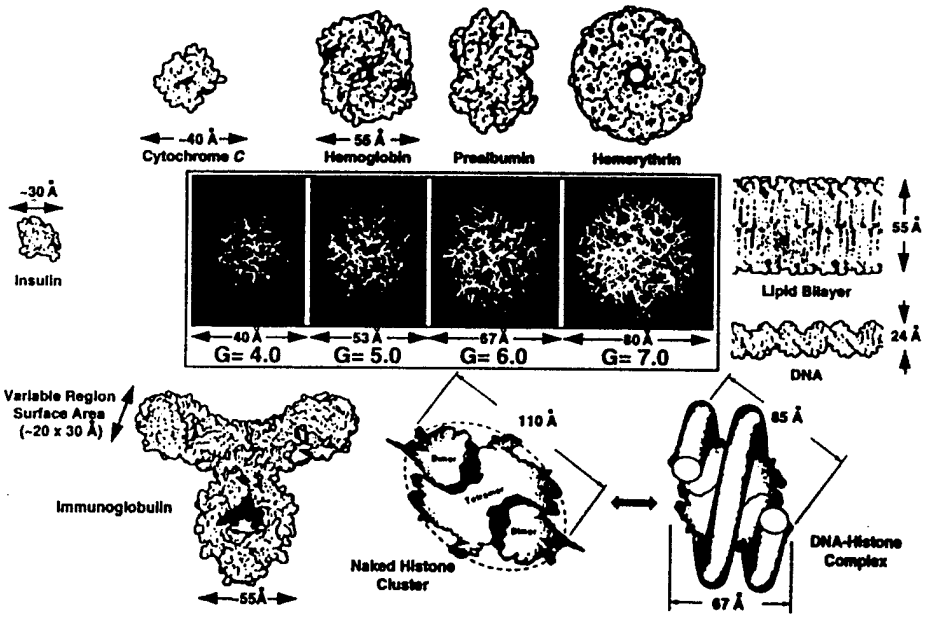

Figure 48 Scaled comparison of tridendron (NH_3 core) poly(amidoamine) dendrimers; generation = 4–7, sizes and shapes with various proteins. (Courtesy of J Mater Chem 1997, 7 (7), 1199. Copyright Royal Society of Chemistry.)

architectures (i.e., linear, crosslinked, etc.) by Staudinger, Carothers, Flory, and others [41,217] provided the basis for the replacement of many natural polymers (i.e., silk, rubber, cotton, etc.) accompanied by many improvements and advantages. With the present understanding of the covalent, supramolecular, and supra*macro*molecular chemistry of both traditional and dendrimeric systems, it is now possible to visualize new architectural possibilities. This area will undoubtedly provide the enabling science for the replacement of many biological nanostructures such as histones, antibodies, hemoglobin, etc. [219]. In fact, recent developments are driving this new and emerging area of science, which is now being referred to as nanoscopic chemistry, biologic nanotechnology, or nanobiology. Briefly defined, it is the science of understanding covalent, structure-controlled synthesis, and characterization, combining rules and the supramolecular/supra*macro*molecular dynamics of molecules and assemblies that manifest complexity and dimensions greater than traditional chemistry [20,218]. This new chemical science will undoubtedly evolve the necessary molecular level understanding to create requisite bridges to biology. These new connections to biology may lead

one to expect many new paradigm shifts in the treatment and remediation of acute/chronic diseases, genetic defects, and enhancements of longevity (aging) leading to improvements in the human condition, as well as the biological environment in general.

Recent successes in the development of dendritic nanodevices reveal progress in this endeavor. It will not be surprising to see the evolution of synthetic immunosystems, gene expression protocol based on artificial histones, or the treatment of cancer with dendritic nanodevices in the foreseeable future.

As proposed earlier, dendritic biomimicry especially as it relates to dimensional size scaling, macromolecular structure control, shape/topological matching, genealogical sequencing, exponential amplification/polyvalency (hypercooperativity), site isolation, unimolecular encapsulation, and self-assembly are now possible with dendritic structures and architecture. In many cases, this mimicry has already been demonstrated in preliminary form (Fig. 47). Recent demonstration of these analogies not only has fulfilled some unexpected prophecies but also more importantly has set the stage (or the table) for an unimaginable banquet of new discoveries and properties. It is hoped that these endeavors will provide solutions to problems that presently plague and hamper the enhancement of the human condition.

Furthermore, we predict that the dendritic state will undoubtedly provide the quintessential scientific bridge by which abiotic molecular level scientists will be able to communicate and collaborate on such critical issues as disease control, increased agricultural production, and finally longevity, with enhanced quality of life. It is with these thoughts and premises that we should be very excited about the future of dendritic macromolecular technology and the role its supraproperties will provide as we enter the next millennium.

ACKNOWLEDGMENTS

The authors would like to thank the U.S. Army Research Laboratory (ARL/MMI Dendritic Polymer Center of Excellence), especially Dr. G. Hagnauer, and Edgewood Research, Dev. & Eng. Center (ERDEC), especially Dr. D. Durst, for financial support of this research and Ms. Linda S. Nixon for manuscript and graphics preparation.

REFERENCES

1. B Pullman. The Atom in the History of Human Thought. New York: Oxford University Press, 1998.
2. SE Mason. Chemical Evolution. Oxford: Clarendon, Oxford University Press, 1991.

3. M Eigen, W Gardiner, P Schuster, R Winkler-Oswatitsch. Evolution Now. New York: Freeman, 1982.
4. M Eigen. Naturwissenschaften 10:465, 1971.
5. H Kuhn, J Waser. Angew Chem Int Ed 20:500, 1981.
6. I Prigogine. Physics Today 25(12):38, 1972.
7. Webster's Third New International Dictionary. Springfield, MA: G & C Merriam, 1981.
8. B Alberts, D Bray, J Lewis, M Raff, K Roberts, JD Watson. Molecular Biology of the Cell. New York, London: Garland, 1994.
9. J Darnell, H Lodish, D Baltimore. Molecular Cell Biology. New York: Scientific American Books, 1986.
10. GF Joyce. Scientific American 90, 1992.
11. HW Salzburg. From Caveman to Chemist. Washington DC: American Chemical Society, 1991.
12. JM Lehn. Angew Chem Int Ed 27:89, 1988.
13. GW Gokel. Crown Ethers & Cryptands. Cambridge, UK: Royal Society of Chemistry, 1991.
14. GR Newkome, CN Moorfield, F Vogtle. Dendritic Molecules. Weinheim: VCH, 1996.
15. D Philip, JF Stoddart. Synlett 7:445, 1991.
16. PR Ashton, NS Isaacs, FH Kohnke, JP Mathias, JF Stoddart. Angew Chem Int Ed 28:1258, 1989.
17. PR Ashton, NS Isaacs, FH Kohnke, GS D'Alcontres, JF Stoddart. Angew Chem Int Ed 28:1261, 1989.
18. FH Kohnke, JP Mathias, JF Stoddart. Molecular Recognition: Chemical and Biochemical Problems. Cambridge, UK: Royal Society of Chemistry, 1989.
19. FH Kohnke, JP Mathias, JF Stoddard. Angew Chem Adv Mater 101:1129, 1989.
20. M Freemantle. Chem Eng News (April 19):51–58, 1999.
21. CM Drain, F Nifiatis, A Vasenko, JD Batteas. Angew Chem Int Ed 37:2344, 1998.
22. CM Drain, JMJ Lehn. J Chem Soc Chem Commun 2313, 1994.
23. RW Wagner, J Seth, SI Yang, D Kim, DF Bocian, D Holten, JS Lindsey. J Org Chem 63:5042, 1998.
24. RV Slone, JT Hupp. Inorg Chem 36:5422, 1997.
25. CM Drain, KS Russell, JM Lehn. Chem Commun 337, 1996.
26. E Alessio, M Macchi, S Heath, LG Marzilli. J Chem Soc Chem Commun 1411, 1996.
27. E Alessio, M Macchi, S Heath. J Chem Soc Chem Commun 36:5614, 1997.
28. Y Kobuke, H Miyaji. Bull Chem Soc Japan 69:3563, 1996.
29. RT Stibrany, J Vasudevan, S Knapp, JA Potenza, T Emge, HJ Schugar. J Am Chem Soc 118:3980, 1996.
30. H Tamiaki, T Miyatake, R Tanikaga, AR Holzwarth, K Schaffner. Angew Chem Int Ed 35:772, 1996.
31. DB Amabilino, CO Dietrich-Bucheker, J-P Sauvage. J Am Chem Soc 188:3285, 1996.
32. S Anderson, HL Anderson, JKM Sanders. Acc Chem Res 26:469, 1993.
33. E Buhleier, W Wehner, F Vögtle. Synthesis 155, 1978.

34. DA Tomalia, R Esfand. Chem Industry 11(2 June):416–420, 1997.
35. DA Tomalia, HD Durst. Genealogically Directed Synthesis: Starburst/Cascade Dendrimers and Hyperbranched Structures. In: E Weber ed. Topics in Current Chemistry vol. 165. Supramolecular Chemistry I—Directed Synthesis and Molecular Recognition, Berlin, Heidelberg: Springer-Verlag, 1993, pp 193–313.
36. DA Tomalia, AM Naylor, WA Goddard III. Angew Chem Int Ed Engl 29(2):138–175, 1990.
37. J Fendler. Membrane Mimetic Chemistry: Characterization and Applications of Micelles, Microemulsions, Monolayers, Bilayers, Vesicles, Host Guest Systems and Polyions. Chichester: Wiley Interscience, 1982.
38. C Tschierske. J Mater Chem 8(7):1485–1508, 1998.
39. C Tanford. The Hydrophobic Effect: Formation of Micelles and Biological Membranes. New York: Wiley, 1973.
40. Macromolekulare Chemie—Das Werk Hermann Staudingers in Seiner Heutigen Bedeutung. Munchen: Schnell und Steiner, 1967.
41. H Morawetz. Polymers: The Origin and Growth of a Science. Chichester, UK: Wiley, 1985.
42. HL Hsieh, RP Quirk. Anionic Polymerization: Principles and Practical Applications. New York: Marcel Dekker, 1996.
43. K Matyjaszewski. Cationic Polymerizations: Mechanisms, Synthesis, and Applications., New York: Marcel Dekker, 1996, pp 1–768.
44. K Matyjaszewski. Controlled Radical Polymerization, ACS Symposium Series 685, vol. 685. Washington, DC: ACS, 1997.
45. K Hatada, T Kitayama, O Vogl. Macromolecular Design of Polymeric Materials. New York: Marcel Dekker, 1997.
46. RB Merrifield. J Am Chem Soc 85:2149–2154, 1963.
47. RB Merrifield. Science 232:341–347, 1986.
48. MK Lothian-Tomalia, DM Hedstrand, DA Tomalia. Tetrahedron 53(45):15495–15513, 1997.
49. DA Tomalia. Scientific American 272(5):62–66, 1995.
50. DA Tomalia. Macromol Symp 101:243–255, 1996.
51. AK Naj. Persistent Inventor Markets a Molecule. In: The Wall Street Journal, New York, 1996, pp B1.
52. JMJ Fréchet. Science 263:1710–1715, 1994.
53. K Dusek. TRIP 5(8):268–274, 1997.
54. S Uppuluri, DR Swanson, HM Brothers II, LT Piehler, J Li, DJ Meier, GL Hagnauer, DA Tomalia. Poly Mater Sci Eng (ACS) 80:55–56, 1999.
55. DA Tomalia, DM Hedstrand, LR Wilson. Dendritic Polymers. In: Encyclopedia of Polymer Science and Engineering, vol. index volume. 2nd ed. New York: Wiley, 1990, pp 46–92.
56. F Zeng, SC Zimmerman. Chem Rev 97:1681–1712, 1997.
57. OA Matthews, AN Shipway, JF Stoddart. Prog Polym Sci 23:1–56, 1998.
58. DA Tomalia. Adv Mater 6(7/8):529–539, 1994.
59. GJ Kallos, DA Tomalia, DM Hedstrand, S Lewis, J Zhou. Rapid Commun Mass Spectrometry 5:383–386, 1991.
60. PR Dvornic, DA Tomalia. Macromol Symp 98:403–428, 1995.

61. HM Brothers II, LT Piehler, DA Tomalia. J Chromatography A 814:233–246, 1998.
62. DA Tomalia, H Baker, J Dewald, M Hall, G Kallos, S Martin, J Roeck, J Ryder, P Smith. Polym J (Tokyo) 17:117–132, 1985.
63. DA Tomalia, JR Dewald, MJ Hall, SJ Martin, PB Smith. Preprints of the First SPSJ International Polymer Conference, Society of Polymer Science, Kyoto, Japan, 65, 1984.
64. DA Tomalia. Akron Polymer Lecture Series, Akron, OH, April, 1984.
65. DA Tomalia. Flory–Pauling Macromolecular Conference—Frontiers in Synthetic Polymer Chemistry, Santa Barbara, CA, January, 1983.
66. DA Tomalia. Sixth Biennial Carl S. Marvel Symposium—Advances in Synthetic Polymer Chemistry, Tucson, AZ, March, 1985.
67. DA Tomalia. ACS Great Lakes/Central Regional Meeting, Kalamazoo, MI, May, 1984.
68. BJ Bauer, A Topp, TJ Prosa, EJ Amis, R Yin, D Qin, DA Tomalia. Polym Materials Sci Eng (ACS) 77:87–88, 1997.
69. AB Padias, HKH Jr. J Org Chem 52:5305–5312, 1987.
70. PG de Gennes, H Hervet. J Physique Lett 44:351–360, 1983.
71. AD Meltzer, DA Tirrell, AA Jones, PT Inglefield, DA Tomalia, DM Hedstrand. Macromolecules 25:4541–4548, 1992.
72. L Balogh, DA Tomalia. J Am Chem Soc 120:7355–7356, 1998.
73. KB Mullis, FA Faloona. Methods Enzymol 155:335, 1987.
74. SC Zimmerman, F Zeng, EC Reichert, SV Kolotuchin. Science 271:1095–1098, 1996.
75. M Conn, J Rebek, Jr. Chem Rev 97:1647–1668, 1997.
76. V Balzani, G Denti, S Serroni, S Campagna, V Ricevuto, A Juris. Proc Indian Acad Sci Chem Sci 105:421–434, 1993.
77. V Balzani, S Campagna, G Denti, A Juris, S Serroni, M Venturi. Coord Chem Rev 132:1–13, 1994.
78. V Balzani, S Campagna, G Denti, A Juris, S Serroni, M Venturi. Sol Energy Mater Sol Cells 38:159–173, 1995.
79. S Campagna, G Denti, S Serroni, A Juris, M Venturi, V Ricevuto, V Balzani. Chem Eur J 1:211–221, 1995.
80. A Juris, M Venturi, L Pontoni, IR Resino, V Balzani, S Serroni, S Campagna, G Denti. Can J Chem 1875–1882, 1995.
81. S Serroni, G Denti, S Campagna, A Juris, M Ciano, V Balzani. Angew Chem Int Ed Engl 31:1493–1495, 1992.
82. S Serroni, S Campagna, A Juris, M Venturi, V Balzani. Gazz Chim Ital 124:423–427, 1994.
83. S Achar, RJ Puddephatt. J Chem Soc Chem Commun 1895–1896, 1994.
84. S Achar, RJ Puddephatt. Angew Chem Int Ed Engl 33:847–849, 1994.
85. S Achar, JJ Vittal, RJ Puddephatt. Organometallics 15:43–50, 1996.
86. WTS Huck, FCJM van Veggel, BL Kropman, DHA Blank, EG Keim, MMA Smithers, DN Reinhoudt. J Am Chem Soc 117:8293–8294, 1995.
87. WTS Huck, FCJM van Veggel, DN Reinhoudt. Angew Chem Int Ed Engl 35:1213–1215, 1996.

88. WTS Huck, R Hulst, P Timmerman, FCJM van Veggel, DN Reinhoudt. Angew Chem Int Ed Engl 36:1006–1008, 1997.
89. WTS Huck, FCJM Van Veggel, DNJ Reinhoudt. J Mater Chem 7:1213–1219, 1997.
90. WTS Huck, LJ Prins, RH Fokkens, NMM Nibbering, FCJM Van Veggel, DN Reinhoudt. J Am Chem Soc 120:6240–6246, 1998.
91. GR Newkome, ZQ Yao, GR Baker, VK Gupta. J Org Chem 50:2003–2004, 1985.
92. CL Jackson, HD Chanzy, FP Booy, BJ Drake, DA Tomalia, BJ Bauer, EJ Amis. Macromolecules 31(18):6259–6265, 1998.
93. JCM van Hest. New Molecular Architectures Based on Dendrimers. PhD dissertation, Eindhoven University, Eindhoven, The Netherlands, 1996.
94. PE Eaton, TW Cole. J Am Chem Soc 86:962–964, 1964.
95. PE Eaton, YS Or, SJ Branka, BKR Shanker. Tetrahedron 42:1621, 1986.
96. LA Paquette, RJ Ternansky, DW Balogh, G Krentgen. J Am Chem Soc 105:5446, 1983.
97. DJ Cram. Science 219:1177, 1983.
98. DJ Cram, JM Cram. Container Molecules and Their Guests. Cambridge, UK: The Royal Society of Chemistry, 1994.
99. RF Curl, RE Smalley. Science 242:1017–1022, 1988.
100. L Balogh, DR Swanson, R Spindler, DA Tomalia. Poly Mater Sci Eng (ACS) 77: 118–119, 1997.
101. M Zhao, L Sun, RM Crooks. J Am Chem Soc 120(19):4877–4878, 1998.
102. NC Beck Tan, L Balogh, SF Trevino, DA Tomalia, JS Lin. Polymer 40:2537–2545, 1999.
103. L Balogh, R Valluzzi, KS Laverdure, SP Gido, GL Hagnauer, DA Tomalia. J Nanoparticle Res 00:1–16, 1999.
104. JFGA Jansen, EMM de Brabander-van den berg, EW Meijer. Science 266:1226–1229, 1994.
105. JFGA Jansen, EW Meijer, EMM de Brabander-van den Berg. J Am Chem Soc 117:4417–4418, 1995.
106. EMM de Brabander-van den Berg, A Nijenhuis, M Mure, J Keulen, R Reintjens, F Vandenbooren, B Bosman, R De Raat, T Frijns, S Wal. Macromol Symposia 77: 51–62, 1994.
107. DA Tomalia, H Baker, J Dewald, M Hall, G Kallos, S Martin, J Roeck, J Ryder, P Smith. Macromolecules 19:2466–2468, 1986.
108. DA Tomalia, M Hall, DM Hedstrand. J Am Chem Soc 109:1601–1603, 1987.
109. RG Denkewalter, JF Kole, WJ Lukasavage. U.S. Pat. 4410688. 1983.
110. RG Denkewalter, JF Kole, WJ Lukasavage. Chem Abstr 100:103907, 1984.
111. SM Aharoni, CR Crosby III, EK Walsh. Macromolecules 15:1093–1098, 1982.
112. SM Aharoni, NS Murthym. Polym Commun 24:132, 1983.
113. DA Tomalia, V Berry, M Hall, DM Hedstrand. Macromolecules 20:1164–1167, 1987.
114. DA Tomalia, DM Hedstrand, LR Wilson, DM Downing. Starburst Dendrimers: Size, Shape and Surface Control of Macromolecules. In: T Saegusa, T Higashimura, and A Abe, eds. Frontiers of Macromolecular Science, 32nd IUPAC Proceedings, Blackwell Publications, 1989, 207–212.

115. AM Naylor, WA Goddard III, GE Kiefer, DA Tomalia. J Am Chem Soc 111:2339–2341, 1989.
116. GR Newkome, CN Moorfield, GR Baker, AL Johnson, RK Behera. Angew Chem Int Ed 30(9):1176–1180, 1991.
117. MC Moreno-Bondi, G Orellana, NJ Turro, DA Tomalia. Macromolecules 23:910–912, 1990.
118. NJ Turro, JK Barton, DA Tomalia. Acc Chem Res 24(11):332–340, 1991.
119. KR Gopidas, AR Leheny, G Caminati, NJ Turro, DA Tomalia. J Am Chem Soc 113:7335–7342, 1991.
120. D Watkins, Y Sayed-Sweet, JW Klimash, NJ Turro, DA Tomalia. Langmuir 13: 3136–3141, 1997.
121. DM Hedstrand, BJ Helmer, DA Tomalia. U.S. Pat. 5,560,929. 1996.
122. Y Sayed-Sweet, DM Hedstrand, R Spindler, DA Tomalia. J Mater Chem 7(7): 1199–1205, 1997.
123. S Stevelmans, JCM van Hest, JFGA Jansen, DAFJ van Boxtel, EMM de Brabander-van den Berg, EW Meijer. J Am Chem Soc 118:7398–7399, 1996.
124. AI Cooper, JD Londono, G Wignall, JB McClain, ET Samulski, JS Lin, A Dobrynin, M Rubinstein, ALC Burke, JMJ Fréchet, JM DeSimone. Nature 389(September 25):368–371, 1997.
125. R Yin, Y Zhu, DA Tomalia. J Am Chem Soc 120:2678–2679, 1998.
126. DB Amabilino, PR Ashton, M Belohradsky, FM Raymo, JF Stoddart. J Chem Soc Chem Commun 751–753, 1995.
127. DB Amabilino, PR Ashton, V Balzani, CL Brown, A Credi, JMJ Fréchet, JW Leon, FM Raymo, N Spencer, JF Stoddart, M Venturi. J Am Chem Soc 118:12012–12020, 1996.
128. FM Menger, CA Littau. J Am Chem Soc 115:10083–10090, 1993.
129. Anionic Surfactants, Physical Chemistry of Surfactant Action. Surfactant Series vol. 11. New York: Marcel Dekker, 1981.
130. S Buckingham, C Garvey, G Warr. J Phys Chem 97:10236–10244, 1993.
131. J Israelachvili, D Mitchell, B Ninham. J Chem Soc Faraday Trans II 72:1525, 1976.
132. SE Friberg, M Podzimek, DA Tomalia, DM Hedstrand. Mol Cryst Liq Cryst 164: 157–165, 1988.
133. H Smith, DA Tomalia. U.S. Pat. 5,331,100. 1994.
134. T Chapman, G Hillyer, E Mahan, K Shaffer. J Am Chem Soc 116:11195–11196, 1994.
135. I Gitsov, KL Wooley, JMJ Fréchet. Angew Chem Int Ed Eng 31(9):1200–1202, 1992.
136. I Gitsov, KL Wooley, CJ Hawker, PT Ivanova, JMJ Fréchet. Macromolecules 26: 5621–5627, 1993.
137. CJ Hawker, KL Wooley, JMJ Fréchet. J Chem Soc Perkin Trans I:1287–1297, 1993.
138. KL Wooley, CJ Hawker, JMJ Fréchet. J Am Chem Soc 115:11496–11505, 1993.
139. JN Israelachvili, D Mitchell, B Ninham. Biophys Acta 470:158, 1977.
140. JN Israelachvili, S Marcelja, R Horn. Rev Biophys (13):121, 1980.
141. GR Newkome, GR Baker, S Arai, MJ Saunders, PS Russo, KJ Theriot, CN Moore-

field, LE Rogers, JE Miller, TR Lieux, ME Murray, B Philips, L Pascal. J Am Chem Soc 112:8458–8465, 1990.
142. DA Tomalia, P Kirchoff. U.S. Pat. 4,694,064. 1987.
143. I Neubert, E Amoulong-Kirstein, A-D Schluter. Macromol Rapid Commun 17: 517–527, 1996.
144. I Neubert, R Klopsch, W Claussen, A-D Schluter. Acta Polymer 47:455–459, 1996.
145. B Karakaya, W Claussen, K Gessler, W Saenger, A-D Schluter. J Am Chem Soc 119:3296–3301, 1997.
146. W Stocker, B Karakaya, LB Schurmann, PJ Rabe, A-D Schluter. J Am Chem Soc 120:7691–7695, 1998.
147. JMJ Fréchet, I Gitsov. Macromol Symp 98:441–465, 1995.
148. G Johansson, V Percec, G Ungar, JP Zhou. Macromolecules 29:646–660, 1996.
149. V Percec, D Schlueter, JC Ronda, G Johansson, G Ungar, JP Zhou. Macromolecules 29:1464–1472, 1996.
150. V Percec, D Schlueter. Macromolecules 30:5783–5790, 1997.
151. S Bauer, H Fischer, H Ringsdorf. Angew Chem Int Ed Engl 32:1589, 1993.
152. V Percec, P Chu, G Johansson, D Schlueter, JC Ronda, G Ungar. Polym Prepr 37: 68, 1996.
153. V Percec, M Kawasumi. Macromolecules 25:3843, 1992.
154. V Percec, P Chu, M Kawasumi. Macromolecules 27:4441, 1994.
155. V Percec, P Chu, G Ungar, J Zhou. J Am Chem Soc 117:11441, 1995.
156. V Percec, G Johansson, G Ungar, JP Zhou. J Am Chem Soc 118:9855–9866, 1996.
157. SD Hudson, H-T Jung, V Percec, W-D Cho, G Johansson, G Ungar, VSK Balaguru-samy. Science 278:449–452, 1997.
158. JH Cameron, A Facher, G Lattermann, S Diele. Adv Mater 9(5):398–403, 1997.
159. V Percec, C-H Ahn, G Ungar, DJP Yeardly, M Moller. Nature 391:161–164, 1998.
160. DLD Gasper. Biophys J 32:103–138, 1980.
161. JD Watson. Molecular Biology of the Gene. W.A. Benjamin, Menlo Park, CA, 1976.
162. AJ Levine. Viruses. New York: W.H. Freeman, 1992.
163. V Percec, C-H Ahn, W-D Cho, G Johansson, D Schlueter. Macromol Symp 118: 33–43, 1997.
164. V Percec, C-H Ahn, B Barboiu. J Am Chem Soc 119:12978–12979, 1997.
165. LL Kiessling, NL Pohl. Chem Biol 3:71–77, 1996.
166. M Mammen, SK Choi, GM Whitesides. Angew Chem Int Ed Eng 37:2754–2794, 1998.
167. SK Choi, M Mammen, M Whitesides. Chem Biol 3:97–104, 1996.
168. KH Mortell, M Gingras, LL Kiessling. J Am Chem Soc 116:12053–12054, 1994.
169. C Fraser, RH Grubbs. Macromolecules 28:7248–7255, 1995.
170. KH Mortell, RV Weatherman, LL Kiessling. J Am Chem Soc 118:2297–2298, 1996.
171. R Roy. J Chem Soc Chem Comm 1869–1872, 1993.
172. R Roy, WKC Park, Q Wu, SN Wany. Tetrahedron 36:4377–4380, 1995.
173. R Roy. Polym News 21(7):226–232, 1996.
174. JD Reuter, A Myc, MM Hayes, Z Gan, R Roy, D Qin, R Yin, LT Piehler, R Esfand, DA Tomalia, J Baker, J.R. Bioconjugate Chem 10(2):271–278, 1999.

175. DA Tomalia, DM Hedstrand, MS Ferritto. Macromolecules 24:1435–1438, 1991.
176. PM Saville, JW White, CJ Hawker, KL Wooley, JMJ Fréchet. J Phys Chem 97: 293–294, 1993.
177. PM Saville, PA Reynolds, JW White, CJ Hawker, JMJ Fréchet, KL Wooley, J Pemford, JRP Webster. J Phys Chem 99:8283–8289, 1995.
178. JP Kampf, CW Frank, EE Malmstrom, CJ Hawker. Langmuir 15:227–233, 1999.
179. JP Kampf, CW Frank, EE Malmstrom, CJ Hawker. Science 282:1730–1733, 1999.
180. APHJ Schenning, C Ellisen-Roman, J-W Weener, MWPL Baars, SJ van der Gast, EJ Meier. J Am Chem Soc 120:8199–8208, 1998.
181. DA Tomalia, G Killat. U.S. Pat. 4,871,779. 1989.
182. ML Mansfield. Polymer 37:3835–3841, 1996.
183. S Watanabe, SL Regen. J Am Chem Soc 116:8855–8856, 1994.
184. M Zhao, H Tokuhisa, RM Crooks. Angew Chem Int Ed Engl 36:2596–2598, 1997.
185. A Hierlemann, JK Campbell, LA Baker, RM Crooks, AJ Ricco. J Am Chem Soc 120:5323–5324, 1998.
186. VV Tsukruk, F Rinderspacher, VN Bliznyuk. Langmuir 13:2171–2176, 1997.
187. VV Tsukruk. Adv Mater 10:253–257, 1998.
188. VN Bliznyuk, F Rinderspacher, VV Tsukruk. Polymer 39:5249–5252, 1998.
189. JMJ Fréchet, T Emrick. Curr Opin Colloid Interface Sci, 4:1999.
190. DC Tully, AR Trimble, JMJ Fréchet. Polym Prepr (ACS) 40(1):402–403, 1999.
191. N Tomioka, D Takasu, T Takahashi, T Aida. Angew Chem Int Ed 37(11):1531–1534, 1998.
192. LL Miller, RG Duan, DC Tulley, DA Tomalia. J Am Chem Soc 119(5):1005–1010, 1997.
193. F Wang, RD Rauh, TL Rose. J Am Chem Soc 119:11106–11107, 1997.
194. G Galileo. Dialogue Concerning the Two Chief World Systems: Ptolemaic and Copernican. Berkeley: University of California Press, 1967.
195. N Bohr. Nobel Laureate Lecture. 1922.
196. T Martin, U Obst, J Rebek, Jr. Science 281(September 18):1842–1845, 1998.
197. X Camps, H Schonberger, A Hirsch. Chem Eur J 3(4):561–567, 1997.
198. DA Tomalia, PR Dvornic. Dendritic Polymers, Divergent Synthesis (Starburst Polyamidoamine Dendrimers). In: JC Salamone, ed. Polymeric Materials Encyclopedia, vol. 3 (D–E). Boca Raton, FL: CRC Press, 1996.
199. A Topp, BJ Bauer, DA Tomalia, EJ Amis. Macromolecules 32:7232–7237, 1999.
200. A Topp, BJ Bauer, JW Klimash, R Spindler, DA Tomalia, EJ Amis. Macromolecules 32:7226–7231, 1999.
201. ML Mansfield, L Rakesh, DA Tomalia. J Chem Phys 105(8):3245–3249, 1996.
202. DA Tomalia, S Uppuluri, DR Swanson, HM Brothers II, LT Piehler, J Li, DJ Meier, GL Hagnauer, L Balogh. Dendritic Macromolecules: A Fourth Major Class of Polymer Architecture—New Properties Driven by Architecture. Boston: Materials Research Society, 1998.
203. S Uppuluri, DA Tomalia. Adv Matrls (in press).
204. S Uppuluri, SE Keinath, DA Tomalia, PR Dvornic. Macromolecules 31:4498–4510, 1998.
205. DA Tomalia. Dendrimers: Nanoscopic Modules for the Construction of Higher Ordered Complexity. In: J Michl ed. Modular Chemistry, Proceedings of the NATO

Advanced Research Workshop on Modular Chemistry, The Netherlands: Kluwer Academic 1997, 183–191.
206. PR Dvornic, DA Tomalia. Macromol Symp 88:123–148, 1994.
207. Z Guan, PM Cotts, EF McCord, SJ McLain. Science 283:2059–2062, 1999.
208. P Singh. Bioconjugate Chem 9:54–63, 1998.
209. A Bielinska, JF Kukowska-Latallo, J Johnson, DA Tomalia, J Baker, Jr. Nucleic Acids Res 24(11):2176–2182, 1996.
210. JF Kukowska-Latallo, AU Bielinska, J Johnson, R Spindler, DA Tomalia, J Baker, Jr. Proc Natl Acad Sci 93:4897–4902, 1996.
211. EC Wiener, MW Brechbiel, H Brothers, RL Magin, OA Gansow, DA Tomalia, PC Lauterbur. Magnetic Resonance Medicine 31(1):1–8, 1994.
212. DS Wilbur, PM Pathare, DK Hamlin, KR Buhler, RL Vesella. Bioconjugate 9: 813–825, 1998.
213. R Duncan. Polym Prepr (ACS) 40(1):285–286, 1999.
214. AH Soloway, W Tjarks, BA Barnum, F-G Rong, RF Barth, IM Codogni, JG Wilson. Chem Rev 98:1515–1562, 1998.
215. C Biemiaz. Dendrimers: Applications to Pharmaceutical and Medicinal Chemistry. In: Encycl of Pharm, Tech, vol. 18. New York: Marcel Dekker, 1998.
216. DA Tomalia, HM Brothers II. Regiospecific Conjugation to Dendritic Polymers to Produce Nanodevices. In: SC Lee and LM Savage, eds. Biological Molecules in Nanotechnology: Convergence of Biotechnology, Polymer Chemistry and Materials Science, vol. 1927. Southborough, MA: IBC, 1998.
217. ME Hermes. Enough for One Lifetime: Wallace Carothers, Inventor of Nylon. American Chemical Society and Chemical Heritage Foundation, 1996.
218. N Zimmerman, JS Moore, SC Zimmerman. Chem Industry (August 3):604–610, 1998.
219. M Freemantle. Chem Eng News (November 1), 77:27–35, 1999.
220. SK Ritter. Chem Eng News (November 8), 77:30–35, 1999.
221. M Kawa and JMJ Fréchet. Chem Mater 10:286–296, 1998.
222. PE Froehling, HAJ Linssen. Macromol Chem Phys 199:1691–1695, 1998.

10

Self-Assembled Monolayers (SAMs) and Synthesis of Planar Micro- and Nanostructures

Lin Yan
Bristol-Myers Squibb, Princeton, New Jersey

Wilhelm T. S. Huck and George M. Whitesides
Harvard University, Cambridge, Massachusetts

I. INTRODUCTION: SAMs AS TWO-DIMENSIONAL POLYMERS

A polymer, by conventional definition, is a macromolecule made up of multiple equivalents of one or more monomers linked together by *covalent bonds* (e.g., carbon–carbon, amide, ester, or ether bonds) [1]. These conventional polymers come in many configurations: for example, linear homopolymers, linear copolymers, block copolymers, crosslinked polymers, dendritic polymers, and others. The most common architecture for polymers is based on linear chains that may have other attached chains (branched, grafted, or crosslinked); that is, they are one-dimensional molecules. A few examples have been claimed as two-dimensional sheet polymers.*

A supramolecular polymer is a structure in which monomers are organized through *noncovalent interactions* (e.g., hydrogen bonds, electrostatic interactions, and van der Waals interactions) [4]. These less familiar types of polymers also exist in many forms. For example, molecular crystals are large collections of molecules arranged in a three-dimensional periodical lattice through noncovalent

* See Refs. 2 and 3 and references therein.

18

Bioapplications of PAMAM Dendrimers

J. D. EICHMAN, A. U. BIELINSKA, J. F. KUKOWSKA-LATALLO, B. W. DONOVAN AND J. R. BAKER, JR
University of Michigan, Center for Biologic Nanotechnology, Department of Internal Medicine, Division of Allergy, Ann Arbor, MI, USA

1 INTRODUCTION

Interest in dendritic polymers (dendrimers) has grown steadily over the past decade due to use of these molecules in numerous industrial and biomedical applications. One particular class of dendrimers, Starburst® polyamidoamine (PAMAM) polymers, a new class of nanoscopic, spherical polymers that appears safe and nonimmunogenic for potential use in a variety of therapeutic applications for human diseases. This chapter will focus on investigations into PAMAM dendrimers for *in vitro* and *in vivo* nonviral gene delivery as these studies have progressed from initial discoveries to recent animal trials. In addition, we will review other applications of dendrimers where the polymers are surface modified. This allows the opportunity to target-deliver therapeutics or act as competitive inhibitors of viral or toxin attachment to cells.

2 DENDRIMER SYNTHESIS AND CHARACTERIZATION

As outlined in other chapters in this volume, Tomalia *et al.* first reported the successful well-characterized synthesis of dendrimers in the early 1980s [1]. These molecules range in size from 10 Å to 130 Å in diameter for generation 0 (G0) through generation 10 (G10). In the ideal situation, PAMAM dendrimers are monodispersed spherical conformation with a highly branched three-dimensional structure (Figure 18.1) that provides a scaffold for the attachment of

Dendrimers and Other Dendritic Polymers. Edited by Jean M. J. Fréchet and Donald A. Tomalia

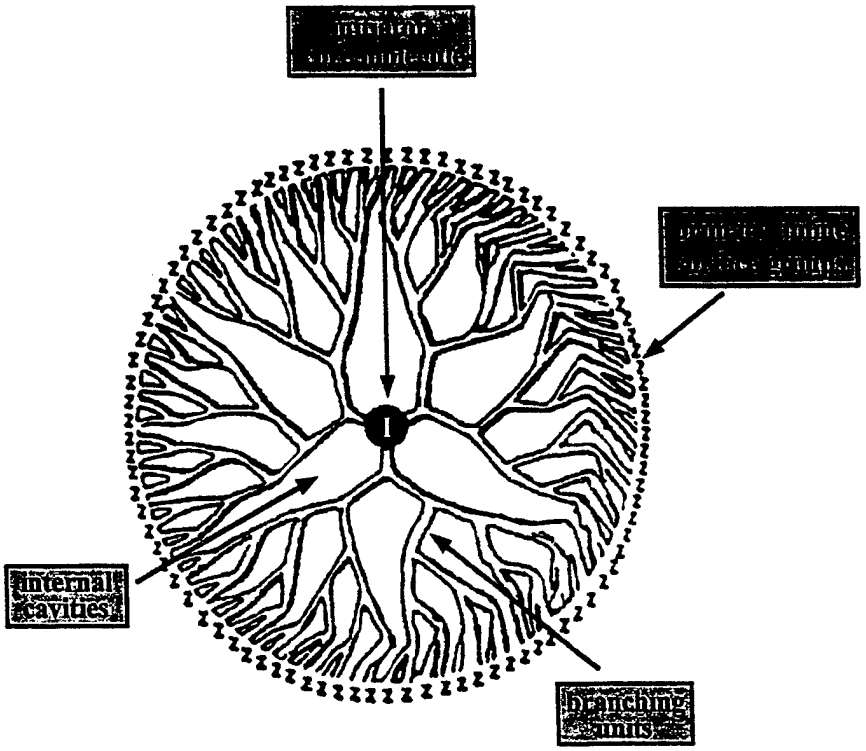

Figure 18.1

multiple biomolecules. With each new layer that is synthesized, the molecular weight of the dendrimer increases exponentially, the number of primary amine surface groups exactly double and the diameter increases by 10 Å (Table 18.1) [2]. As dendrimers grow in generation, the subsequent increase in exterior branching density begins to impart various structural effects to the polymer shape. Lower generation dendrimers (0 through 4) manifest a flexible, somewhat flat shape, while at the higher generations (5 through 10), the congested branching induces a persistent, robust spherical conformation [3]. Beginning at generation 4 (ethylenediamine core), the interior of the dendrimer develops internal void spaces that are accessible to molecules that may be encapsulated for drug delivery or other potential applications [4, 5]. Dendritic purity (isomolecularity) is typically around 98% due to small defects in branch formation during synthesis. These defects may be due to retro-Michael reactions or intramolecular macrocycle formation [6]. Dendrimer preparations are purified using ultrafiltration techniques. Subsequent structural characterization is performed by a number of analytical methods including: high performance liquid chromatography (HPLC), size exclusion chromatography (SEC), nuclear magnetic resonance

Table 18.1 Physical characteristics of PAMAM dendrimers (EDA core)

Dendrimer generation	Molecular weight	Primary amino surface groups	Diameter (Å)
0	517	4	15
1	1430	8	22
2	3256	16	29
3	6909	32	36
4	14215	64	45
5	28826	128	54
6	58048	256	67
7	116493	512	81
8	233383	1024	97
9	467126	2048	114
10	934787	4096	135

(NMR) techniques (^{1}H, ^{13}C, ^{15}N, ^{31}P), electron paramagnetic resonance (EPR), electrospray-ionization mass spectroscopy (ESI–MS), capillary electrophoresis, or gel electrophoresis [7–11]. Analytical methodology usually requires a combination of the above techniques in order to provide a detailed account of the exact identity and composition of the dendrimer sample. PAMAM dendrimers are currently commercially available with production occurring under good manufacturing procedures (GMP) to provide suitable samples for various biomedical and gene therapy applications [11b]. Atomic force microscope images of generation 9 (G9 EDA) dendrimers are shown in Figure 18.2. Li *et al.* have also recently obtained AFM images of PAMAM dendrimers ranging from G5 EDA to G10 EDA [12]. These studies clearly demonstrate the shape and consistency of these molecules.

3 DNA DELIVERY *IN VITRO* WITH UNMODIFIED DENDRIMERS

3.1 DENDRIMER/DNA INTERACTIONS: CHARACTERIZATION OF THE COMPLEX FORMATION

Formation of a complex between DNA and polycationic compounds appears to be the initial and quite possibly a critical parameter for nonviral gene delivery. Several synthetic vector systems, which are generally cationic in nature, including poly(lysines), cationic liposomes or various types of block copolymers and recently dendrimers, have been shown to self-assemble with plasmid DNA [13–15] [16]. Specific physicochemical properties manifested by these DNA complexes depend on the type of cationic agent used; however, interesting patterns for such interactions are beginning to evolve [17, 18]. Under certain conditions, the interaction of DNA with polyvalent cations results in

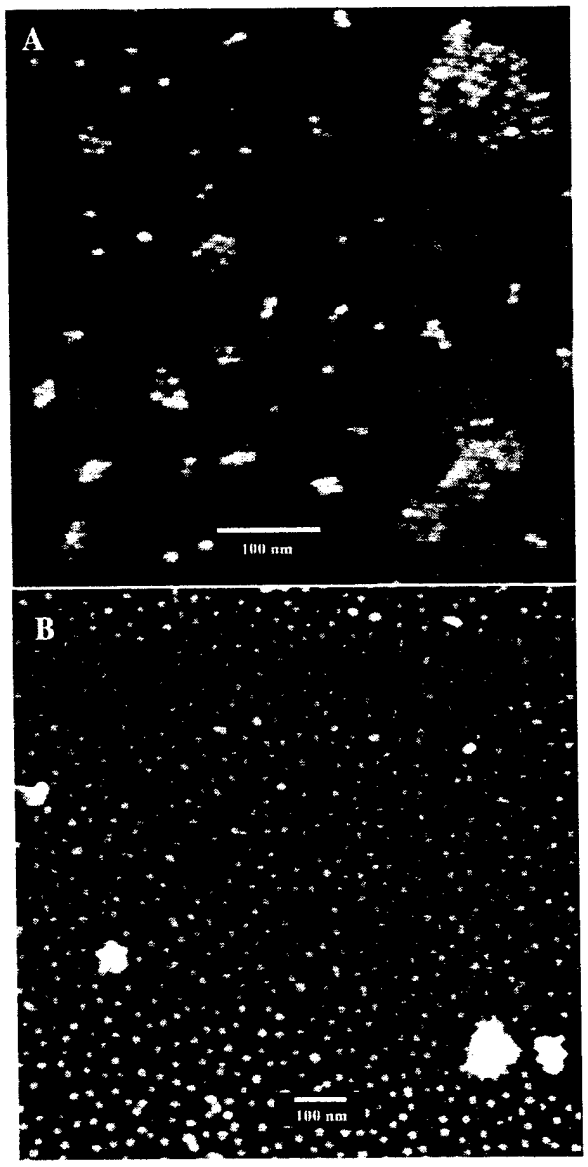

Figure 18.2

compaction of extended DNA structures to produce aggregation and precipitation from the solution [19–21]. Similar to other large polycationic compounds, PAMAM dendrimers form complexes with DNA through sequence-independent electrostatic interactions between negatively charged phosphate groups of the nucleic acid components and the cationic primary amino groups on the dendrimer surface (Figure 18.3). Charge neutralization of both components and alterations of the net charge of the complex lead to changes in both physicochemical and biologically relevant properties.

Complex formation analysis and characterization as soluble–insoluble or low–high density particles can be performed by various methods including UV light absorption, laser light scattering (LLS) and measurements that utilize radiolabeled DNA and/or dendrimers. The actual binding affinity constant (K_a) of DNA and dendrimers are difficult to determine in part because of the tendency to aggregation and precipitation [22]. However, the formation of high molecular weight and high-density complexes depends strongly on the DNA concentration (Figure 18.4). In salt-free water solutions, the precipitate formation increases as the DNA concentration rises from 10 ng/ml to 1 mg/ml. At DNA concentrations of 10 ng/ml, the complex formed with various dendrimer generations (i.e. G5, G7 and G9, with both NH_3 and EDA cores) form soluble, low density aggregates that remain suspended in water. Complex formation is facilitated by increasing the dendrimer concentration that effectively increases the dendrimer–DNA charge ratio [21].

Electrostatic charge effects (attraction or repulsion of charged molecules) appear to be modulated by the dendrimer generation (size of the polymer). Figure 18.5 illustrates that, although generally parallel, the precipitation curves shift as a result of the size (i.e. generation) of the dendrimer. Complexing of the

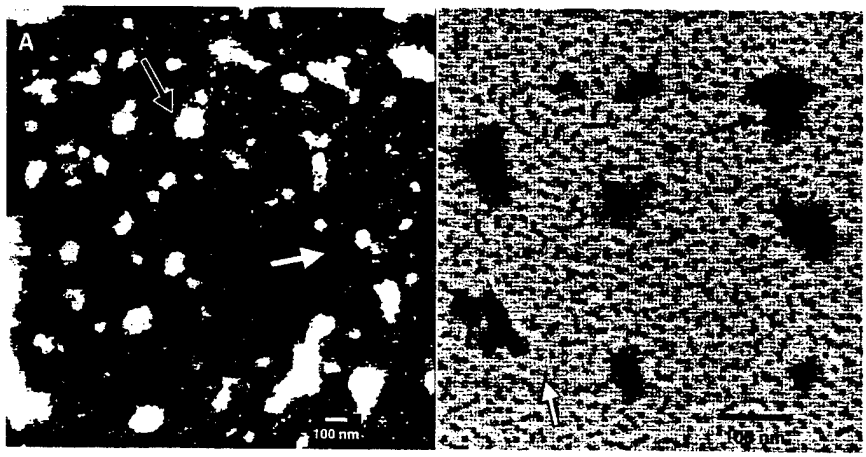

Figure 18.3

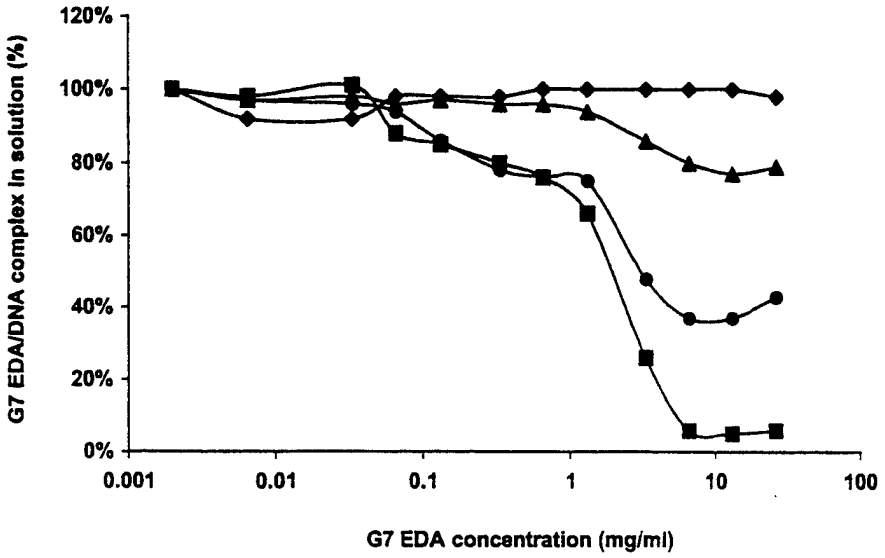

Figure 18.4

smaller G5 and G7 EDA dendrimers with DNA leads to highly aggregated forms of the complex at lower charge ratios than with larger, G9 EDA dendrimers [21]. This suggests that a purely electrostatic effect is modulated by the size and molecular weight of the dendrimer. PAMAM dendrimers readily form complexes with various forms of nucleic acids including single stranded oligonucleotides, circular plasmid DNA, linear RNA and various sizes of linear double stranded DNA. The larger the nucleic acid molecule, the lower the dendrimer concentration that is required to generate high-density complexes. With progressive increases in the dendrimer–DNA charge ratio (> 20), an increase in the quantity of low-density, soluble complexes is observed. Functional analysis revealed that the majority (> 90%) of transfection is carried by low-density, soluble, subpopulations of complexes, which may represent approximately 10–30% of the total complexed DNA (Figure 18.6).

The continuous distribution of the radioactively labeled dendrimer–DNA complexes in glycerol density gradients indicates the heterogeneous nature of the complex population. The size evaluation of dendrimer–DNA complexes (in water) using dynamic LLS, further reveals the polydispersed nature of particles with hydrodynamic diameters ranging from 30–100 nm to 20–200 μm depending on DNA concentration, size of dendrimer and charge ratio between each polymeric component. Complexes formed at very low DNA concentrations (e.g. 1–10 ng/ml) are usually smaller and more uniform than particles generated at high DNA concentrations. Complex formation at higher DNA concentrations results

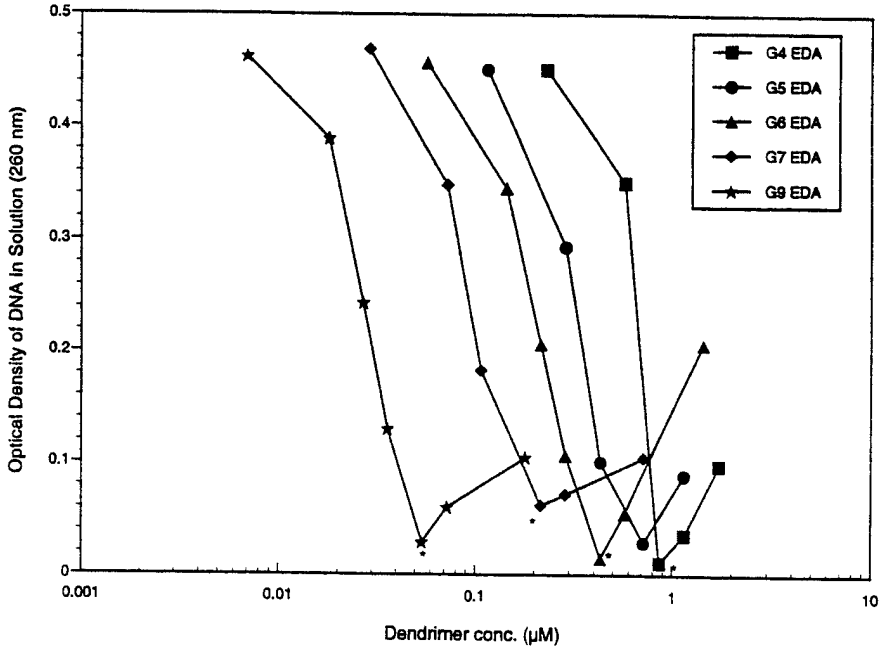

Figure 18.5

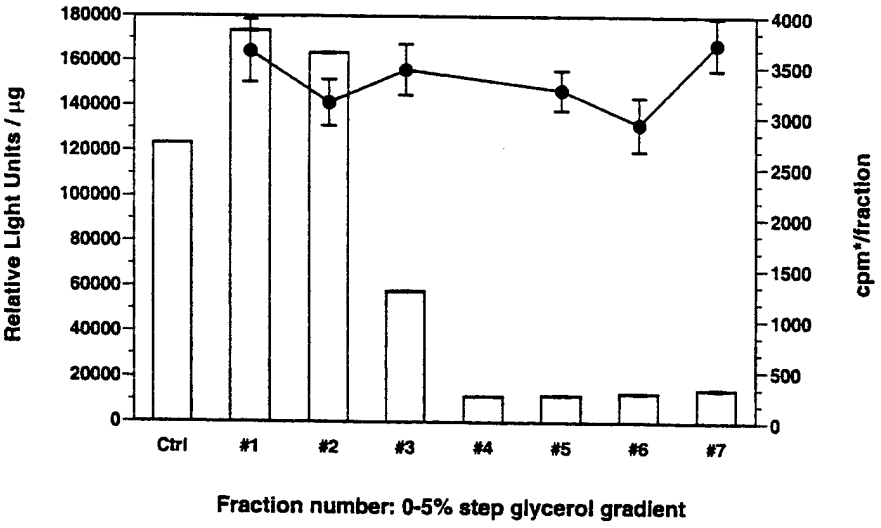

Figure 18.6

in the nonuniform distributions of larger, high-density aggregates and precipitates.

3.2 MECHANISM OF DENDRIMER-MEDIATED CELL ENTRY

Studies that focus on the cell entry mechanisms for several nonviral vectors, including liposomes, lipospermines, poly(ethylenimine) and PAMAM dendrimers have been previously reported [23–27]. Figure 18.7 shows a proposed dendrimer–DNA complex pathway into cells with subsequent processing [28, 29]. The cationic surface charge imparted to the complex through high dendrimer–DNA charge ratios (e.g. 5–20) is required for subsequent interaction with the anionic glycoproteins and phospholipids that reside on the cell membrane surface. This interaction initiates the interior movement of the dendrimer–DNA complex into the cell cytosol, either by passive transport through membrane or by endocytosis [30]. Complexes formed without an excess cationic surface charge do not mediate high gene transfection efficiency, which furnishes support for the importance of the initial electrostatic interaction between the complex and cell membrane. Studies following the incorporation of radiolabeled DNA and/or dendrimer components into cells established that the uptake in most cells was primarily via an active endocytosis mechanism [31]. Cells preincubated with inhibitors of endocytosis (i.e. cytochalasin B and deoxyglucose) or cellular metabolism (i.e. sodium azide) reduced the uptake that corresponded to lower transgene expression, regardless of cell type. After being entrapped within the endosome, complex release into the cytosol is essential

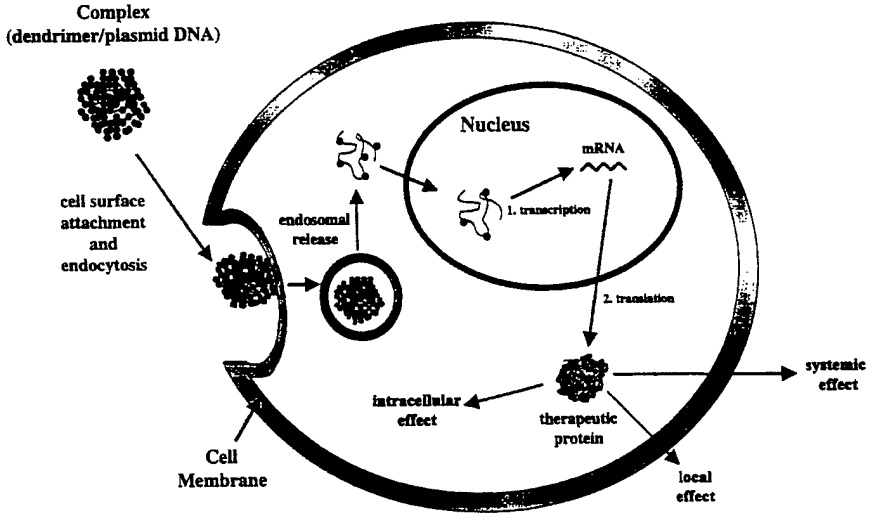

Figure 18.7

before acidic or enzymatic DNA degradation within the endosomal/lysosomal compartment takes place. The enhanced dendrimer-mediated transfection can be obtained in several cell types using chloroquine, an inhibitor of endosomal acidification.

It has been postulated that branched cationic polymers have a high buffer capacity owing to the basic amine groups [25, 32]. This characteristic enables dendrimers to act as a weak base and retard degradation caused by acidification within the endosome-lysosome. A reduction in pH might also lead to polymeric swelling within the endosome, thus disrupting the membrane barrier of the organelle and promoting DNA and/or complex release [23, 25]. After discharge from the endosome, DNA must penetrate the nuclear membrane for transcription and subsequent expression to occur. Translocation into the nucleus does occur within 30 min post-transfection, but the exact molecular and cellular mechanisms that mediate these events are unclear at this time, and are probably different for each cell type [33]. Recent studies tracing the movement of poly(ethylenimine) (PEI)–DNA complexes within cells indicated that complete separation of the polymer–DNA complex was not necessary for DNA entry into the nucleus [34]. Therefore, it might be possible that PAMAM dendrimers are also associated with DNA as it crosses into the nuclear compartment.

3.3 PLASMID DNA DELIVERY

The ability of PAMAM dendrimers to associate electrostatically with polyanionic DNA imparts a unique property to these polymers that enables them to be used as a synthetic vector for delivery of genes. Other cationic vectors such as poly(lysine), PEI, liposomes and block copolymers can also interact with plasmid DNA, resulting in successful gene transfer *in vitro* [13, 35–37]. Initially Haensler and Szoka performed studies to investigate the application of PAMAM den-drimers as nonviral vectors for *in vitro* gene transfer [32]. Their results demonstrated that complexes consisting of G5 PAMAM dendrimer and expression plasmid DNA had enhanced transfection efficiency over naked plasmid DNA in many cells, particularly cell lines derived from monkey and human neoplasms [32]. Further work from these investigators revealed that the transfection observed in their experiments was improved by thermally degraded dendrimers [23]. Thermally degraded dendrimers appear to be polydispersed in size and structure enhance transfection efficiency when compared with the intact G5 dendrimer. The enhanced transfection activity of the degraded polymer was attributed to increased flexibility of the structure. However, the exact structural changes that account for this have not been identified. Independent studies by Baker and co-workers documented the efficiency of intact dendrimers as synthetic vectors for the delivery of genetic material into cells

[31, 38]. They used different generations of intact dendrimers to transfect plasmid DNA in a variety of cells (Table 18.2) using luciferase, CAT (chloramphenicol acetyltransferase) and β-galactosidase reporter genes to quantify transfection efficiency.

In contrast to the results obtained with degraded PAMAM dendrimers, only intact dendrimers of G5 mediated significant transfection, and this required the addition of a dispersing agent such as (diethylamino)ethyl (DEAE) dextran [31]. In a number of cells analyzed, typified by the rat embryonal fibroblast cell line Rat 2, an exponential rise in transfection efficiency was observed using G5–G10 of either NH_3 or EDA core dendrimers [31]. High transfection levels of the luciferase reporter gene were obtained in non-adherent cells of lymphoid lineage (i.e. Jurkat and U937) and adherent cells (COS-1 and Rat 2). Expression levels of luciferase in Jurkat and U937 cells was one to two orders of magnitude greater than those obtained in experiments using the commercial lipid prepara-

Table 18.2 Cell lines transfected with PAMAM dendrimers

Cell line	Cell type
Rat 2	Rat embryonal fibroblast
Clone 9	Rat liver epithelium
rat Clone B	Rat mesothelium
YB2	Rat myeloma, nonsecreting
NRK52E	Rat kidney epithelial-like
NIH3T3	Mouse embryonal
10′	Mouse embryonal, 3T3-like, p53 deficient
EL4	Mouse lymphoma
D5	Mouse melanoma
Cos1	Monkey kidney fibroblast
Cos7	Monkey kidney fibroblast
CHO	Chinese hamster ovary
HMEC-1	Human microvascular endothelium
MSU1.2	Human fibroblast
NHFF3	Normal human foreskin fibroblast
QS	Human synoviocyte
HepG2	Human liver hepatoblastoma
Jurkat	Human T cell leukemia
JR	Human T cell leukemia
SW 480	Human colon adenocarcinoma
COLO 320 DM	Human colon adenocarcinoma
SW 837	Human rectum adenocarcinoma
YPE	Porcine vascular endothelial
BHK-21	Hamster kidney fibroblast-like
NHBE	Normal human bronchial epithelium
SAEC	Small airway epithelium
CCD-37Lu	Human normal lung fibroblast
A549	Human lung carcinoma epithelial-like

tions, Lipofectamine and DMRIE-C (1,2-dimyristyloxy-3-dimethylhydroxy ethyl ammonium bromde formulated with cholesterol) [33]. Typically, nonviral vectors do not mediate high levels of expression in primary cell lines. PAMAM dendrimers are highly efficient in transfecting a wide array of primary cells of various origins including human fibroblasts (HF1) and human lung epithelial cells [31]. Each cell line reacts differently to transfection with this agent, owing to subtle changes in physiological makeup, so the dendrimer generation that is optimal for each particular cell line must be determined experimentally.

The addition of other agents to the DNA–dendrimer complex can markedly alter transfection. For example, chloroquine or cationic DEAE dextran added to dendrimer–DNA complexes significantly increase transgene expression in a number of cell lines [31]. DEAE dextran alters the dendrimer–DNA complex by dispersing the complex aggregates [31]. However, it is cytotoxic and might prevent stable gene integration.

3.4 STABLE TRANSFORMED CELL LINES

One of the most important goals of gene therapy is the transfer of genetic material that is permanently integrated and expressed in cells. A large percentage of cells must be transfected for a few to retain stable gene integration. This is owing to the low efficiency of DNA integration that is observed with nonviral vector systems (as compared with retroviruses). To overcome these problems, *ex vivo* approaches have been used, in which a small quantity of tissue is removed from the patient and the cells within that tissue are placed into culture. After clonal expansion of the cells, transfection of the desired gene is performed *in vitro*. The genetically modified cells are then returned to the patient by transplantation or implantation to obtain a limited number of stable clones expressing the gene [39, 40]. Transfections with calcium phosphate–DNA precipitates, DEAE–dextran–DNA, or dendrimer–DNA complexes with expression plasmids carrying both β-galactosidase and neomycin resistance genes were performed on D5 mouse melanoma cells [41]. Dendrimer–DNA complexes produced approximately 90-fold more neomycin-resistant stable clones than other complexes, including calcium phosphate precipitation and DEAE dextran [41]. It was demonstrated that up to one-third of the neomycin resistant colonies produced β-galactosidase activity. This indicates that a nonselected gene was integrated into the cellular genomic DNA and expressed. It also suggested that if cells are transfected with dendrimer–DNA complexes *in vivo*, the transfected DNA will integrate into the host chromosome and be permanently expressed [41].

3.5 OLIGONUCLEOTIDE DELIVERY

Antisense oligonucleotides are short, gene-specific sequences of nucleic acids, typically 15–25 bases in length. These molecules are designed to interact with complementary sequences on a targeted mRNA and, in principle, prevent the message from being translated into a protein. Protein synthesis is inhibited by initiating enzymatic degradation of the mRNA by RNAse H or by interfering with ribosomal reading of the message to form the encoded protein [42]. There are approximately 10 different phosphorothioate oligonucleotides that are presently being tested in human clinical trials [42]. Additional experiments have also demonstrated that some antisense oligonucleotides can inhibit gene expression selectively [43]. The biological effect of an oligonucleotide will ultimately correspond to its intracellular concentration and the rate of degradation. One of the primary difficulties associated with the delivery of antisense nucleic acids is obtaining a sufficient intracellular concentration. The second problem is preventing its rapid degradation by cellular endo- and exonucleases. Methods such as enhancing the chemical stability through modifications of the phosphodiester bond attempt to increase the half-life of the oligonucleotide [44]. Other techniques aim to increase cellular uptake, including the use of high initial concentrations, use of cationic lipids as carriers and microinjection [44–46]. However, these methods have encountered various problems associated with their use *in vivo*. Therefore, more efficient delivery systems are needed to achieve successful applications of antisense technology.

Recent studies by Bielinska *et al.* have shown that PAMAM dendrimers can be complexed to antisense oligonucleotides or plasmid expression vectors coding antisense mRNA, to inhibit specific reporter luciferase gene expression by 30% to 60% (Figure 18.8) [38]. These results were obtained in several stable cell clones that demonstrated long-term luciferase expression of cDNA from mouse melanoma (D5) and rat embryonal fibroblast (Rat 2) cells. The wide variety of inhibition depends on DNA concentration, charge ratios of the dendrimer–DNA complex and generation of dendrimer used in the particular study. Specific inhibition of gene expression is obtained in picomolar concentrations with dendrimer delivery. When Bielinska *et al.* attempted to use Lipofectamine (Life Technologies, Gaithersburg, MD, USA) a commercial liposome preparation, consistent results were not obtained because of cytotoxicity. Dendrimers were not cytotoxic at the concentrations required for gene delivery [38]. Oligonucleotide stability is required for successful inhibition of gene expression through antisense application. Exposure of 'naked' oligonucleotide leads to its rapid degradation in serum and endosomes, or by cellular enzymes. An increase in phosphodiester oligonucleotide stability occurs when such oligonucleotides are complexed with dendrimers [38]. A later study was performed evaluating PAMAM dendrimers as an adjuvant to enhance the delivery of antisense phosphorothioate deoxyoligonucleotides (PODN) directed against chloramphenicol

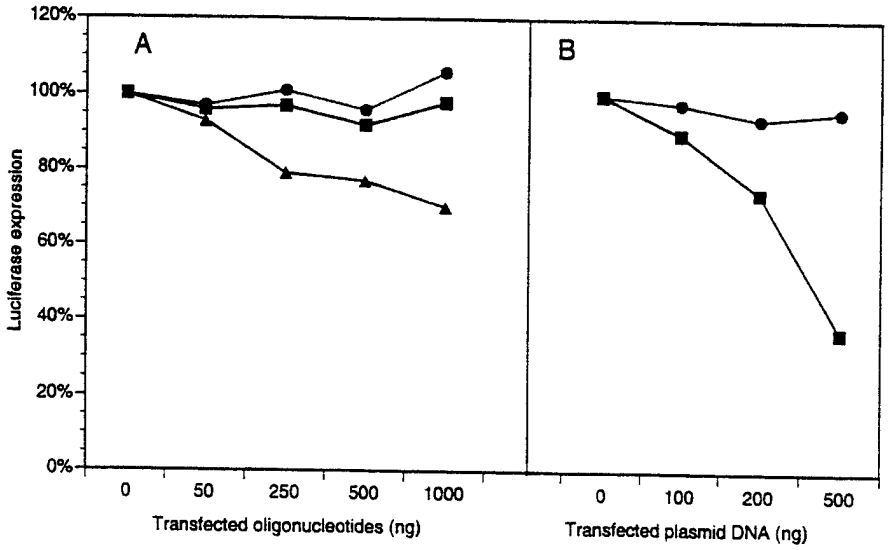

Figure 18.8

acetyltransferase (CAT) in Chinese hamster ovary (CHO) cells [47]. The level of antisense inhibition could be modulated as a function of DNA concentration, and by generation of dendrimer and dendrimer–DNA charge ratio. The use of G5 dendrimers resulted in a 35–40% reduction in CAT expression. G3 (EDA core) dendrimers also enhanced PODN uptake 50-fold in human astrocytoma cells (U251) and improved delivery to the nucleus [48]. Other transfection studies achieved targeted gene expression inhibition in nano- to micromolar oligonucleotide concentrations [49–51]. Thus the complexation of oligonucleotides with dendrimers might enable DNA delivery in a manner that could lead to *in vivo* uses for a variety of regulatory nucleic acid applications.

3.6 ENHANCEMENT OF IN VITRO GENE DELIVERY

The major limitation of nonviral-based gene delivery is low transfection efficiency when compared with viral vectors. Various techniques have been developed in an attempt to increase the quantity of therapeutic genes delivered intracellularly, including mechanical enhancements such as electroporation, the gene gun and membrane permeability enhancers [52–59]. It has been demonstrated that pulmonary surfactants increase *in vitro* adenoviral-mediated gene transfer, but have the reverse effect when used in conjunction with cationic liposomes [58, 60]. Recently, Exosurf Neonatal® (GlaxoWellcome, Research Triangle Park, NC, USA) a commercialized pulmonary surfactant preparation used for treatment of neonatal respiratory distress syndrome, was investigated for enhance-

ment of dendrimer-mediated transgene expression *in vitro* [61]. Exosurf Neonatal® is a mixture of three components: dipalitoylphosphatidylcholine (DPPC), tyloxapol and cetyl alcohol.

Studies with Exosurf Neonatal® have demonstrated a significant enhancement in luciferase reporter gene expression in a variety of cells, including primary cells of different origins [61]. Primary human lung epithelial (NHBE) and porcine vascular endothelial (YPE) cells showed the highest enhancement with a 41.4- and 25.3-fold increase in luciferase expression, respectively, over the control [61]. Exosurf Neonatal® also significantly enhanced luciferase expression in a nonadherent lymphoid Jurkat cell line by 11.5-fold over control [61]. Jurkat cells are historically difficult to transfect by nonviral transfection techniques. It was determined that tyloxapol, a formaldehyde polymer of a polyoxyethylene condensate of *p*-(1,1,3,3-tetramethylbutyl)phenol, was the sole component inducing the den-drimer-mediated expression enhancement [61–63]. Tyloxapol is also classified as a nonionic surfactant. Substitution of Exosurf Neonatal® with tyloxapol in transfection experiments produced comparable transfection enhancement, while DPPC and cetyl alcohol alone had no effect [61]. Tyloxapol did not induce significant toxicity at concentrations required for enhanced transgene expression (0.25–0.50 mg/ml) [61].

Surfactants are commonly used as absorption enhancers and typically act by destabilizing the cell membrane [64–67]. Initial studies seeking the mechanism(s) of tyloxapol-mediated enhancement have been performed, but the mechanism has not been completely defined (J. D. Eichman, unpublished). Membrane permeability studies measuring intracellular enzyme release (i.e. lactate dehydrogenase; LDH) and fluorescent marker leakage (i.e. fluorescein diacetate) and uptake (i.e. propidium iodide) indicated in part an enhancement of permeability [61]. Preincubation of cells with tyloxapol with subsequent washing prior to transfections was shown to elevate transgene expression (A. U. Bielinska, unpublished). This indicates that tyloxapol might temporarily activate certain cell membrane properties, which promote DNA uptake even after surfactant removal [61].

4 DNA DELIVERY *IN VIVO*

Many human diseases, including cancer and inherited illness such as cystic fibrosis are caused by genetic disorders. The progress in biotechnology, such as being able to synthesize DNA constructs containing genes of interest, has effected dramatic changes in therapeutic agents. Recent advances in molecular biology leads to greater understanding of the molecular genetic basis for human diseases, as well as the promise for the development of novel treatment through gene therapy [68]. The feasibility of using gene therapy to correct human genetic disorders has led to a flurry of excitement in both the scientific community and

biotechnology industry [68, 69]. However, a major obstacle for successful *in vivo* gene therapy has been the absence of suitable DNA delivery vectors [70]. The therapeutic application of genes requires non-toxic, cost effective methods for gene delivery that are safe, non-immunogenic and provide producible levels of the gene products [71]. Viral vectors such as adenovirus are highly efficient for gene transfer and have been used for various clinical trials such as cystic fibrosis [72, 73]. However, a number of problems with the adenoviral vector have limited its use. The major drawback is immunogenicity associated with the adenovirus that may have played an important role in the recent death of a patient enrolled in a gene therapy clinical trial. Owing to the potential limitations of viral vectors, non-viral *in vivo* strategies that employ plasmid DNA encoding a target gene are seen to be a promising alternative. Cationic lipids have been used in gene delivery to the lung. However, an inflammatory response to the lipid limits its use [74]. PAMAM dendrimers have recently been tested as a synthetic vector system for gene therapy to the lung [75].

Poly(amidoamine) (PAMAM) dendrimers, as well as other families of dendrimers are finding utility in a wide variety of uses, from particle size standards to a number of biological applications [5]. In order for PAMAM dendrimers to be useful for *in vivo* applications, studies establishing various parameters such as pharmacokinetics and biocompatibility are necessary. The criteria for choice of carrier molecules can be summarized as follows. The carrier should be (1) non-toxic, (2) non-immunogenic, (3) biocompatible, (4) have adequate functional groups for chemical fixation, (5) limited body accumulation and (6) maintain the original drug activity until reaching the site of action.

4.1 *IN VIVO TOXICITY*

Evaluation of dendrimer toxicity was recently performed utilizing specific pathogen-free, female CBA/J mice. The mice were injected intravascular (i.v.) with G5, G7 or G9 EDA PAMAMs dissolved in physiological saline at doses of 10, 50, 100, 200, 300, 600 μg/mice. Control animals received saline alone. The animals were observed for behavioral abnormalities, activity level and eating/drinking behavior. Dendrimers were injected every four days up to four times per mouse. Changes in body weight over the 30-day observation period were recorded as a measure of overall health. Groups of mice were sacrificed on days 4, 8, 16, 20 and 30 after treatment. Results indicated that dendrimer toxicity is dependent on both the concentration and polymer generation. High doses of G5 EDA (200 μg/mouse) and G7 EDA (300 μg/mouse) dendrimers showed signs of toxicity. Tissue pathology and toxicity studies with G9 EDA dendrimer i.v. administration up to 600 μg/mouse has not indicated lung inflammation and pneumonitis. Dendrimers also did not induce an immune response when administered alone or in combination with adjuvant [76].

4.2 BIODISTRIBUTION

Biodistribution of G3 and G4 ^{125}I-labelled PAMAM dendrimers after administration by intravenous (i.v.) or intraperitoneal (i.p.) routes accumulated primarily in the liver (60–90%) with only 0.1–1.0% of the recovered dose detected in the blood after 60 min in Wistar rats [77]. This distribution is different from that obtained with studies using i.v. delivery of generation 3, 5 and 7 on Swiss-Webster mice. G3 dendrimers showed the highest accumulation in the kidney, with G5 and G7 dendrimers mainly localized in the pancreas [76]. The differences between the studies may be attributable to the choice of animal model and/or dendrimer generation used. When dendrimers interact with DNA to form complexes of varying charge ratios, complex distribution patterns would be expected to be entirely different from that obtained for naked dendrimer administration. This is due to changes in the size, density and surface charge of the complex compared to individual dendrimer molecules. To date, the *in vivo* distribution patterns of dendrimer/DNA complexes have not yet been established.

4.3 EXPERIMENTAL TRIALS

A number of experimental *in vivo* gene therapy trials on animals using PAMAM dendrimers are in their preliminary stages. Numerous *in vivo* experiments are currently being conducted in order to optimize the dendrimer generation, concentration, and complex charge ratio to obtain optimal transfection efficiency.

Complexes of dendrimer and DNA have been administered to the lungs of mice and rats by intranasal delivery. Preliminary results have indicated that administration by this route may not led to optimal gene expression when compared to 'naked' DNA delivery [78]. Polymerase chain reaction (PCR) confirmed long-term plasmid DNA survival when complexed with dendrimer. Amplification was performed directly with lung homogenate and/or nucleic acids isolated from lung tissue [33]. Semiquantitative PCR of plasmid DNA removed from lung tissue showed up to a 10^3-fold increase in its survival when complexed with dendrimer than when plasmid DNA was administered alone.

Recently, i.v. delivery of dendrimer/DNA complexes was evaluated on mice. When delivered by i.v. administration, the greatest amount of gene expression in Balb/C mice has been obtained in the bronchial and alveolar regions of the lung [75]. It is also possible that *in vivo* targeted gene delivery using antibody-conjugated dendrimers may eventually be achieved. Antibody–dendrimer conjugates have already been used in tumor imaging, diagnostics and radioimmunotherapy [79, 80] More recently, dendrimers were investigated as a method to increase plasmid DNA gene transfer in a murine cardiac transplantation model.

4.4 GENETIC APPROACHES TO THE THERAPY INFLAMMATORY AND FIBROTIC LUNG DISEASE

Pulmonary diseases are present in a heterogeneous group of lung disorders of known or unknown etiology. Gene therapy has been a useful tool against these diseases for a variety of reasons. First, the genetic basis for lung cancer and common inherited pulmonary disease such as cystic fibrosis has been identified. Secondly, there are no effective therapies for many lung diseases, especially for chronic inflammatory lung diseases such as idiopathic pulmonary fibrosis (IPF). IPF is a progressive disease resulting in respiratory failure. Recent progress in understanding the pathogenic mechanisms of lung fibrosis has provided insights into the inflammatory process underlying this disorder. IPF is commonly characterized by inflammation of the alveolar wall leading to disruption of the normal alveolar architecture and interstitial as well as intra alveolar fibrosis. The process involves cellular interactions via a complex cytokine network and heightened collagen gene expression with abnormal deposition in the lung. Recent studies have identified a myriad of cytokines with potential roles in pulmonary fibrosis (PF) including transforming growth factor β_1 (TGFβ_1), tumor necrosis factor α (TNF-α), platelet derived growth factor (PDGF), interleukin 5 (IL-5), and IL-8. Of the investigations so far, the TGFβ_1 family has the most potent stimulatory effect on extracellular matrix deposition. TGFβ_1 stimulates fibroblast procollagen gene expression and protein synthesis. The murine model of bleomycin induced lung fibrosis, increased TGFβ_1 gene expression and collagen elevation. This information provides a rational basis for developing anticytokine agents. Furthermore, recent studies have shown that *in vivo* administration of antisense oligonucleotides (ONDs) against TGFβ_1 reduced malignant mesthelioma tumor growth in mice. Antisense ODNs can block the translation of particular gene products within cells and represent a unique method of specifically inhibiting the effects of target proteins in the cells. The ability of the antisense technique to down-regulate the expression of specific genes is well documented both *in vitro* and *in vivo*. In animal models, gene transfer was achieved with a variety of vectors such as lipids, virus or naked plasmid DNA. In a recent study, Baker *et al.* investigated the ability of G9 (EDA core) dendrimers complexed with TGFβ_1 ODN to inhibit pulmonary fibrosis in a well-characterized model of bleomycin induced pulmonary fibrosis utilizing CBA/J mice. Intravenous G9 (EDA core) dendrimer/TGFβ_1 antisense ODN complex administration caused a significant reduction in lung fibrosis as indicated by TGFβ_1 mRNA suppression and inhibition of lung hydroxyproline contents, collagen synthesis, cytokine expression and pulmonary eosinophilia. Administration of either TGFβ_1 antisense ODNs alone or sense oligos complexed to G9 EDA dendrimers did not produce an equivalent inhibition in pulmonary fibrosis indicators. These results suggest the possibility for *in vivo* use of dendrimer vectors with antisense ODNs to combat pulmonary fibrosis as well as other diseases.

5 CONCLUSION

PAMAM dendrimers are a highly efficient non-viral vector for gene delivery into numerous cell lines *in vitro* and *in vivo*. Results obtained from *in vitro* studies do not always correlate to similar observations obtained in the *in vivo* experiments. The use of dendrimers for *in vivo* gene delivery is in its initial stages with studies primarily focusing on optimizing localized transgene expression. The ability of certain dendrimer generations to transfect cells without inducing biocompatibility issues or toxicity confers a significant advantage over other gene delivery vectors for use *in vivo*. Preliminary studies delivering plasmid DNA and antisense oligonucleotides in mice for gene therapy in cancer, pulmonary fibrosis and other diseases have resulted in a positive outlook for the future use of dendrimers as an *in vivo* synthetic gene delivery vector.

6 REFERENCES

1. Tomalia, D. A., Baker, H., Dewald, J., Hall, M., Kallos, G., Martin, S., Roeck, J., Ryder, J. and Smith, J. *Polymer J.*, **17**, 117–132 (1985).
2. Lothian-Tomalia, M. K., Hedstrand, D. M., Tomalia, D. A., Padia, A. B. and Hall, Jr. H. K. *Tetrahedron*, **53**(45), 15495–15513 (1997).
3. Pötschke, D., Ballauff, M., Lindner, P., Fischer, M. and Vögtle, F. *Macromolecules*, **32**, 4079–4087 (1999).
4. Tomalia, D. A., Hall, M. and Hedstrand, D. M. *J. Amer. Chem. Soc.*, **109**, 1601–1603 (1987).
5. Bieniarz, C. Dendrimers: applications to pharmaceutical and medicinal chemistry, in Swarbrick, J. and Boylan, J. C. (eds) *Encyclopedia of Pharmaceutical Technology*, v. **18**, Marcel Dekker Inc, New York, 1999, pp. 55–89.
6. Tomalia, D. A., Uppuluri, S., Swanson, D. R., Brothers II, H. M., Piehler, L. T., Li, J., Meier, D. J., Hagnauer, G. L. and Balogh, L. *Mater. Res. Soc. Symp. Proc.*, **543**, 289–298 (1999).
7. Tomalia, D. A., Naylor, A. M. and Goddard III, W. A. *Angewandte Chem.*, **29**, 138–175 (1990).
8. Ottaviani, M. F., Montalti, F., Turro, N. J. and Tomalia, D. A. *J. Phys. Chem. B*, **101**, 158–166 (1997).
9. Pesak, D. J., Moore J. S. and Wheat, T. E. *Macromolecules*, **30**, 6467–6482 (1997).
10. Kallos, G. J., Tomalia, D. A., Hedstrand, D. M., Lewis, S. and Zhou, J. *Rapid Commun. Mass Spectrom.*, **5**, 383–386 (1991).
11. Weiner, E. C., Brechbiel, M. W., Brothers, H., Magin, R. L., Gansow, O. A., Tomalia, D. A. and Lauterbur, P. C. *Mag. Reson. Med.*, **31**, 1–8 (1994).
12. Li, J., Piehler, L. T., Qin, D., Baker, J. R. and Tomalia, D. A. *Langmuir*, **16**, 5613–5616 (2000).
13. Wolfert, M. A., Schacht, E. H., Toncheva, V., Ulbrich, K., Nazarova, O. and Seymour, L. W. *Hum. Gene Ther.*, **7**, 2123–2133 (1996).
14. Rädler, J. O., Koltover, I., Salditt, T. and Safinya, C. R. *Science*, **275**, 810–814 (1997).
15. Bielinska, A. U., Kukowska-Latallo, J. F. and Baker, J. R. Jr, *Biochim. Biophys. Acta*, **1353**, 180–190 (1997).

16. Ottaviani, M. F., Sacchi, B., Turro, N. J., Chen, W., Jockusch, S. and Tomalia, D. A. *Macromolecules*. **32**, 2275–2282 (1999).
17. Bloomfield, V. A., Ma, C. and Arscott, P. C. in K. S. Schmitz (ed.), *Macro-Ion Characterization from Dilute Solutions to Complex Fluids*, American Chemical Society, Washington DC; 1994, pp. 195–209.
18. Post, C. B. and Zimm, B. H. *Biopolymers*, **21**, 2123–2137 (1982).
19. Pelta, J., Livolant, F. and Sikorav, J. L. *J. of Biol. Chem.*, **271**, 5656–5662 (1996).
20. Dunlap, D. D., Maggi, A., Soria, M. R. and Monaco, L. *Nucl. Acids Res.*, **25**, 3095–3101 (1997).
21. Bielinska, A. U., Chen, C., Johnson, J. and Baker, J. R. Jr. *Bioconj. Chem.*, **10**, 843–850 (1999).
22. Rau, D. C. and Parsegian, V. A. *Biophys. J.*, **61**, 246–259 (1992).
23. Tang, M. X., Redemann, C. T. and Szoka, F. C. Jr. *Bioconj. Chem.*, **7**, 703–714 (1996).
24. Zabner, J., Fasbender, A. J., Moninger, T., Poellinger, K. A. and Welsh, M. J. *J. of Biol. Chem.*, **270**, 18997–19007 (1995).
25. Boussif, O., Lezoualc'h, F., Zanta, M. A., Mergny, M. D., Scherman, D., Demeneix, B. and Behr, J.-P. *Proc. Natl Acad. Sci. U.S.A.*, **92**, 7297–7301 (1995).
26. Remy, J.-S., Abdallah, B., Zanta, M. A., Boussif, O., Behr, J.-P. and Demeneix., B. *Adv. Drug Del. Rev.*, **30**, 85–95 (1998).
27. Pollard, H., Remy, J.-S., Loussouarn, G., Demolombe, S., Behr, J.-P. and Escande, D. *J. of Biol. Chem.*, **273**, 7507–7511 (1998).
28. Tomalia, D. A. and Brothers II, H. M. *Biological Molecules in Nanotechnology: The Convergence of Biotechnology, Polymer Chemistry and Material Science*. IBC Library Series Publication No. 1927, 1998, pp. 107–119.
29. Tomalia, D. A. in Walsh, B. (ed.), *Non-Viral Genetic Therapeutics Advances, Challanges and Applications for Self-Assembling Systems*, IBC USA Conferences, Inc., Westborough, MA, 1996, pp. 1.2–1.2.36.
30. Dvornic, P. R. and Tomalia, D. A. *Sci. Spectra*, **5**, 36–41 (1996).
31. Kukowska-Latallo, J. F., Bielinska, A. U., Johnson, J., Spindler, R., Tomalia, D. A. and Baker J. R. Jr. *Proc. Natl Acad. Sci. USA*, **93**, 4897–4902 (1996).
32. Haensler, J. and Szoka, F. C. Jr. *Bioconj. Chem.*, **4**, 372–379 (1993).
33. Kukowska-Latallo, J. F., Bielinska, A. U., Chen, C., Rymaszewski, M., Tomalia, D. A. and Baker J. R. Jr. 'Gene transfer using starburst dendrimers', in Kabanov, A. V., Felgner, P. L. and Seymour, L. W. (eds) *Self-Assembling Complexes for Gene Delivery*, John Wiley & Sons, New York, 1998, pp. 241–253.
34. Godbey, W. T., Wu, K. K. and Mikos, A. G. *Proc. Natl Acad. Sci. USA*, **96**, 5177–5181 (1999).
35. Wagner, E., Cotten, M., Foisner, R. and Birnstiel, M. L. *Proc. Natl Acad. Sci. USA*, **88**, 4255–4259 (1991).
36. Zhou, X. and Huang, L. *Biochim. Biophys. Acta*, **1189**, 195–203 (1994).
37. Astafieva, I., Maksimova, I., Lukanidin, E., Alakhov, V. and Kabanov, A. *FEBS Lett.*, **389**, 278–280 (1996).
38. Bielinska, A., Kukowska-Latallo, J., Johnson, J., Tomalia, D. A., Baker, J. R. Jr. *Nucl. Acids Res.*, **24**, 2176–2182 (1996).
39. Chowdhury, J. R., Grossman, M., Gupta, S., Chowdhury, N. R., Baker, J. R. Jr. and Wilson, J. M. *Science*, **254**, 1802–1805 (1991).
40. Anderson, W. F. *Scientific Amer.*, **273**, 124–128 (1995).
41. Baker, J. R. Jr. in Heller, M. J., Lehn, P. and Behr, P. (eds), *Conference Proceedings Series. Artificial Self-Assembling Systems for Gene Delivery*, American Chemical Society, Washington DC, 1996, pp. 129–145.
42. Phillips, M. I. and Gyurko, R. in Weiss, B. (ed.), *Antisense Oligodeoxynucleotides and*

Antisense RNA. Novel Pharmacological and Therapeutic Agents, CRC Press, New York, 1997, pp. 131–148.
43. Crooke, S. T. and Bennett, C. F. *Ann. Rev. Pharmacol. Toxicol.*, **36**, 107–129 (1996).
44. Bennett, C. F. in Stein, C. A. and Krieg, A. M. (eds), *Applied Antisense Oligonucleotide Technology*, Wiley-Liss, Inc., New York, 1998, pp. 129–145.
45. Lewis, J. G., Lin, K.-Y., Kothavale, A., Flanagan, W. M., Matteucci, M. D., DePrince, R. B., Mook, R. A., Hendren, R. W. and Wagner, R. W. *Proc. Natl Acad. Sci. USA*, **93**, 3176–3181 (1996).
46. Giles, R. V., Spiller, D. G. and Tidd, D. M. *Antisense Res. Develop.*, **5**, 23–31 (1995).
47. Hughes, J. A., Aronsohn, A. I., Avrutskaya, A. V. and Juliano, R. L. *Pharm. Res.*, **13**, 404–410 (1996).
48. Delong, R., Stephenson, K., Loftus, T., Fisher, M., Alahari, S., Nolting, A. and Juliano, R. L. *J. Pharm. Sci.*, **86**, 762–764 (1997).
49. Bennett, C. F., Chiang, M. Y., Chan, H., Shoemaker, J. E. and Mirabelli, C. K. *Mol. Pharmacol.*, **41**, 1023–1033 (1992).
50. Goodarzi, G., Gross, S. C., Tewari, A. and Watabe, K. *J. Gen. Virol.*, **71**, 3021–3025 (1990).
51. Colige, A., Sokolov, B. P., Nugent, P., Baserga, R. and Prockop, D. J. *Biochem.*, **32**, 7–11 (1993).
52. Yang, N. S., Burkholder, J., Roberts, B., Martinell, B. and McCabe, D. *Proc. Natl Acad. Sci. USA*, **87**, 9568–9572 (1990).
53. Matthews, K.E. and Keating, A. *Exp. Hematol.*, **22**, 702 (1994).
54. Takahashi, M., Furukawa, T., Nikkuni, K., Aoki, A., Nomoto, N., Koike, T., Moriyama, Y., Shinada, S. and Shibata, A. *Exp. Hematol.*, **19**, 343–346 (1991).
55. Wagner, E. *J. Controlled Rel.*, **53**, 155–158 (1998).
56. Freeman, D. J. and Niven, R. W. *Pharm. Res.*, **13**, 202–209 (1996).
57. Midoux, P., Kichler, A., Boutin, V., Maurizot, J.-C. and Monsigny, M. *Bioconj. Chem.*, **9**, 260–267 (1998).
58. Manuel, S. M., Guo, Y. and Matalon, S. *Am. J. Physiol.*, **273**, L741–L748 (1997).
59. Van Der Woude, I., Wagenaar, A., Meekel, A. A. P., Ter Beest, M. B. A., Ruiters, M. H. J., Engberts, J. B. F. N. and Hoekstra, D. *Proc. Natl Acad. Sci. USA*, **94**, 1160–1165 (1997).
60. Duncan, J. E., Whitsett, J. A. and Horowitz, A. D. *Hum. Gene Ther.*, **8**, 431–438 (1997).
61. Kukowska-Latallo, J. F., Chen, C., Eichman, J., Bielinska, A. U., Baker, J. R. Jr. *Biochem. Biophys. Res. Commun.*, **264**, 253–261 (1999).
62. Westesen, K., *Inter. J. Pharm.*, **102**, 91–100 (1994).
63. Westesen, K. and Koch, M. H. J. *Inter. J. Pharm.*, **103**, 225–236 (1994).
64. O'Hagan, D. T. and Illum, L. *Crit. Rev. Ther. Drug Carrier Syst.*, **7**, 35–97 (1990).
65. Muranishi, S., *Crit. Rev. Ther. Drug Carrier Syst.*, **7**, 1–33 (1990).
66. Lee, V. H., Yamamoto, A. and Kompella, U. B. *Crit. Rev. Ther. Drug Carrier Syst.*, **8**, 91–192 (1991).
67. Elbert, K. J., Schäfer, U. F., Schäfer, H. J., Kim, K. J., Lee, V. H. and Lehr, C. M. *Pharm. Res.*, **16**, 601–608 (1999).
68. Hug, P. and Sleight, R. G. *Biochim. Biophys. Acta*, **1097**, 1–17 (1991).
69. Ledley, F. D. *Hum. Gene Ther.*, **6**, 1129–1144 (1995).
70. Lee, R. J. and Huang, L. *Crit. Rev. Ther. Drug Carrier Syst.*, **14**, 173–206 (1997).
71. Huber, B. E. *Ann. N. Y. Acad. Sci.*, **716**, 1–5 (1994).
72. Miller, N. and Vile, R. *FASEB*, **9**, 190–199 (1995).
73. Uckert, W. and Walther, W. *Pharmacol. Ther.*, **63**, 323–347 (1994).
74. Logan, J. J., Bebok, Z., Walker, L. C., Peng, S., Felgner, P. L., Siegal, G. P., Frizzell, R. A., Dong, J., Howard, M., Matalon, *et al.*, *Gene Ther.*, **2**, 38–49 (1995).

75. Kukowska-Latallo, J. F., Raczka, E., Quintana, A., Chen, C., Rymaszewski, M. and Baker, J. R. Jr. *Hum. Gene Ther.*, **11**, 1385–1395 (2000).
76. Roberts, J. C., Bhalgat, M. K. and Zera, R. T. *J. Biomed. Mater. Res.*, **30**, 53–65 (1996).
77. Malik, N., Wiwattanapatapee, R., Klopsch, R., Lorenz, K., Frey, H., Weener, J. W., Meijer, E. W., Paulus, W. and Duncan, R. *J. Control. Rel.*, **65**, 133–148 (2000).
78. Raczka, E., Kukowska-Latallo, J. F., Rymaszewski, M., Chen, C. and Baker J. R. Jr, *Gene Ther.*, **5**, 1333–1339 (1998).
79. Singh, P., Moll III, F., Lin, S. H., Ferzli, C., Yu, K. S., Koski, R. K., Saul, R. G. and Cronin, P. *Clin. Chem.*, **40**, 1845–1849 (1994).
80. Wu, C. *Bioorg. Med. Chem. Lett.*, **4**, 449–454 (1993).
81. Lamb, R. A. and Krug, R. M. 'Orthomyxoviridae: the viruses and their replication', in Fields, B. N., Knipe, D. M. and Howley, P. M. (eds), *Fields and Virology*, Lippincott-Raven Publ., Philadelphia, 1996, pp. 1353–1395.
82. Schulze, I. T. *J. of Infectious Dis.*, **176** (Suppl. 1), S24–S28 (1997).
83. Weis, W., Brown, J. H., Cusack, S., Paulson, J. C., Skehel, J. J. and Wiley, D. C. *Nature*, **333**, 426–431 (1988).
84. Pritchett, T. J. and Paulson, J. C. *J. Biol. Chem.*, **256**, 9850–9858 (1989).
85. Reuter, J. D., Myc, A., Hayes, M. M., Gan, Z., Roy, R., Qin, D., Yin, R., Piehler, L. T., Esfand, R., Tomalia, D. A. and Baker, J. R. Jr. *Bioconj. Chem.*, **10**, 271–278 (1999).

Chapter 5

Dendrimer-mediated cell transfection *in vitro*.

James R. Baker Jr. M.D., Anna U. Bielinska Ph.D., and Jolanta F. Kukowska-Latallo Ph.D.

Department of Internal Medicine and Center for Biologic Nanotechnology,
The University of Michigan Health System, Ann Arbor, Michigan 48109-0648.

Corresponding author:
James R. Baker Jr. M.D.
9220 MSRB III, Ann Arbor, Michigan 48109-0648
ph: 734-647-2777
fax:734-936-2990
e-m:jbakerjr@umich.edu

1. Introduction

In recent years, Starburst^R PAMAM dendrimers, a class of polyamidoamine polymers have become an interesting alternative vector for non-viral delivery of DNA *in vitro* and *in vivo* (1, 2, 3, 4, 5, 6). These nanoscopic polymers characterized by regular dendritic branching, radial symmetry and uniform size ranging from 4 to 11nm, have excellent water solubility and are biocompatible in a broad range of concentrations. Non-modified dendrimers have a high density of positively charged primary amino groups on the surface, which is essential for their interaction with counter-charged nucleic acids. Positively charged dendrimers bind DNA through electrostatic interactions with negatively charged phosphates on the DNA molecule (1). The consistent and predictable formation of dendrimer-DNA complexes allows for the design of efficient DNA transfections into variety of eukaryotic cell lines and primary cells *in vitro* (1, 2, 4, 5, 7). The positively charged dendrimer-DNA complexes facilitate transfer of DNA into a cell primarily through endocytosis. DNA in a complexed form is protected from nuclease activity while the majority of the DNA template remains transcriptionaly active (8). The well designed dendrimer-based transfection is characterized by the lack or minimal cytotoxicity, high transfection efficiency, and stability of complexed plasmid DNA and oligonucleotides (8, 9). PAMAM dendrimers can be used for gene delivery *in vivo* and *ex vivo* (6, 10, 11, 12). The majority of chemical and structural differences in PAMAM dendrimers relate to the core molecule, either ammonia (NH3) as a trivalent initiator core or ethylenediamine (EDA) as a tetravalent initiator core. The core starts the stepwise polymerization process and dictates several structural characteristics of the molecule, including the overall shape, density, and surface charge. With each new layer or generation, the diameter of molecule increases approximately 1nm, the molecular weight of the dendrimer more than doubles and the number of surface amine groups exactly doubles. Such regularity of the dendrimer architecture provides for the convenient calculations of electrostatic charge ratios between dendrimers and nucleic acids for transfection. All types of nucleic acids including plasmid DNA, short single stranded and double stranded oligonucleotides (ODNs), as well as RNA can be used for transfection with dendrimers *in vitro* and *in vivo* (9, 13). The quality of DNA preparation (e.g. presence of low molecular weight nucleic acids and bacterial endotoxins) affects the efficiency of transfection and cytotoxicity, especially gene transfer *in vivo* (6).

2. Material

2.1. Dendrimers

A number of dendrimers are available commercially. Generations 1 - 4 of Starburst^{R} (PAMAM) dendrimers are available from The Sigma-Aldrich Family (Milwaukee, WI). Generations 5, 7, 9 of PAMAM dendrimers are available from Dendritech (Midland, MI). In the presented method we have used dendrimers with ethylenediamine (EDA) as a tetravalent polymerization initiator core. Generations (G) 5, 7, and 9 EDA core dendrimers have molar masses of 28 826, 116 493, and 467 162 kDa, respectively. The number of surface charges (amine groups) is 128, 512, and 2048 for the same dendrimers.

2.2. Plasmids

The reporter gene plasmids coding luciferase (luc), chloramphenicol acetyltransferase (CAT), β-galactosidase or green fluorescence protein (GFP) can be purchased (Promega Co. Madison, WI; Invitrogen, Rockville, MD; Clontech, Palo Alto, CA) or constructed specifically for the project.

Prepare plasmid DNA by any standard method (14). The preferable method for purification used in the dendrimer-based protocol is double CsCl-gradient centrifugation and dialysis into sterile TE buffer or water.

2.3. Cell lines and cells

Transfections of Rat 2 (rat embryonal fibroblast), NHFF1 (normal human forskin fibroblast), COS-1 (monkey kidney SV40 transformed fibroblast-like) and Jurkat (human acute T cell leukemia) cell lines are presented in this protocol.

For optimum results transfections should be performed on actively dividing cells, preferably from cultures at the logarithmic phase of growth.

2.4. Cell culture medium and solutions

The cell culture media should be used as recommended by the supplier of cells or ATCC. Cells in the presented method are maintained in appropriate growth medium, primarily DMEM or RPMI 1640 (Invitrogen) supplemented with 10% FBS serum (HyClone, Logan, UT) and 1% penicillin-streptomycin solution (Invitrogen) at 37^{O}C in 5% CO_2.

Molecular biology grade PBS buffer pH 7.4 (Invitrogen,) is used for cell washes.

Luciferin substrate and luciferase reporter buffer is needed to measure luciferase gene expression (Promega Co.). CAT protein expression is quantified using CAT ELISA assay

kit (Roche Diagnostics Co., Indianapolis, IN). The protein concentration of the sample is measured with BCA Protein Assay Reagent (Pierce, Rockford, IL).

2.5. Equipment

Chemiluminometer LB96P is used for measurement of light emission (EG & G/Berthold, Gaithersburg, MD). For spectrophotometric measurements of protein and ELISA assays SPECTRA MAX 340 microtiter plate reader is used (Molecular Devices Corp., Sunnyvale, CA). Flow cytometry analysis is conducted using FACScan Becton-Dickinson and CellQuest software (Becton-Dickinson, San Jose, CA). *In situ* cell analysis is performed with Nikon fluorescent microscope (Eclipse TE 200).

3. Methods

3.1. Preparation of plasmid DNA-dendrimer complex

Prepare dendrimer and DNA complex based on the calculated dendrimer to DNA charge ratio. Mix 0.65μg of dendrimer with 1.0μg of DNA to obtain charge ratio of 1. Form complexes at various charge ratios of 1, 5, 10 and 20 at room temperature for 15 minutes before adding into transfection medium (see example in *Transfection protocol*).

3.2. Transfection protocol

1. Plate adherent cells (e.g. Rat2, NHFF1, COS-1) 12 - 24hrs prior to transfection so that they are 60 – 70% confluent at the time of DNA delivery. Required cell density depends on cell type and size, growth rate and serum concentration in the growth medium. Generally, seeding at 2 to 4 $x10^4$ cells/cm^2 of a plate surface is optimal for transfection of the majority of cell lines. Inoculate suspension cell line (e.g. Jurkat) with $5x10^5$ to 10^6 cells 18 - 24 hrs prior to transfection from culture that is in a mid-logarithmic phase of growth. Resuspend 10^6 to $5x10^6$ cells in serum free (or 1% FBS) medium at the density of 1-$5x10^6$/ml for transfection.
2. If cells are grown in medium containing > 10% serum, wash the cells once with PBS or serum-free medium. Aspirate the medium or wash.
3. Add an appropriate volume of serum free medium on the plate (e.g. 2-3 ml for 100mm plate, 0.3-0.5 ml/well of 6-well plate, 0.2-0.3 ml/well of 24-well plate).
4. Prepare dendrimer/DNA complex. For example, for 60μl of dendrimer/DNA complex at a charge ratio of 10, mix 50μl of plasmid DNA at 0.02μg/μl (up to 0.08μg/μl) with 10μl of dendrimer at 0.65 μg/μl (up to 2.6 μg/μl), respectively.

5. Add an aliquot of dendrimer/DNA complex into the cells. For example, a 10-25µl volume of the complex for transfection in 24-well plate, 10-50µl for transfection in 6-well plate. Generally, complex made in water should not constitute more than 10% of the total volume of serum-free transfection medium.

a. Incubate cells with transfection mixture for 3 hr to 6 hr at 37°C, 5% CO_2.

b. Remove transfection medium, wash once gently, with serum free medium (it is not necessary when low concentration of dendrimer is used, and no augmenting agents are added).

c. Add fresh, full growth medium.

d. Incubate for the required time (24, 36, 48, 72hr etc.) before harvesting cells.

e. Remove medium, wash twice with PBS and prepare cell lysate for assay. For example, use 50µl or 100 µl of luciferase reporter buffer to lyse the cells for 5min in a well of 24-well or 6-well plate, respectively or follow the supplier's protocol (Promega, Roche Diagnostics Co.)

3.3. Measurement of expression

a. Assay transfected cells for expression of introduced transgene. Measure luciferase activity in a chemiluminescence assay. Incubate cell extract (typically 10µl) with 2.35 x 10^{-2} µmol of luciferin substrate injected automatically in 50µl or 100µl volumes. Measure light emission in the chemiluminometer for 10sec and adjuste for the protein concentration of the sample.

b. Measure the protein concentration of the sample (typically 10µl) using BCA Protein Assay Reagent. The absorbance of the sample measure at 562nm using a microtiter plate reader.

c. To quantify chlormaphenicol acetyl transferase (CAT) protein centrifuge cell lysate at 12,000xg for 10-15 minutes at 4°C. Measure the amount of CAT in 10 to 50µl of the supernatant in ELISA assay. Measure the absorbance of the samples at 405nm using a microtiter plate reader and adjust for the protein concentration of the samples.

d. Analyze cells transfected with the plasmid coding GFP gene using flow cytometry Wash harvested cells twice with PBS and fix in 2% paraformaldehyde for 15 minutes before analysis. Determine the green fluorescence of GFP on FACScan from at least 10,000 cells per sample and analyze using CellQuest software.

e. Assess the expression of green fluorescence protein (GFP) *in situ* using an inverted fluorescent microscope at 450-480 nm excitation and 515 nm emission wavelength. Take photographs at 20X magnification.

4. Notes

Dendrimer-mediated DNA transfection is a straightforward technique which can be applied to gene delivery in order to modify cellular genetic makeup (i.e. to generate a stably transfected cell line), in studies on regulation of gene expression, and due to lack of immunogenicity, for gene transfer *in vivo*. The reporter plasmids are very useful for determination of the transfection conditions for the experimental cDNA. They can also be used in co-transfection with the DNA of interest for tracing the efficiency and kinetics of gene expression.

1. Preparation of the dendrimer/DNA complex for *in vitro* transfection is based on the charge ratio of both components. Calculations use maximal theoretical electrostatic charge present on each component (1, 15). For example, the number of phosphate groups (i.e. negative charges) in 1.0μg of DNA equals 1.71×10^{15} and the number of positive charges of dendrimer equals 2.65×10^{15} per μg. This calculation is independent of molecular properties of both components, including the size and form of nucleic acid or generation of dendrimer. It was determined that for practical reasons dendrimer/DNA complexes should be formed in water at appropriate DNA and dendrimer concentrations (see *Transfection protocol*). For consistency, complexes are formed at room temperature before adding into transfection medium. However, the dendrimer/DNA complex is stable for a prolonged (up to few days) time and can be used after remixing when precipitation occurs.

a. Figure 1 illustrates the effect of increasing the charge ratio on the efficiency of transfection. Most impressive improvement is obtained when a low amount (e.g. 0.25μg per transfection) of DNA is used. With higher amounts of DNA at 1μg to 5μg per transfection, the maximum efficiency is achieved at the relatively low charge ratio of 10. Maximal gene expression can be optimized for the amount of DNA available for delivery, the amount of dendrimer, and consequently dendrimer to DNA charge ratio. Generally, the lower the amount of DNA, the higher dendrimer/DNA charge ratio (and *vice versa*) is required for transfection.

b. In addition to charge ratio, the DNA concentration during complex formation significantly affects efficiency of transfection (Figure 2). Empirical data indicate that complexes formed with DNA concentrations ranging from 20 to 80 μg/ml are most

efficient. In such conditions, dendrimer/DNA complexes formed at a broad range of charge ratios do not tend to aggregate or precipitate and remain in suspension. This low density complex mediates the majority of transfections *in vitro* (15). Soluble dendrimer formulations, obtained either in excess of dendrimer or DNA, also appear to be more effective for *in vivo* transfection of solid tissues (6, 12).

c. Another essential step in optimizing *in vitro* transfection is the choice of generation (type) of dendrimer. As shown on Figure 3A, the preferred dendrimer for transfection of Rat2 cells is generation 9 EDA core dendrimer. Generation 5 EDA core dendrimer and to a lesser degree generation 7 EDA dendrimer are better for NHFF-1 cells (Figure 3B). However, transfection obtained with the intermediate G7 EDA dendrimer indicates that size preference may not be an absolute property of either cells or dendrimer and can be affected by other parameters of the complex mentioned above.

2. The design of the transfection-based experiments would not be complete without elementary consideration of cellular biology. Most model systems employ cell lines dividing and metabolizing rapidly.

a. The experiment presented in Figure 3 involved active cell cultures. However, growth, metabolic rate and transcriptional milieu were manipulated by varying the initial density of cell seeding. Cultures of Rat2 and NHFF1 cells seeded at $1x10^4$ cells/cm^2 and $5x\ 10^4/cm^2$ cells had a similar growth rate but very different levels of transfection. At 24 hr after transfection, Rat 2 cells at both densities express similar levels of luciferase, but no enzyme activity is detected in NHFF1 cells in the same conditions. Practically, no expression is achieved with either of the cell types when they are transfected in near-confluent densities (initial seeding at $1\ x10^6$cells/cm^2).

b. Cellular differences can also be pronounced in the kinetics of transgene expression with a maximum level for NHFF1 at approximately 48 hr and for Rat2 at 72 hr after transfection. The time of harvest and analysis should be chosen depending on the goals of experiment, since the prolonged presence of the expressed protein may not only be a result of efficient transfection and transcription, but also reflect a difference of a specific rate of degradation in a particular cell type.

3. There is no cell origin or cell type limitation on the use of dendrimers for *in vitro* transfections. In our extensive studies on the efficiency and mechanism of dendrimer-mediated transfection we have transfected a broad variety of cells (1, 7).

a. The efficiently transfected cell lines include established CCD-37Lu (human normal lung fibroblast); A549 (human lung carcinoma epithelial-like), COS-7 (monkey kidney SV40 transformed fibroblast-like), Clone9 (rat normal liver epithelium), BHK-21 (hamster kidney fibroblast-like), MC7 (human breast cancer line), B/6 (mouse melanoma), RAW264 (mouse monocyte -macrophage), NIH 3T3 (mouse embryonal), HeLa (human cervical adenocarcinoma epithelium), U937 (human histiocytic lymphoma), MDCK (dog normal kidney epithelium), P815 (mouse mastocytoma).

b. The primary cell cultures, efficiently transfected with dendrimer/DNA complex, include normal human bronchial epithelium (NHBE) and small airway epithelium (SAEC) grown in serum-free SABM/SAGM (collection and medium from Clonetics Co., San Diego, CA). Also, successful and efficient transfection was achieved in primary cells from human and mouse thyrocytes, normal human skin kerationocytes (NHSK) and human mucosal keratinocytes (NHMK), either isolated from patients or from Clonetics Co. collection (7, 12). Generally, the optimal conditions of cell culture growth are similar for adherent and suspension cell lines.

4. The transfection can be carried out for 3 to 6 hr. Further extension of time does not result in an appreciable increase of transfection efficiency. After removal of transfection solution, cells are washed once in serum free medium. An appropriate amount of fresh complete medium (i.e. a 5 to 10-fold volume of the transfection medium) is added to obtain cultures of approximately 1-5 x 10^5 cells/ml. The single wash after removal of transfection medium is not necessary if no toxicity was observed during transfection or if cytotoxic augmentation reagents such as chloroquine (CLQ) or DEAE-dextran are not used. The incubation time has to be assessed based on the results of cell expression after 24, 36, and 48 hr after transfection.

a. As with other polymer-based systems the dendrimer mediated transfection can be augmented with chloroquine and DEAE-dextran. A typical transfection experiment can be performed in serum-free medium, augmented with chloroquine at 50 μM final concentration (effective concentration varies from 10 to 100μM depending on cell

type) or augmented with DEAE-dextran at 0.5μM final concentration. Combination of chloroquine and DEAE-dextran in transfection medium can be used at 50 μM and 0.5 μM final concentrations, respectively. Chloroquine, a weak acidotropic base, neutralizes the endosomal compartment and possibly enables endosomal escape of DNA. We found that chloroquine alone does not greatly improve dendrimer-mediated transfection, but in conjunction with DEAE-dextran, the complex dispersing agent, the efficiency can be enhanced up to two orders of magnitude (Figure 4A). Unfortunately, both of these agents are cytotoxic, requiring careful experimental adjustments, and cannot be applied *in vivo*.

b. We have identified that incubation with the non-ionic surfactant tyloxapol results in an increase in transfection efficiency *in vitro*, possibly through interaction with cellular membranes (Figure 4B). Dendrimer/DNA complex can be added to medium containing tyloxapol at 0.1–0.5 mg/ml final concentration or dendrimer /DNA complex can be mixed in the presence of tyloxapol.

5. The dendrimer/DNA complex composition and architecture seems to be critical for its transfection activity. The interaction of both components is affected by pH and/or salt concentration. Data in Figure 5 clearly shows that the initial condition of complex formation has consequences on transfection. A high concentration of NaCl present during complex formation at charge ratios of 5 to 10 initially resulted in enhanced DNA expression, but this effect disappeared with an increase in dendrimer concentration (Figure 5A). We recommend lower than neutral pH of water or very diluted buffer for the formation of active complexes (Figure 5B). Our experience with various laboratory sources of distilled and deionized water indicate that all of them produce H_2O at pH 5 to 5.5 which is suitable for preparation of dendrimer/DNA complexes.

References

1. Kukowska-Latallo, J.F., Bielinska, A.U., Johnson, J., Spindler, R., Tomalia, D.A., and Baker Jr., J.R. (1996) Efficient transfer of genetic material into mammalian cells using Starburst polyamidoamine dendrimers. *Proc. Natl. Acad. Sci. USA* **93**, 4897-4902.
2. Baker Jr., J.R., Bielinska, A., Johnson, J., Yin, R., and Kukowska-Latallo, J.F. (1996). Efficient transfer of genetic material into mammalian cells using polyamidoamine dendrimers as synthetic vectors: Dendrimer -mediated transfection. In: Conference Proceedings Series: Artificial Self-Assembling Systems for GeneDelivery (Felgner, P.L., Heller, M.J., Lehn, P., Behr, J.P., Szoka Jr., F.C., eds.), American Chemical Society, Washington, DC, p.129-145.
3. Kukowska-Latallo, J.F., Bielinska, A.U., Chen, C., Rymaszewski, M., Tomalia, D.A., and Baker Jr., J.R. (1998). Gene transfer using starburst dendrimers. In: Self-Assembling Complexes for Gene Delivery: From Chemistry to Clinical Trial (Kabanov, A.V., Felgner, P.L., Seymour, L.W. eds.), J Wiley & Sons, Ltd. Sussex, England, p.241-253.
4. Eichman, J.D., Bielinska, A.U., Kukowska-Latallo, J.F., and Baker Jr., J.R. (2000). The use of PAMAM dendrimers for the efficient transfer of genetic material into cells. *Pharm. Sci. Technol. Today*. **7**, 232-245.
5. Eichman, J.D., Bielinska, A.U., Kukowska-Latallo, J.F., Donovan, B.W., and Baker Jr., J.R. (2001). Bioapplications of PAMAM dendrimers. In: Dendrimers and Other Dendritic Polymers (Frechet, J.M.J. and Tomalia, D.A., eds.), J Wiley & Sons, Ltd. Sussex, England, p441-461.
6. Kukowska-Latallo, J.F, Raczka, E., Quintana A., Chen, C., Rymaszewski, M., and Baker Jr., J.R. (2000). Intravascular and endobronchial DNA delivery to murine lung tissue using a novel, nonviral vector. *Hum. Gene Ther*. **11**, 1385-1395.
7. Kukowska-Latallo, J.F., Chen, C., Eichman, J., Bielinska, A.U., and Baker Jr., J.R. (1999). Enhancement of dendrimer-mediated transfection using synthetic lung surfactant Exosurf Neonatal *in vitro*. *Biochem. Biophys. Res. Commun*. **264**, 253-261.
8. Bielinska, A.U., Kukowska-Latallo, J.F., and Baker Jr., J.R. (1997) The interaction of plasmid DNA with polyamidoamine dendrimers: mechanism of complex formation and

analysis of alterations induced in nuclease sensitivity and transcriptional activity of the complexed DNA. *Biochim. Biophys. Acta* **1353**, 180-190.

9. Bielinska, A., Kukowska-Latallo, J.F., Johnson, J., Tomalia, D.A., and Baker Jr., J.R. (1996) Regulation of in vitro gene expression using antisense oligonucleotides or antisense expression plasmids transfected using starburst PAMAM dendrimers. *Nucleic Acids Res.* **24**, 2176-2182.
10. Qin, L., Pahud, D.R., Ding, Y., Bielinska, A.U., Kukowska-latallo, J.F., Baker Jr., J.R., and Bromberg, J.S. (1998). Efficient transfer of genes into murine cardiac grafts by starburst polyamidoamine dendrimers. *Hum. Gene Ther.* **9**, 553-560.
11. Wang, Y., Boros, P., Liu, J., Qin, L., Bai, Y., Bielinska, A.U., Kukowska-Latallo, J.F., Baker, Jr., J.R., and Bromberg, J.S. (2000). DNA/dendrimer complexes mediate gene transfer into murine cardiac transplants ex vivo. *Mol. Ther.* **2**, 602-608.
12. Bielinska, A.U., Yen, A., Wu, H.L., Zahos, K.M., Sun, R., Weiner, N.D., Baker, Jr., J.R., and Roessler, B.J. (2000). Application of membrane-based dendrimer/DNA complexes for solid phase transfection in vitro and in vivo. *Biomaterials* **21**, 877-887.
13. Raczka, E., Kukowska-Latallo, J.F., Rymaszewski, M., Chen, C., and Baker Jr., J.R. (1998). The effect of synthetic surfactant Exosurf on gene transfer in mouse lung in vivo. *Gene Ther.* **5**, 1333-1339.
14. Sambrook, J., Fritsch, E. F., and Maniatis, T. (1989) *in* Molecular Cloning: A Laboratory Manual, 2nd ed. pp. 142-143 Cold Spring Harbor Laboratory Press, Cold Spring Harbor, NY.
15. Bielinska, A. U., Chen, C., Johnson, J., and Baker, Jr., J. R. (1999) DNA complexing with polyamidoamine dendrimers: implications for transfections. *Bioconjugate Chem.* **10**, 843-850.
16. Roessler, B.J., Bielinska, A.U., Janczak, K., Lee, I., and Baker Jr., J.R. (2001). Substituted b-cyclodextrins interact with PAMAM dendrimer-DNA complexes and modify transfection efficiency. *Biochem. Biophys. Res. Commun.* **283**, 124-129.

Figure Legends

Figure 1.

The effect of DNA amount on dendrimer-mediated transfection *in vitro*. An excess of positive charge is required for efficient transfection. The G9 EDA/DNA complexes for transfection of Rat2 embryonic fibroblasts were prepared with an increasing amount of CMV-luciferase plasmid DNA (pCF1-Luc). The efficiency of transfection was analyzed at a broad range [1 to 100] of dendrimer/DNA charge ratio. Luciferase activity (RLU) was measured 36 hr after transfection and normalized per microgram of protein in the cell lysate.

Figure 2.

The effect of DNA concentration during complex formation and dendrimer/DNA charge ratio on the efficiency of transfection. Rat2 cells were transfected with 1μg of pCF1-Luc complexed with G9 EDA dendrimer. Complexes of equal amount of DNA and the same dendrimer/DNA charge ratio differ in DNA concentration during complex formation. Data indicate that the optimal DNA concentration range from 0.04-0.08 μg/μl results in most efficient transfection.

Figure 3.

Optimization of the transfection conditions for Rat2 (panel A) and NHFF1 (panel B) cells *in vitro*. Note that transfection conditions and the resulting kinetics of the transgene expression is cell specific, including dendrimer requirements, cell density and growth rate. Transfections were performed with 1 μg of pCF1-Luc DNA complexed with G5, G7 and G9 EDA dendrimers at the dendrimer/DNA charge ratio 10. Cells were seeded at 10^4, 5 x 10^4 and $10^5/cm^2$ 12 hr before transfection, and incubated for 24, 48 and 72 hr after transfection. For both cell lines, the highest luciferase expression was obtained in cells seeded at the lowest density.

Optimal transfection in Rat2 cells (A) was achieved with G9 EDA dendrimer and in NHFF1 cells (B) with E5 EDA dendrimer. Kinetics of expression indicates that maximum level of reporter protein production can be most likely detected at 24 to 48 hr after transfection.

Figure 4.

Augmentation of the dendrimer-mediated transfection by the addition of chloroquine (CLQ) and DEAE-dextran (panel A) and tyloxapol (panel B). Rat 2 (A) and Jurkat (B) cells were transfected with 0.5μg of pCF1-Luc DNA complexed with G9 EDA at charge ratio 5 and 10 (A) and 10 (B). Luciferase activity was measured 36 hr after transfection.

Figure 5.

Salt concentration and pH during dendrimer/DNA complex formation and their effect on transfection efficiency. COS-1 cells were transfected with 1 μg of pCF1-Luc DNA (0.05μg/μl) complexed with G7 EDA at specified dendrimer/DNA charge ratios 1, 5, 10 and 20 (panel A). Complexes (20 μl) formed in water or in the presence of 2 M NaCl were added to 400μl of medium (1:20 dilution) to avoid a hypertonic effect of salt or hypotonic effect of water on cell physiology. Transfection efficiency predictably increased with the increasing charge ratios for the complexes formed in water. To achieve enhancement with monovalent salt, the condition would have to be carefully adjusted for the specific concentrations of dendrimer, DNA as well as charge ratio because of the narrow functional optimum.

In panel B COS-1 cells were transfected with G5 EDA/DNA complex formed in aqueous solution adjusted to below neutral, neutral and alkaline pH. Complexes initially formed at the low pH are the most efficient despite the fact that transfections are routinely performed in standard growth media, buffered to neutral pH.

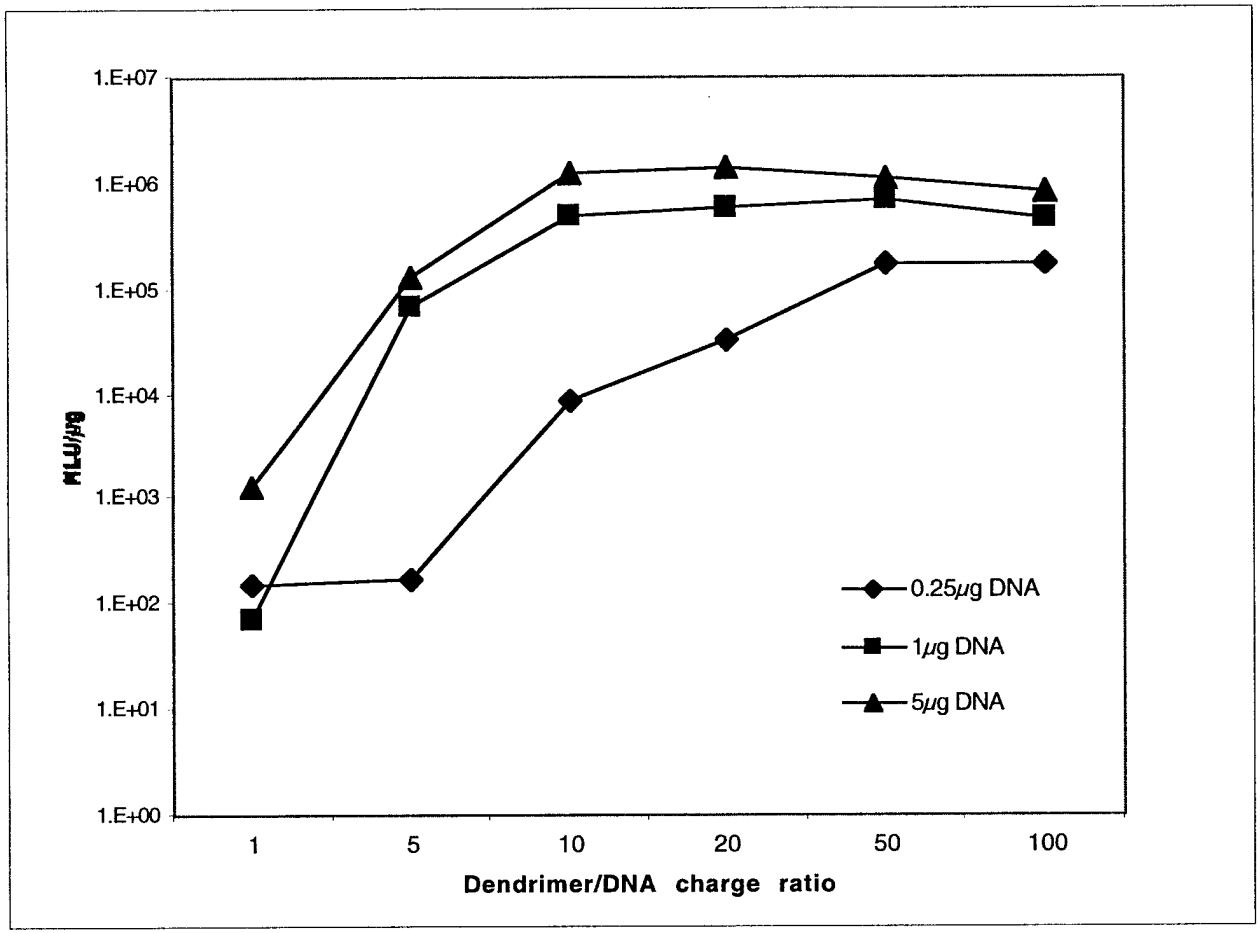
1.E+07
1.E+06
1.E+05
1.E+04
1.E+03
1.E+02
1.E+01
1.E+00
RLU/μg
1
5
10
20
50
100
Dendrimer/DNA charge ratio
0.25μg DNA
1μg DNA
5μg DNA

Fig.1

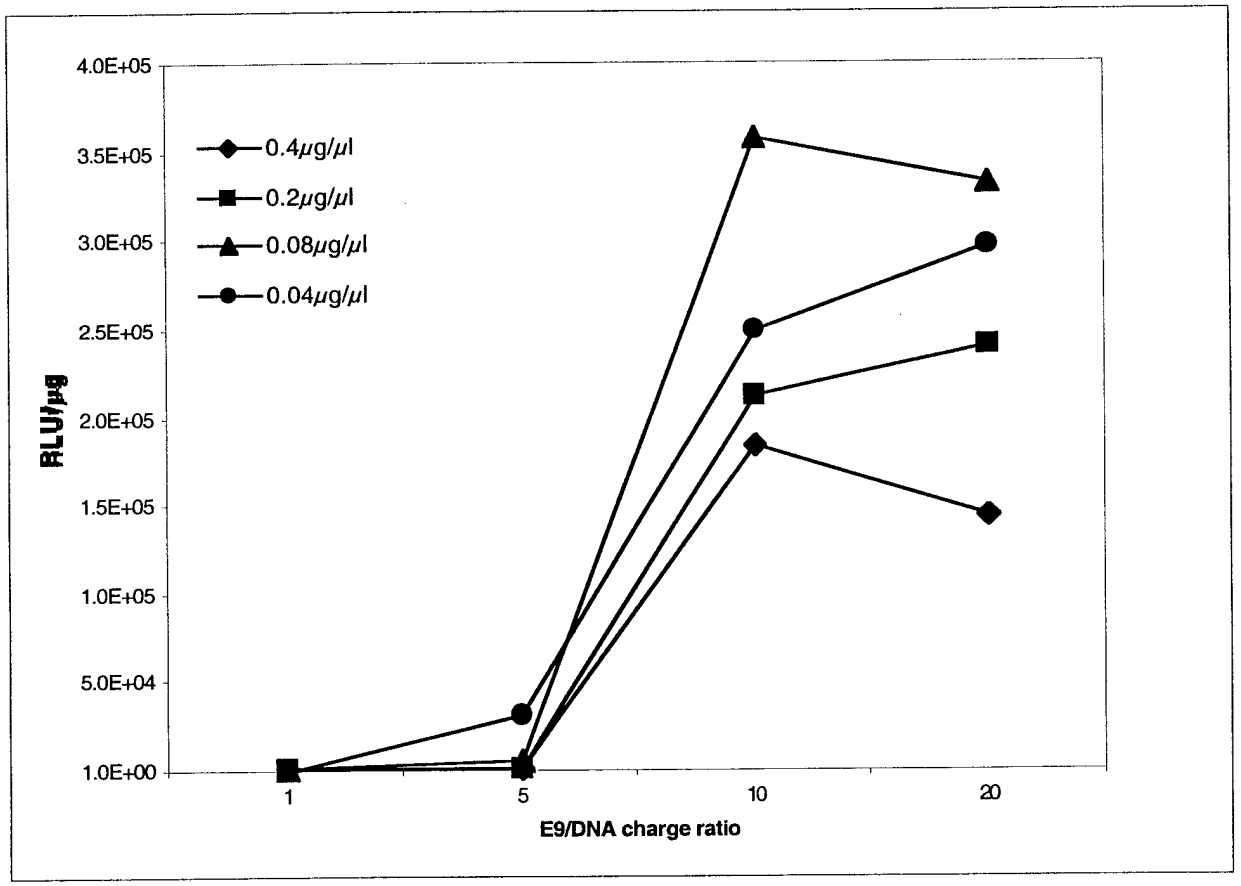
4.0E+05
3.5E+05
3.0E+05
2.5E+05
2.0E+05
1.5E+05
1.0E+05
5.0E+04
1.0E+00
RLU/µg
0.4µg/µl
0.2µg/µl
0.08µg/µl
0.04µg/µl
1
5
10
20
E9/DNA charge ratio

Fig. 2

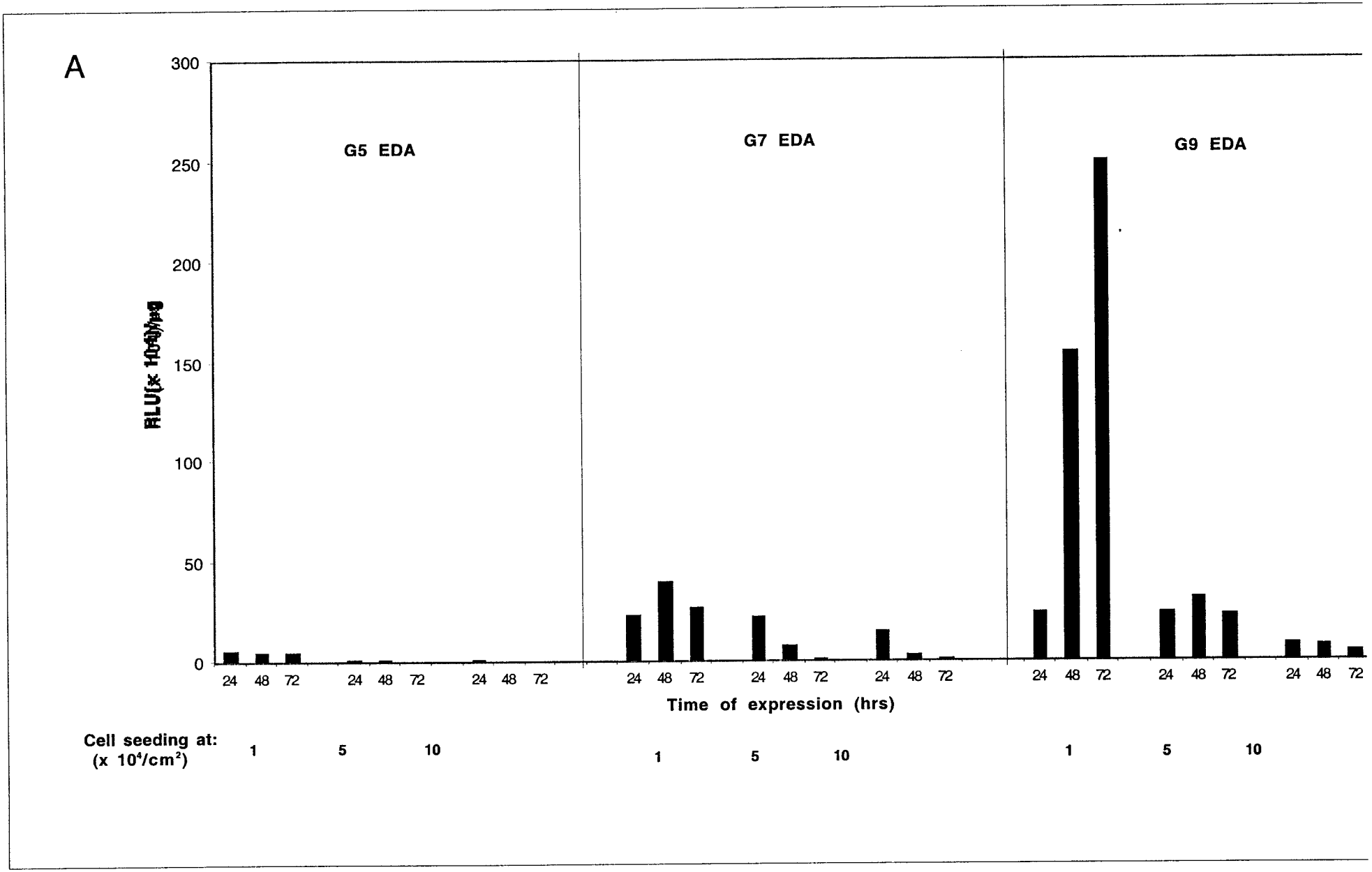
A
300
250
200
150
100
50
0
G5 EDA
G7 EDA
G9 EDA
24 48 72 24 48 72 24 48 72 24 48 72 24 48 72 24 48 72 24 48 72 24 48 72 24 48 72
Time of expression (hrs)
Cell seeding at:
(x 10⁴/cm²)
1 5 10 1 5 10 1 5 10

Fig. 3A

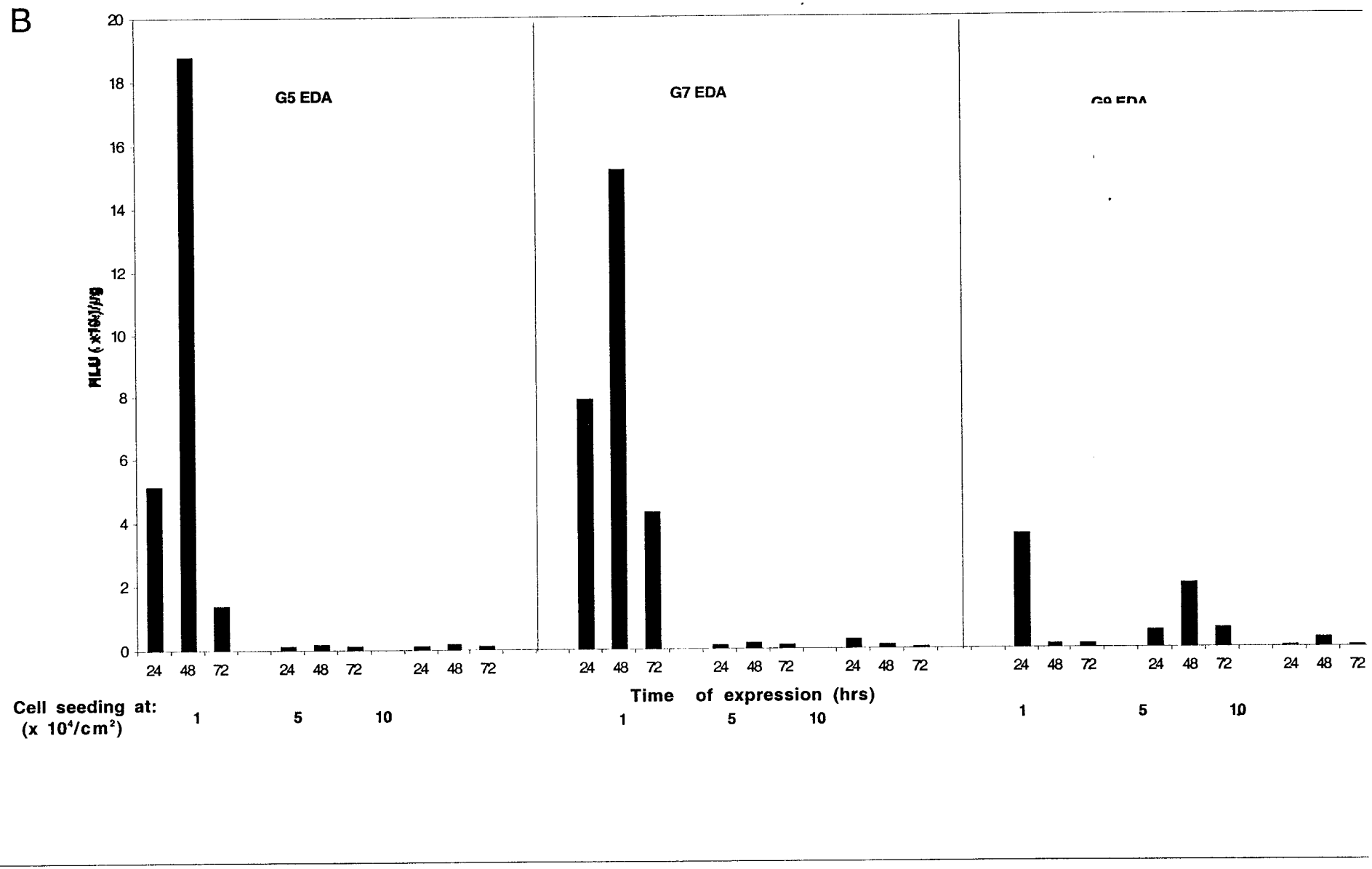
B
G5 EDA
G7 EDA
G9 EDA
RLU (x10³)/µg
0
2
4
6
8
10
12
14
16
18
20
24 48 72 24 48 72 24 48 72
Time of expression (hrs)
Cell seeding at:
(x 10⁴/cm²)
1
5
10

Fig. 3B

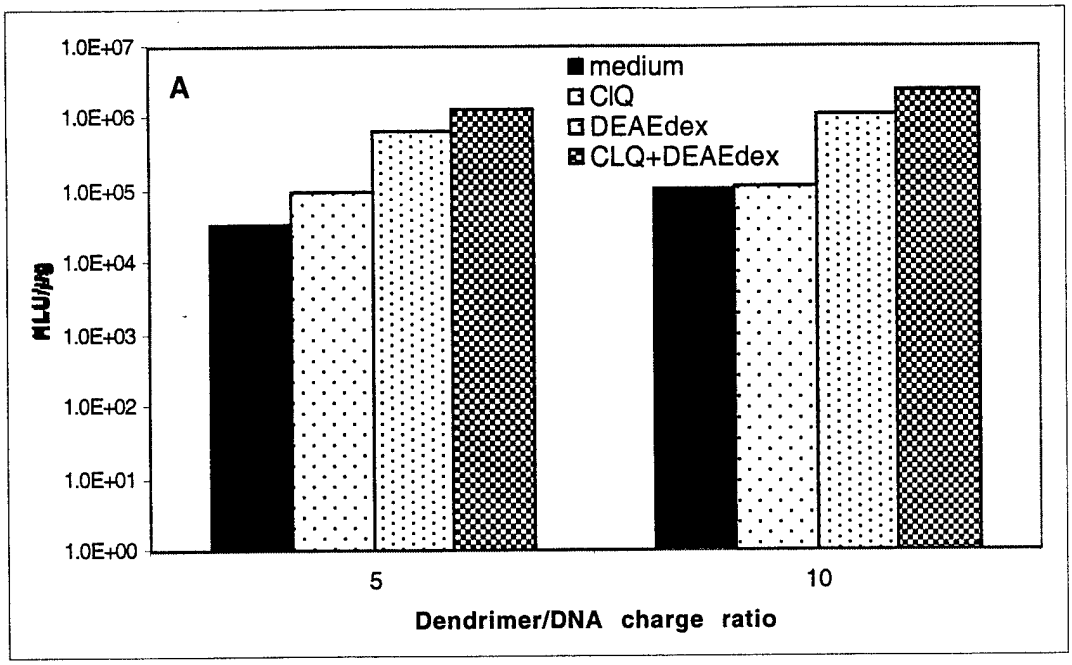
A
medium
ClQ
DEAEdex
CLQ+DEAEdex
1.0E+07
1.0E+06
1.0E+05
1.0E+04
1.0E+03
1.0E+02
1.0E+01
1.0E+00
RLU/µg
5
10
Dendrimer/DNA charge ratio

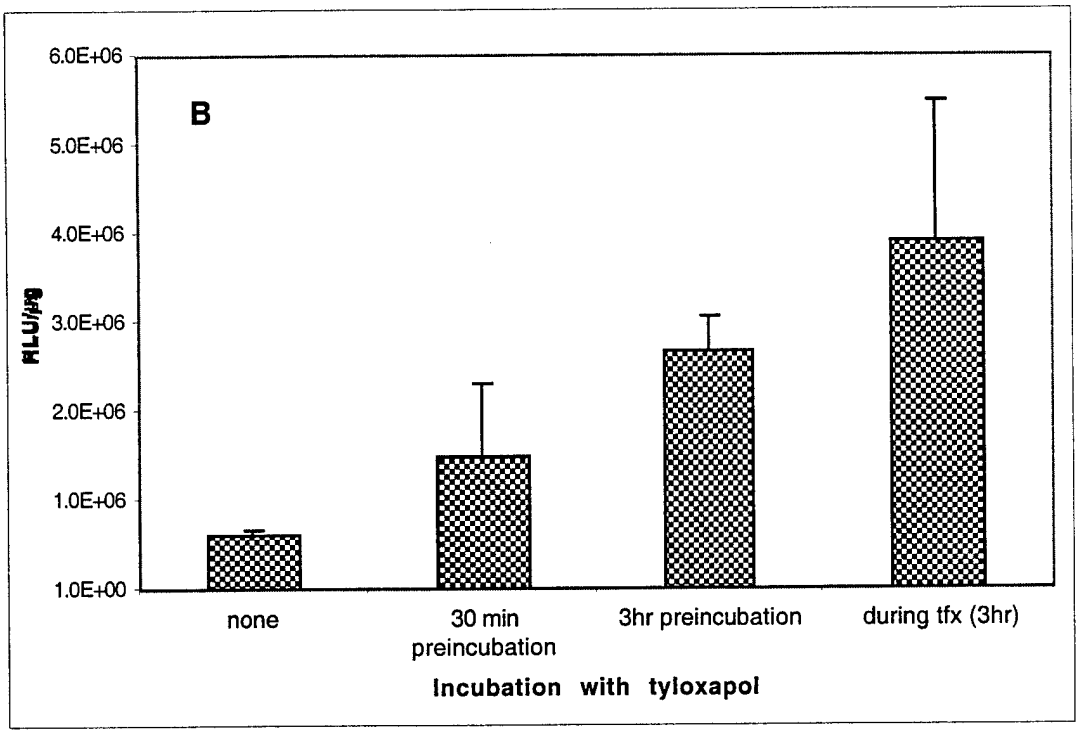
B
6.0E+06
5.0E+06
4.0E+06
3.0E+06
2.0E+06
1.0E+06
1.0E+00
RLU/µg
none
30 min preincubation
3hr preincubation
during tfx (3hr)
Incubation with tyloxapol

Fig. 4

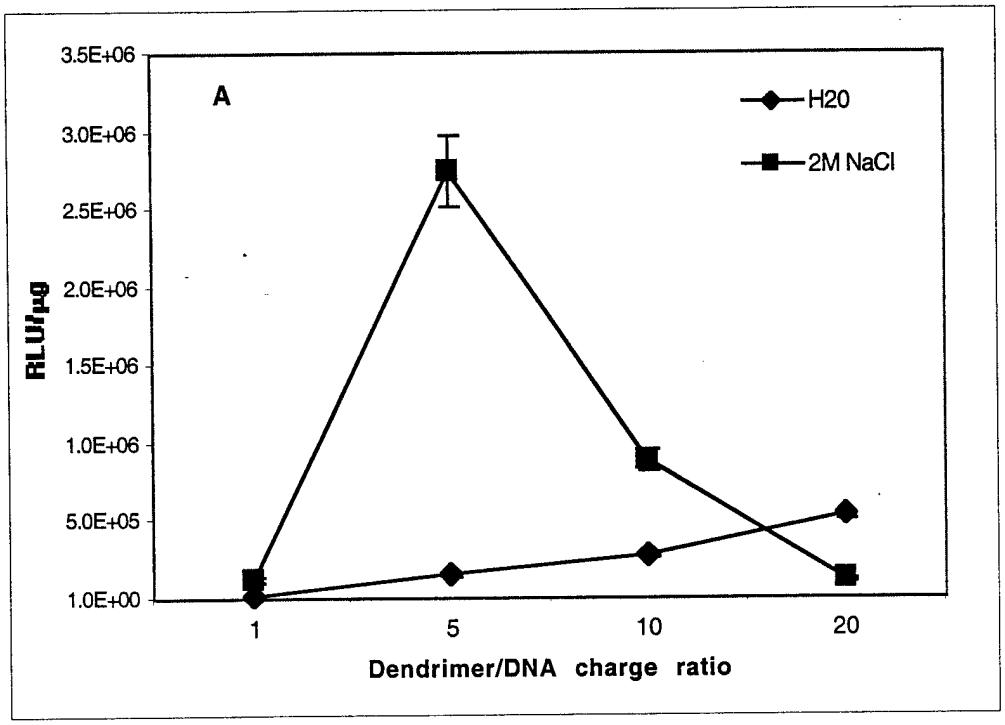
A
H20
2M NaCl
RLU/µg
3.5E+06
3.0E+06
2.5E+06
2.0E+06
1.5E+06
1.0E+06
5.0E+05
1.0E+00
1
5
10
20
Dendrimer/DNA charge ratio

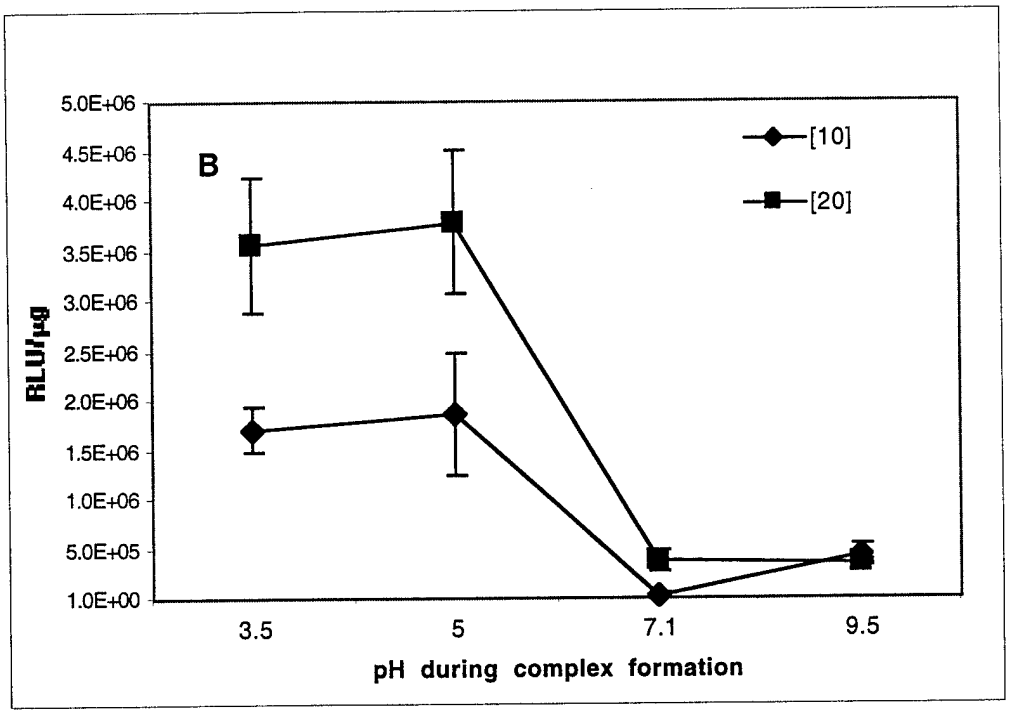
B
[10]
[20]
RLU/µg
5.0E+06
4.5E+06
4.0E+06
3.5E+06
3.0E+06
2.5E+06
2.0E+06
1.5E+06
1.0E+06
5.0E+05
1.0E+00
3.5
5
7.1
9.5
pH during complex formation

Fig. 5